Distribution Agreement

In presenting this thesis or dissertation as a partial fulfillment of the requirements for an advanced degree from Emory University, I hereby grant to Emory University and its agents the non-exclusive license to archive, make accessible, and display my thesis or dissertation in whole or in part in all forms of media, now or hereafter known, including display on the world wide web. I understand that I may select some access restrictions as part of the online submission of this thesis or dissertation. I retain all ownership rights to the copyright of the thesis or dissertation. I also retain the right to use in future works (such as articles or books) all or part of this thesis or dissertation.

Signature:

_____ _____

Juyoung Kim Date

Role of OVOL2 and miR-126 in ETV2-regulated cardiovascular development

By

Juyoung Kim
Doctor of Philosophy

Graduate Division of Biological and Biomedical Science
Molecular and Systems Pharmacology

_____

Changwon Park, Ph. D.
Advisor

_____

Roy L. Sutliff, Ph. D.
Committee Member

_____

Young-sup Yoon, M.D, Ph. D.
Committee Member

_____

Renhao Li, Ph. D.
Committee Member

Accepted:

_____

Lisa A. Tedesco, Ph.D.
Dean of the James T. Laney School of Graduate Studies

_____

Date

Role of OVOL2 and miR-126 in ETV2-regulated cardiovascular development

By

Juyoung Kim
M.S., Kyungpook National University

Advisor: Changwon Park, PhD.

An abstract of
A dissertation submitted to the Faculty of the
James T. Laney School of Graduate Studies of Emory University
in partial fulfillment of the requirements for the degree of
Doctor of Philosophy
in the Graduate Division of Biological and Biomedical Sciences,
Molecular and Systems Pharmacology
2018

Abstract

Role of OVOL2 and miR-126 in ETV2-regulated cardiovascular development

By Juyoung Kim

FLK1, the receptor for VEGF (vascular endothelial growth factor), has been identified as an essential factor for cardiovascular development and post-natal life. Accordingly, extensive efforts have been made to understand FLK1-mediated signaling, but the underlying mechanisms of *Flk1* gene regulation remain largely unknown. In this regard, my laboratory revealed for the first time the critical function of ETV2, a member of the ETS transcription factor family, for cardiovascular development. Further, ETV2 was identified as a direct upstream regulator for *Flk1* gene as well as other genes critical for both vascular endothelial and hematopoietic cell lineages development.

To understand the molecular mechanisms of ETV2 in regulating the development of the cardiovascular system, I set out two independent, but closely related projects for my Ph.D. thesis. First, I sought to identify the proteins that can interact with ETV2, since transcription factors often form the transcriptional complex with other transcription regulatory proteins to regulate the expression of the target genes. I revealed that ETV2 can directly interact with OVOL2, a zinc finger transcription factor. The interaction of ETV2-OVOL2 cooperatively regulates not only for the generation of $FLK1^+$ cells, but also the generation of vascular endothelial and hematopoietic cell lineages from mouse embryonic stem cells (mESCs). Second, I performed experiments to identify ETV2-regulated microRNA (miRNA) using next generation sequencing and found a subset of miRNAs regulated by ETV2. These miRNAs were closely related to cardiovascular development; particularly miR-126 was of special interest, since my experiments showed that the expression of miR-126 was directly activated by ETV2. Further, I demonstrated that the miR-126/MAPK pathway is critical for the generation of $FLK1^+$ cells from mESCs. Mechanistically, c-JUN/FOS (AP1 complex), a downstream of the MAPK pathway, binds to the enhancer region of *Flk1* via AP1 binding sequences, leading to the activation of *Flk1* expression.

In my dissertation, I have revealed the novel functions of ETV2; the interaction of ETV2-OVOL2 and the role of the miR-126/MAPK pathway in ETV2-mediated $FLK1^+$ cell generation. Therefore, these findings will advance our understanding on cardiovascular development, which could provide fundamental research directions for designing therapeutic approaches for cardiovascular disease.

Role of OVOL2 and miR-126 in ETV2-regulated cardiovascular development

By

Juyoung Kim
M.S., Kyungpook National University

Advisor: Changwon Park, Ph. D.

A dissertation submitted to the Faculty of the
James T. Laney School of Graduate Studies of Emory University
in partial fulfillment of the requirements for the degree of
Doctor of Philosophy
in the Graduate Division of Biological and Biomedical Sciences,
Molecular and Systems Pharmacology
2018

Acknowledgement

First of all, I would like to give all thanks to my Jesus, who was sacrificed on the cross for me. He is good all the time. 8 years ago, I was a young lady from South Korea who came to United States not to study science, but to expand experiences. However, God allowed me to meet my advisor Changwon Park and his wife Yunhee Kang, and gave me a chance to expand my knowledge so that I may dream the better future for the next generation in this world.

From the bottom, my advisor Dr. Changwon Park taught me enormous things about science and life. He made my eyes to open to science and gave me the motivation when I was exhausted. During my journey, he also taught me how to learn and study as a scholar with some criticism whenever it was needed. I became a scientist through him.

I also would like to thank Dr. Sutliff Roy my committee member, DGS, and supporter. After I got my Ph.D. candidacy, he supported me in various ways. He always gave me the best answers whenever I really needed help in science and life.

My other committee member, Dr. Young-sup Yoon taught me so many things. Every week, I learned from you how to present, discuss, and collaborate in the science field. Also, I would like to thank Dr. Renhao Li, who guided me to learn how to be professional. His brilliant comment about my thesis helped me to go through the problem.

In Emory, I also met my spiritual supporter, Eddie T. Morgan. He always encouraged me to go through all these steps. Moreover, he always came to my presentations, listened carefully, and helped me to realize the strength that I had inside of me.

I've received lots of help from all MSP people. Especially, I appreciate Susan Hoffstadter and my classmates. Without them, I may not have been able to finish my journey for Ph. D. MSP program was the best program for me to become a real scientist and scholar.

To all of my friends from Saehan Church, I appreciate your prayers, care, and love from heart. Especially, I appreciate Changkyo Lee, Sunhae Kim and Chaeum Lee, you are the most warm-hearted persons I've ever met. And, my old friend Minyoung Lee, she is my best friend and mentor. She helped all my steps with her wisdom.

To my loving family in Korea, especially my parents Jungyeon Kim and Geumja Shin, I cannot express my thanks to you. Without your love, I would not be able to be here today. You raised me up when I was very weak and sick physically and mentally during this Ph.D. journey. Finally, I would like to dedicate this dissertation to my grandmother whom I lost along this journey. I could not see her last moment, but I know she loved me until her last moment in this world, and she loves me now in heaven. Wolsoon Lee you faithfully provided unending love and encouragement. You are always in my heart.

Table of Contents

List of Abbreviations

AP1	Activator Protein 1
bFGF	Basic Fibroblast Growth Factor
BGLAP	Bone Gamma-Carboxyglutamate Protein
BMP	Bone Morphogenetic Protein
CDH5	Cadherin 5 (also known as Ve-Cadherin)
CREB	Cyclic Adenosine 3,5-Monophosphate Response Element-Binding Protein
DGCR8	DiGeorge syndrome critical region gene 8
DICER	Dcr-1 Homolog
DOX	Doxycycline
Drosha	Drosha Ribonuclease III
E	Embryonic day
EB	Embryoid body
EC	Endothelial cell
EGFL7	Epidermal Growth Factor-Like Protein 7
ERG	Ets-related gene
ERK1/2	Extracellular Signal-Regulated Kinase 1/2
ESC	Embryonic stem cell
ETS	E-26
etsrp	ets-related protein
ETV2	Ets Variant Gene 2 (also known as ER71)
FACS	Fluorescence-activated cell sorter
FDR	False discovery rate
FGF8	Fibroblast Growth Factor 8
FLI1	Friend leukemia integration 1
FLK1	Fetal Liver Kinase 1 (also known as KDR or VEGFR2)
FLT4	Fms Related Tyrosine Kinase 4 (also known as VEGFR3)
FOS	Fos Proto-Oncogene
FOXC2	Forkhead Box C2
GATA	GATA binding protein
GO	Gene Ontology
HAND2	Heart And Neural Crest Derivatives Expressed 2
ISLET1	Insulin gene enhancer binding protein-1
JUN	Jun Proto-Oncogene
KEGG	Kyoto Encyclopedia of Genes and Genomes
LMO2	LIM Domain Only 2
MAPK	Mitogen-Activated Protein Kinase
MEF2C	Myocyte Enhancer Factor 2C
MEK1	MAPK/ERK Kinase (also known as MAPKK1or MKK1)
MESP1	Mesoderm Posterior Basic Helix-Loop-Helix Transcription Factor 1
miR	micro RNA
MYOD	Myogenic Differentiation
NEUROD	Neuronal Differentiation
NKX2-5	Nk2 homeobox 5

NRP	Neuropilin
OVOL2	Ovo Like Zinc Finger 2
PAX6	Paired Box 6
PDGFRα	Platelet-derived growth factor receptor α
PIK3R2	Phosphoinositide-3-Kinase Regulatory Subunit 2
Pre-miRNA	Premature miRNA
Pri-miRNA	Primary miRNA
RGS5	Regulator of G Protein Signaling 5
RHOJ	Ras Homolog Family Member J
RISC	RNA-induced silencing complex
RUNX2	Runt related transcription factor 2
SCL	Stem cell leukemia (also known as TAL1)
SOX	Sry-related high mobility group box
SPRED	Sprouty-Related, EVH1 Domain-Containing Protein
T	T-Box Transcription Factor T
TEL1	ETS-related protein Tel1
TIE2	Tyrosine Kinase With Ig And EGF Homology Domains-2
VEGF	Vascular Endothelial Growth Factor

CHAPTER I

Introduction

An Overview on ETV2 in hematopoietic and endothelial cell development

In consonant with a close proximity in anatomy, coordinated development of the circulatory system including vessels, blood and the heart is prerequisite for securing successful embryogenesis. In developing embryos, the growth of the circulatory system is identifiable first and abnormalities in the establishment of the system frequently cause embryonic lethality. As early as embryonic day (E) 7.5 in mice, the first structure with the signature of endothelial and hematopoietic cells is the blood islands of the extraembryonic yolk sac (Haar and Ackerman, 1971). Shortly after, the blood islands, which have erythrocytes inside the lumen circled by a layer of endothelial cells, fuse together to create primitive forms of vessels (i.e., primary plexus), which then undergo a remodeling process, generating the complex vascular network interwoven by small capillary vessels and large vessels. On the other hand, angioblasts (also known as endothelial precursor cells) initiate the formation of the vascular structures in the embryonic proper such as dorsal aorta, cardinal veins, vitelline vessels (Drake and Fleming, 2000; Flamme et al., 1997; Patan, 2004). The more elaborated vasculatures are further completed through vascular reshaping, recruitment of perivascular cells and deposition of the extracellular matrix (Carmeliet and Jain, 2011; Jain, 2003). While the blood cells that first appear in the yolk sacs are mainly erythrocytes and macrophages in the blood islands (Choi, 2002; Palis et al., 1999), hematopoietic stem cells, which can supply all types of blood cells throughout the adult life, are detected in the specialized region of the dorsal aorta (Bertrand et al., 2010; Boisset et al., 2010; Kissa and Herbomel, 2010; Zovein et al., 2008) and sequentially populate the fetal liver, spleen and bone marrow.

Transcriptional factors have been implicated in a myriad of biological processes including embryogenesis, tumor, and cell proliferation. Among are the E26 transforming sequence or E-twenty-six specific sequence (ETS) transcription factors, which are categorized by the presence of the ETS DNA binding domain (Hollenhorst et al., 2004; Hollenhorst et al., 2011). Extensive studies have revealed important functions of the ETS factors in endothelial and hematopoietic cell development (Bartel et al., 2000; Ciau-Uitz et al., 2013; Dejana et al., 2007a; Findlay et al., 2013; Randi et al., 2009). For example, compound knockouts of *Ets1* and *Ets2* show abnormal endothelial cell branching (Wei et al., 2009). While *Fli1* null mouse embryos develop vascular leakage due to enhanced endothelial cell death (Hart et al., 2000; Spyropoulos et al., 2000), the lack of *Tel1* in mice leads to defective vascular remodeling in the yolk sac and is accompanied by considerable apoptosis (Wang et al., 1997). However, emergence of the vascular structures is not blocked by the absence of these ETS factors and the inactivation of *Ets1* does not cause vascular defects (Barton et al., 1998). This fact suggests the redundant functions of the ETS factors for at least some members in vessel development (Craig et al., 2015; Pham et al., 2007; Wei et al., 2009). In contrast, recent studies have discovered the non-redundant and indispensable role of one of the ETS factors, ETV2 in vessel as well as blood cell development (Ferdous et al., 2009b; Kataoka et al., 2011a; Lee et al., 2008b).

ETV2 is essential for vascular endothelial and hematopoietic cell development.

ETV2 has drawn a great deal of attention as an important regulator for embryonic vessel and blood cell development. Structurally, ETV2 shares a conserved ETS DNA binding domain with other ETS factors but does not exhibit any similarities outside this domain (Brown and McKnight, 1992; De Haro and Janknecht, 2002, 2005). Although identified as

a testis specific protein in adults (Brown and McKnight, 1992; De Haro and Janknecht, 2005), accumulative data show that ETV2 is expressed in early mouse embryos. Its expression is first recognizable in mesodermal progenitors, which can generate cardiovascular lineages between E7.0 and E7.5 (Ferdous et al., 2009b; Kataoka et al., 2011a; Lee et al., 2008b; Rasmussen et al., 2011). At later stages, ETV2 is detected in specific vasculatures including the dorsal aorta, endocardium and cardinal vein. From E11.5 and onwards, the ETV2 message becomes extinct (Ferdous et al., 2009b; Kataoka et al., 2011a; Lee et al., 2008b; Rasmussen et al., 2011). The importance of ETV2 in embryogenesis was revealed by a series of seminal findings from three independent groups. In 2005, Lin and fellow colleagues (Sumanas et al., 2005) reported that *etsrp,* the *zebrafish* homologue to mammalian ETV2, is one of the significantly downregulated genes in the *zebrafish cloche* mutant, which displays defects in both vessel and blood cell development (Stainier et al., 1995), compared to controls. Subsequently, the same group demonstrated the vasculogenic function of etsrp in zebrafish (Sumanas and Lin, 2006). In agreement with its endothelial specific expression, *etsrp* morpholino led to a significant impairment of vessel formation, whereas overexpression of *etsrp* resulted in an enhanced generation of embryonic vasculature. Rescuing the vascular defects in the *cloche* mutants upon overexpression of *etsrp* indicates that etsrp functions downstream of the cloche when generating embryonic vasculatures. In mice, we, for the first time, revealed an indispensable function of ETV2 in the development of vessels and blood cells (Lee et al., 2008b). Complete absence of both vascular structures and hematopoietic cells in *Etv2* deficient mice embryos leads to embryonic lethality between E9.5 and E10.5. Mechanistically, ETV2 directly binds promoters or enhancers of genes that are critical for

endothelial and hematopoietic cell lineages. Similar findings were reported by two groups as the two generated Etv2 gene trap mice and ETV2-knockin mice, respectively (Ferdous et al., 2009b; Kataoka et al., 2011a). With the addition of the finding that *Xenopus er71* has a potent vasculogenic function (Neuhaus et al., 2010a), it is clear that ETV2 is indispensable in vessel and blood cell development.

Molecular mechanisms of ETV2 in regulating cardiovascular development.

The very first clue as to how ETV2 regulates cardiovascular cell lineage development was reported by our group and showed that ETV2 directly binds to the ETS consensus sequence (GGAA/T) (Hollenhorst et al., 2004; Hollenhorst et al., 2011) in the promoter of the *Flk1* gene, leading to the induction of the gene expression (Lee et al., 2008b). In this study, it was also shown that overexpression of ETV2 can generate $FLK1^{+}$ mesoderm as well as endothelial and hematopoietic cells in differentiating ESCs in a serum-free condition. In subsequent studies, *Sox7, Lmo2*, *Tie2*, *Nfac1*, were identified as direct targets of ETV2 (Behrens et al., 2014; Koyano-Nakagawa et al., 2012; Lee et al., 2011; Palencia-Desai et al., 2011). Rather than performing Chromatin Immunoprecipitation (ChIP) assay on the targeted ones, a recent study (Liu et al., 2015) performed a ChIP-sequencing analysis to reveal the direct downstream target genes of ETV2 at a genome wide analysis level and found that ETV2 can not only bind to promoters or enhancers of already known target genes including *Flk1 and Cdh5* but also other genes that perform critical roles in vascular endothelial and hematopoietic cells. Among these genes are *Scl, Gata2, Meis1, Dll4, Notch1, Nrp1/2, Flt4, Fli1, RhoJ, Mapk*. Thus, these results strongly

indicate that ETV2 regulates the endothelial and hematopoietic programs in early stage embryos through direct binding to the ETS elements present in the aforementioned genes.

One of the major outstanding questions would be the mechanisms, which regulates the expression of ETV2. In the first report conducted by our group, treatment of inhibitors of BMP (noggin), NOTCH (DAPT) and WNT (DKK1) led to a significant decrease in the expression of *Etv2* and the generation of $FLK1^{+}$ mesoderm (Lee et al., 2008b). The reduced genesis of the $FLK1^{+}$ mesoderm in the presence of the inhibitors was reversed upon the overexpression of *Etv2*, suggesting that ETV2 functions downstream of these signaling pathways. In addition, several studies reported the transcriptional regulation of ETV2. Ferdous et al (2009) reported that the upstream region of the *Etv2* promoter can be bound by NKX2-5, a key transcription factor for heart development (Lyons et al., 1995; Tanaka et al., 1999), positing NKX2-5 as an direct upstream factor of *Etv2* in the generation of endocardium in the heart (Ferdous et al., 2009b). However, no defects were observed in endothelial cell development in *Nkx2-5* deficient mouse embryos and the failure of increasing endothelial genes upon overexpression of *Nkx2-5* in differentiating mouse ESCs (Caprioli et al., 2011; Lyons et al., 1995; Tanaka et al., 1999). Indeed, overexpression of *nkx2-5* in *zebrafish* significantly decreases the expression of *etsrp* with concomitant upregulation of cardiac genes (Simoes et al., 2011), suggesting that endothelial expression of ETV2 is NKX2-5 independent. In addition to the role of FOXC2 as an ETV2 interacting protein, it was reported that Fox proteins could function upstream of *etsrp* when generating endothelial and hematopoietic cells in *zebrafish* (Veldman and Lin, 2012). In this study, the authors found enhancers that drove the endothelial expression of *etsrp*. While one of the enhancers of *etsrp* was occupied by foxc1a/fox1b,

the expression of *etsrp* was significantly reduced by *foxc1a/fox1b* morpholino. Given the finding that FOXC2 can interact with ETV2 to modulate the expression of vascular endothelial and hematopoietic genes (De Val et al., 2008b), these results suggest the critical function of FOXC protein in ETV2-mediated cardiovascular development. Through the use of the mouse ESC differentiation system and mouse genetics, it was shown that Mesoderm posterior 1 (MESP1) and CREB (CRE binding protein) play important roles in *Etv2* transactivation (Shi et al., 2015; Yamamizu et al., 2012). *Etv2* expression can be activated by cAMP/PKA/CREB signaling in differentiating mouse ESCs (Yamamizu et al., 2012). In this study, the authors showed that CREB can directly bind to the CRE binding elements in *Etv2* upstream regions. Blocking ETV2 expression using siRNA leads to the reduction of PKA/CREB-mediated induction of endothelial and hematopoietic cell lineages. In accordance to this, a recent study reported (Shi et al., 2015) that Mesp1 can activate the expression of *Etv2* through binding to the CRE element. This transactivation appears to be CREB-dependent as shown by the abrogated *Etv2* promoter activity upon co-transfection of MESP1 and dominant negative form of CREB. Interestingly, the study found that the majority of $ETV2^{+}$ cells originate from $MESP1^{+}$ cells and that the deficiency of *Etv2* in $MESP1^{+}$ cells causes embryonic lethality that leads to defects in vascular and blood cell generation, which is reminiscent of *Etv2* knockout mice. This supports the linear correlation between MESP1 and ETV2 in vascular endothelial and hematopoietic cell development. However, given that the overexpression of *Mesp1* can promote the generation of cardiac lineage cells with suppression of hematopoiesis (Bondue et al., 2008; Lindsley et al., 2008), this appears contradictory to the results. Nonetheless, these studies clearly indicate that the transcription factors involved in early mesoderm

development as well as cardiovascular generation and maturation play an important role in the regulation of ETV2 expression. Not only mapping sequential order of the transcription factors and identifying additional factors required for ETV2 expression, but it would also be interesting to study how these transcription factors cross talk with the aforesaid signaling pathways in governing ETV2 expression.

Interplay between ETV2 and other ETS factors in establishing cardiovascular system

As discussed, there are more than 20 ETS factors found in mammals and some of them play significant roles in vascular system development and function (Findlay et al., 2013; Meadows et al., 2011; Randi et al., 2009). Having confirmed the transient but potent vasculogenic activity of ETV2 in early mouse embryos (i.e. its expression is not detectable beyond E11.5) (Ferdous et al., 2009b; Kataoka et al., 2011a; Lee et al., 2008b), many have been puzzled by how the vasculatures develop and are maintained throughout embryogenesis. In this regard, two groups have demonstrated a positive feedback loop mechanism between ETV2 and other ETS factors, at least Fli1 (Abedin et al., 2014; Liu et al., 2015). In 2014, Abedin et al., showed using *Fli1* knockout mice that while *Fli1* messages were significantly decreased in *Etv2* knockout mouse embryos, other ETS factors such as *Ets1/2, Elf1/2* and *Etv6* showed comparable levels of expression (Abedin et al., 2014). The expression of *Fli1* is directly upregulated by ETV2 as well as by FLI1 itself through the ETS binding sites on the *Fli1* promoter as demonstrated by the ChIP-PCR and luciferase-based promoter assays. Interestingly, that fact that FLI1 binds to its own promoter was observed at E11.5, which is the time in which the ETV2 expression

becomes extinct, but not at E9.5, which is when the ETV2 message is still abundant. Also, the ChIP-PCR analysis revealed *in vivo* occupancy of FLI1 on the promoters of *Tie2* and *Cdh5* at E11.5, but not at E9.5 embryos. Consistently, several key endothelial genes, such as *Tie2* and *Cdh5,* induced by ETV2 showed reduced levels of expression in *Fli1* deficient embryos as well as *Fli1* knockdown primary endothelial cells. These results suggest that the function of FLI1 replaces the function of ETV2 at least partly for endothelial cell survival and vascular maintenance at the mid-gestation stage. Subsequently, Liu et al (2015) reported a similar feedback regulation mechanism between ETV2 and FLI1 (Liu et al., 2015). Performing genome wide analysis with ChIP-sequencing comprehensively revealed direct targets of ETV2, which can be classified into VEGF signaling/endothelial lineage specification genes, NOTCH/MAPK signaling and RHO GTPase. The ETS factors such as *Fli1*, *Ets1/2, Erg* and notably *Etv2* itself were identified as potential targets of ETV2 in differentiating mESCs. In agreement with the results, overexpression of *Etv2* led to the immediate induction of *Fli1*, suggesting that *Fli1* is a direct downstream target of ETV2. Indeed, the ChIP-PCR experiment showed *in vivo* occupancy of ETV2 on *Fli1* genomic DNA. The findings that *Fli1* null embryos and mouse ESCs showed comparable levels of expression of *Etv2* compared to wild type controls but overexpression of *Fli1* in mouse ESCs did not induce *Etv2* message further support the argument (Liu et al., 2015). Similar to the findings discussed above (Abedin et al., 2014), key endothelial and hematopoietic genes such as *Tie2*, *Cdh5, Lmo2* and *Scl*, which are the direct targets of ETV2, can also be directly regulated by *Fli1* when ETV2 expression is not detected in differentiating ESCs. Given that ETV2 can activate its own promoter, these results suggest the following model; ETV2 triggers a genetic program for

endothelial and hematopoietic lineage development through its transcriptional activation function (i.e. positive autoregulation and transactivation of target genes). Once the endothelial cells and hematopoietic cells are generated when the ETV2 expression is silent, other ETS factors, especially FLI1 induced by ETV2 ensure further establishment and maintenance of the vessel and blood systems. Thus, molecular and biochemical studies that uncover the functional significance of other ETS factors in the context of FLI1 in generating vessel and blood cells would be worthy areas to pursue.

Cardiovascular cell fate determining role of ETV2

The first emerging FLK1^{+} mesoderm in developing mouse embryos have the potential to differentiate into vascular endothelial, hematopoietic, muscle cell lineages including cardiomyocyte and smooth muscle cells(Chung et al., 2002; Ema et al., 2003; Ema et al., 2006; Faloon et al., 2000; Motoike et al., 2003; Yamashita et al., 2000), suggesting that FLK1^{+} mesoderm functions as a multipotent progenitor in cardiovascular cell lineages. A series of studies showed that FLK1^{+} mesoderm can be subdivided into two distinct cell populations; FLK1^{+}PDGFRα^{+} (platelet-derived growth factor receptor α) with cardiogenic potential and FLK1^{+}PDGFRα^{-} cells with endothelial and hematopoietic potential (Hirata et al., 2007; Liu et al., 2012b; Sakurai et al., 2006). However, mechanisms that determine the cell fate of FLK1^{+} mesoderm into the cell population remain to be elucidated. Given the role of transcription factors in determining cell identity (Frum and Ralston, 2015; Hatakeyama and Kageyama, 2004; Iwafuchi-Doi and Zaret, 2014; Park et al., 2013; Weintraub et al., 1991), it is plausible that ETV2 regulates the multipotency of the FLK1^{+} mesoderm. Indeed, the lack of *Etv2* in mice and mouse ESCs leads to the failure to

generate FLK1^{+}PDGFRα^{-} cells (we refer this hemoangiogenic FLK1^{+} cells) with concomitant augmentation of FLK1^{+}PDGFRα^{+} cells (we refer this cardiogenic FLK1^{+} cells) (Liu et al., 2012c; Liu et al., 2015). Also, reduced expression of genes of vascular endothelial and blood cells and augmentation of cardiac genes were observed in *Etv2* knockout embryos (Lee et al., 2008b). Inversely, the overexpression of *Etv2* in differentiating mouse ESCs leads to a significant increment of hemoangiogenic FLK1^{+} cells at the expense of cardiogenic FLK1^{+} cells. The capability of ETV2 to induce hemoangiogenic potential is further strengthened when GATA2 and SCL are co-expressed (Liu et al., 2013). Additional supporting results in this field have been reported from studies in *zebrafish*. In 2007, Schoenebeck et al., showed that the overexpression of *etsrp* together with *scl* leads to the expansion of hematopoietic and endothelial cell area with a reduction in the cardiac field as well as heart size (Schoenebeck et al., 2007). The observed phenotype was reversed upon injection of *etsrp* and *scl* morpholino in *zebrafish* embryos. A similar finding was reported by the knockdown of *etsrp* alone in *zebrafish* embryos (Palencia-Desai et al., 2011). In this study, the authors further showed using etsrp-gfp cells that etsrp^{+} cells are deficient in *etsrp* fated to cardiogenic cell lineages. These results suggest that ETV2 functions as an essential cell fate determinant between hemoangiogenic and cardiogenic mesoderm. Likewise, transcriptional regulation of such antagonistic relationships between hemoangiogenic and cardiogenic cell lineage specification is evident in other studies as well. Injection of *nkx2-5* into zebrafish embryos reduced the expression of endothelial and blood cell markers such as *etsrp, scl* and *pu.1,* but significantly expanded the hand2^{+} cardiac boundary (Simoes et al., 2011). When *Mesp1*, another key cardiogenic transcription factor in differentiating

mESCs, *was* overexpressed, the antagonistic developmental outcomes have also been reported (Bondue et al., 2008; Lindsley et al., 2008).

Further insight as to how ETV2 regulates the cell fate of $FLK1^+$ mesoderm was suggested by Liu et al. (2012) as the study reported the first evidence of the role of ETV2 and WNT-β-catenin signaling in this process (Liu et al., 2012b). The authors found reduced expression of genes involved in WNT-β-CATENINE signaling with decreased cardiomyocyte generation when *Etv2* was overexpressed in differentiating ESCs. In sharp contrast, overexpressing *β-catenin* reversed the ETV2-induced hemoangiogenic cell lineage generation. However, the proposed mechanism was not consonant with the knockout mice study in which deficiency of *β-catenin* in $FLK1^+$ mesoderm resulted in no obvious phenotypic defects in heart formation (Stenman et al., 2008). Therefore, further investigation to explain the molecular mechanism of ETV2 in determining the cell fate of $FLK1^+$ mesoderm is required.

A

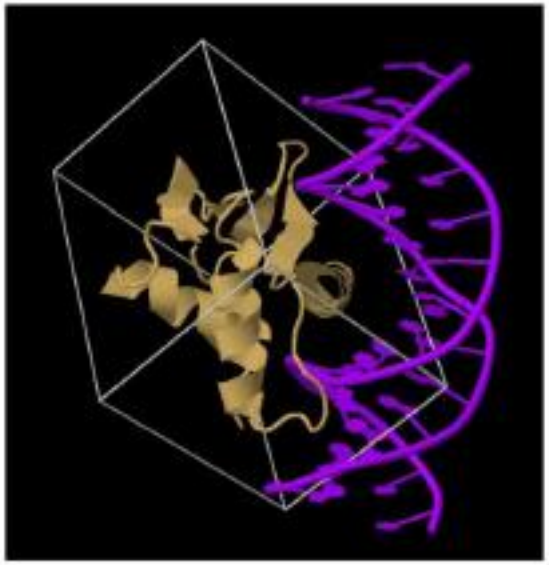

B

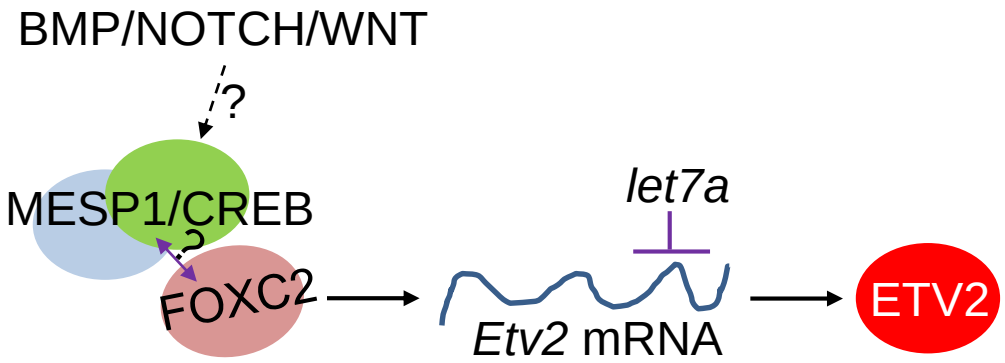

Figure 1

Figure legends

Figure 1. Regulation of the expression and function of ETV2.

(A) A schematic structural diagram of the complex of the ETS domain of PU.1 in gold and DNA in purple (deposited on The RCSB PDB www.rcsb.org; DOI: 10.2210/pdb1pue/pdb) (Berman et al., 2000; Kodandapani et al., 1996). (B) In early embryos or differentiating mouse ES cells, BMP/NOTCH/WNT pathways act upstream of ETV2 expression. During this process, transcriptional activation of *Etv2* is induced by at least MESP1, CREB and FOXC2. let7a functions to inhibit ETV2 protein synthesis. It is of note that the relationship between BMP/NOTCH/WNT pathways to MESP, CREB and FOXC2 is not known. Also, whether the three transcription factors interact each other in regulating *Etv2* gene expression remain elucidated.

CHAPTER II

OVOL2 is a critical regulator of ER71 in generating FLK1^{+} cells, hematopoietic and endothelial cells from embryonic stem cells

This has been published in Blood (2014) 124:2948-2952. PMCID:PMC4224193

OVOL2 is a critical regulator of ER71 in generating FLK1^{+} cells, hematopoietic and endothelial cells from embryonic stem cells

Running title: OVOL2 as a novel ER71-interacting protein

Ju Young Kim,[1,2,8] Ra Ham Lee,[3,8] Tae Min Kim,[2,8] Dong-Wook Kim,[3,9] Young-Joo Jeon,[3] Sung-Ho Huh,[4] Se-Yeong Oh,[1] Michael Kyba,[5] Hiroshi Kataoka,[6] Kyunghee Choi,[7] David M. Ornitz,[4] Jung-IL Chae,[3] and Changwon Park[1,2]

[1]Department of Pediatrics, Center for Cardiovascular Biology, Emory University School of Medicine, GA, USA, [2]Department of Pharmacology, College of Medicine, University of Illinois, IL, USA, [3]Department of Oral Pharmacology, School of Dentistry, Brain Korea 21 Project, Chonbuk National University, Jeonju, Republic of Korea, [4]Department of Developmental Biology, [7]Department of Pathology and Immunology, Washington University School of Medicine, Saint Louis, MO, USA, [5]Department of Medicine, Medical School, University of Minnesota, Minneapolis, Minnesota, USA, [6]Laboratory for Stem Cell Biology, RIKEN Center for Developmental Biology, 2-2-3 Minatojima-Minamimachi, Chuo-ku, Kobe, Japan,

[8]These authors equally contributed to this work.

Correspondence: Jung-IL Chae, jichae@jbnu.ac.kr, Phone:82-63-270-4024,
664, 1Ga DeokJin, Jeonju 561-756, Republic of Korea, or
Changwon Park, cpark23@emory.edu, Phone:404-727-7143, Fax: 404-727-5737
2015 Uppergate Dr. #208b, Atlanta, GA 30322, USA

[9]Current Address: Department of Microbiology, Immunology, and Cancer Biology, School of Medicine, University of Virginia, Charlottesville, USA

Article components: 120 words (abstract), 1500 words (text), 2 figures, and 25 references.

Key points

1. OVOL2 is identified as a novel binding protein of ER71.
2. Interaction between ER71 and OVOL2 cooperatively regulates the generation of FLK1^{+} mesoderm and endothelial and erythroid cells.

Abstract

We here report that OVOL2, a C_2H_2 zinc finger protein, is a novel binding protein of ER71 which is a critical transcription factor for blood and vessel development. OVOL2 directly interacted with ER71, but not with ETS1 or ETS2, in the nucleus. ER71-mediated activation of the *Flk1* promoter was further enhanced by OVOL2, although OVOL2 alone failed to activate it. Consistently, co-expression of ER71 and OVOL2 in differentiating embryonic stem cells (ESCs) led to a significant augmentation of $FLK1^+$, endothelial and hematopoietic cells. Such cooperative effects were impaired by the shRNA-mediated inhibition of *Ovol2*. Collectively, we show that ER71 directly interacts with OVOL2 and that such interaction is critical for $FLK1^+$ cell generation and their differentiation into downstream cell lineages.

Introduction

It is widely accepted that blood cells are generated from two distinct cell populations during embryogenesis; hemangioblast and hemogenic endothelium (Hirschi, 2012; Park et al., 2005). The blood islands in the extraembryonic yolk sac as early as embryonic day (E) 7.5 is the first site of hematopoiesis. Both blood and endothelial cells in the blood islands are generated from the hemangioblast. On the other hand, the hemogenic endothelium, a specialized endothelial cell population within the aorta-gonad-mesonephros, generates hematopoietic stem cells which can populate hematopoietic organs including bone marrow. Despite the unsettled controversy regarding the hemangioblast and the hemogenic endothelium, it is evident that the generation of FLK1(VEGFR2)$^{+}$ cells in the developing embryos is an essential step for both hematopoiesis and vessel development (Carmeliet et al., 1996; Shalaby et al., 1995). In this regard, we and others have demonstrated that *Er71*/*Etv2*, a member of the ETS transcription factor family, is indispensable for specification of mesodermal precursors into endothelial and hematopoietic lineages during mouse embryogenesis (Ferdous et al., 2009a; Kataoka et al., 2011b; Lee et al., 2008a; Liu et al., 2012a). ER71 activates genes critical for both hematopoiesis and vessel development including *Flk1*, *VECadherin*, *Scl* and *Lmo2* through direct binding to gene-associated promoters/enhancers (De Val et al., 2008a; Koyano-Nakagawa et al., 2012; Lee et al., 2008a; Liu et al., 2012a). Studies in zebrafish and Xenopus also reported *er71*'s potent function (Neuhaus et al., 2010b; Sumanas and Lin, 2006), indicating an evolutionally conserved and essential role for ER71 in the establishment of the cardiovascular system.

The specificity and function of the majority of ETS-domain transcription factors are dependent upon their interacting proteins (De Haro and Janknecht, 2005; Dejana et al., 2007b; Sharrocks, 2001a). However, very few studies have examined the role of ER71 interacting proteins (Knebel et al., 2006). Here, we show that ER71 interacts with OVOL2, a C_2H_2 ZF transcription factor essential for early embryogenesis (Unezaki et al., 2007), and that this interaction plays an important role in the generation of $FLK1^+$ as well as endothelial and erythroid cells.

Methods

Plasmid vector construction

The PCR products of ER71, ETS1 or ETS2 were cloned into modified pcDNA6-HA-MYC-HIS eukaryotic expression vector (ER71-MYC, ETS1-MYC, ETS2-MYC). For purification of GST fusion proteins of ER71, PCR products corresponding to full-length ER71 cDNA were cloned into pGEX-4T1 vector (GST-ER71). The full-length of wild type (isoform A) of OVOL2 was cloned into the modified pcDNA6-HA-MYC-HIS vector (HA-OVOL2-wt). To generate OVOL2 deletion mutants, PCR products of each mutant were cloned into pcDNA6-HA-MYC-HIS vector.

ESC culture and flow cytometry

ESC culture, in vitro differentiation and flow cytometry were conducted as previously described.(Lee et al., 2008a; Park et al., 2004) For flow cytometry, all primary and secondary antibodies were purchased from eBioscience; FLK1 (AVAS12), PE-CD31 (MEC 13.3), biotin-VE-Cadherin (eBioBV13), SA/APC (0.5 g/ml; eBioscience). Data were

acquired by CyAN ADP analyzer, and analyzed by Summit Software v4.0 (Beckman Coulter).

Generation of inducible ES cells

Full-length cDNA of FLAG-ER71, HA-OVOL2, or bicistronic FLAG-ER71-P2A-HA-OVOL2 sequences in p2lox, respectively, were inserted into the tet-responsive locus of A2Lox ESCs by nucleofection (Lonza) as previously described (Iacovino et al., 2009; Kim et al., 2011). The positive clones were selected with G418 for two weeks, and individually expanded and then the correct targeting event was confirmed by a tet-responsive locus/cDNA vector-specific PCR. To verify protein expression, each iESCs were differentiated in serum condition without DOX for 48 hrs followed by culture in the presence or absence of DOX (±DOX) for additional 2 days. After being lysed with RIPA buffer, lysates were then electrophoresed on a 12% SDS PAGE and transferred to a nitrocellulose membrane (Bio-Rad). The membrane was then probed with mouse anti-FLAG M2 antibody (Sigma-Aldrich) or goat anti-HA antibody (Roche), followed by being incubated with HRP-conjugated anti-mouse or anti-goat IgG (Santa Cruz Biotechnology). For loading control, goat anti-α-tubulin antibody (Cell Signaling) was used.

GST-pull down assay

Control GST or GST-ER71 were expressed in BL-21 (Agilent Technologies), and purified by binding with GSH-agarose (Sigma-Aldrich) followed by being washed for four times with washing buffer (20 mM Tris, 120 mM NaCl, 5 mM EDTA, 5 mM EGTA, 1% NP40) containing proteinase inhibitor cocktail (Roche). For pull-down, purified GST or GST-

ER71 was incubated overnight with 1 milligram of whole cell lysate of D3.5 EBs, and washed six times using washing buffer. The resulting beads were then subjected to LC/MS analysis. For Western blot analysis, GST- or GST-ER71-bound proteins were electrophoresed on a 12% SDS polyacrylamide gel and transferred to a nitrocellulose membrane (Bio-Rad). The membrane was probed with rabbit anti-OVOL2 antibody(1:1,000; Abcam), followed by being incubated with HRP-conjugated anti-rabbit antibody (Santa Cruz Biotechnology).

In-solution tryptic digestion

The bound proteins were eluted from Glutathione Sepharose beads (GE Healthcare) with 200 μl of rehydration solution (7 M urea, 2 M thiourea, 4% CHAPS). The eluted solution was applied in 800μl of 50mM ammonium bicarbonate. The protein solution was reduced by final DTT concentration of 5 mM and then incubated with 14 mM of iodoacetamide for alkylation of the reduced proteins. Excess iodoacetamide was quenched by adding DTT, to provide final concentration of 7mM. The reduced and alkylated proteins were digested by treatment of trypsin (the content of 2% (w/w)) at 37°C overnight. This reaction was terminated by adding 2% formic acid. The tryptic peptides were dried in speed-vac.

Desalting of tryptic peptide

Tryptic peptides were desalted using Sep-Pak C18 cartridge (Waters) prior to MS analysis according to manufactured protocol. Briefly, the cartridge was washed with 100% acetonitrile and equilibrated with 0.1% formic acid. The tryptic peptides dissolved in 0.5% formic acid were loaded and bound in the cartridge. Bound peptides were washed with

0.1% formic acid and 5% MeOH, which in turn were eluted with 70% acetonitrile. The eluted tryptic peptides were dried in speed-vac, and stored at -80°C.

Mass spectrometer configuration

Mass spectrometry analysis of tryptic peptides was performed using a Waters SynaptTM HDMS. The mass spectrometer was operated in V-mode for all measurements. All analyses were performed using a positive mode Nano ESI with a NanoSpray source. The lock mass channel was sampled every 30 seconds. The mass spectrometer was calibrated using a [Glu1] fibrinopeptide solution (400 fmol/µl) delivered through the reference sprayer of the NanoLockSpray source. Accurate mass LCMS data was collected via Data Dependent Acquisition (DDA) mode of acquisition.

Data processing and protein identification

Continuum LC-MS/MS data were processed and used in database searches using the Protein Lynx Global Server (PLGS), version 2.3 (Waters). The data were automatically smoothed, background-subtracted, centered and deisotoped. In addition, the charge state was reduced and masses were corrected based on reference scans. Ion detection, clustering and normalization were performed using PLGS. Processed data were used to search the IPI human database (Liu et al., 2004; Wang et al., 2005a). Processed ions were sequenced and mapped against the IPI human database using the PLGS and MASCOT DAEMON programs (http://www.matrixscience.com). The PLGS search parameters were defined by the software, with systematic settings used. Peptides were

restricted to trypsin fragments with a maximum of one missed cleavage and cysteine carbamidomethylation.

In vitro transcription and translation reactions

For synthesis of ^{35}S-labeled ER71, OVOL2 wild type (isoform A), or OVOL2 deletion mutant proteins, each protein was generated using a coupled transcription and translation (TNT) system (Promega) from eukaryotic constructs (pcDNA6-ER71-MYC-HIS, pcDNA6-HA-OVOL2, or pcDNA6-HA-OVOL2 deletion mutants). Briefly, 1 μg of DNA and 2 μl of ^{35}S-methionine (>1,000Ci/mmol, Perkin Elmer) were added directly to methionine absence rabbit reticulocyte lysates, and then incubated for 2 hrs at 30°C for radiolabeled proteins synthesis.

Peptide competition assay

For peptides competition assays, 100 pmole of glutathione-Sepharose beads bound GST-ER71 were incubated in 1 ml of pull-down reaction buffer (50 mM Tris-HCl, pH 7.6, 150 mM NaCl, 0.1% Triton X-100) containing 20 nmole (200-fold molar excess of GST-ER71) of the synthesized peptides corresponding to each zinc finger domain sequences of OVOL2 for 3 hrs followed by the addition of radiolabeled in vitro transcription and translation mixture of each OVOL2 mutant for a further 6 hrs at 4°C. And then glutathione-Sepharose beads were centrifuged and washed six times with washing buffer (50 mM Tris-HCl, pH 7.6, 300 mM NaCl, 0.5% Triton X-100). After washing, beads bound proteins were dissociated by boiling in SDS loading buffer and separated on 12% SDS polyacrylamide gel. The radioactive signals were visualized by autoradiography (Thypoon,

GE). The peptide sequences are as follows: Zn1;NCDLCGKSFRLQRMLNRHLKCHN, Zn2; LCTFCGKGFNDTFDLKRHVRTHT, Zn3; KCEVCNKAFTQRCSLESHLKKIHG, Zn4; VCEDCGYTGPTQEDLYLHVNSDHP (Peptron).

Co-immunoprecipitation assay

Plasmids encoding ER71-MYC, ETS1-MYC, ETS2-MYC, HA-OVOL2 were transfected into 293T cells. After 48 hours, cells were lysed using NP40 lysis buffer and the resulting cell lysate (500 μg each) were incubated in IP buffer (20mM Tris-HCl, pH 8.0, 137 mM NaCl, 10 % glycerol, 1% IGEPAL, 2 mM EDTA, pH 8.0) with 10 μg of anti-MYC or anti–HA antibodies (Santa Cruz Biotechnology) overnight at 4°C. Then, 30 μl (50% suspension) of protein A/G agarose beads (GenDEPOT) were added and incubated for 4 hrs at 4°C. The antibody-beads complex were then washed three times with IP buffer and analyzed by immunoblotting with anti-MYC or anti-HA antibodies.

FACS sorting of ER71-VENUS embryonic cells

E8.5 ER71-VENUS mice embryos were obtained from timed mating between ER71-VENUS mice (Kataoka et al., 2011b) and C57/BL6. Both yolk sac and embryo proper was digested with 0.1% collagenase for thirty minutes, and $VENUS^{+}$ and $VENUS^{-}$ cells were sorted using a MoFlo high-speed flow cytometer (Dako Cytomation).

Hematopoietic replating assay

Hematopoietic colonies were generated as described previously (Lee et al., 2008a; Park et al., 2004). Briefly, EBs differentiated for 6 days in serum-free condition were

dissociated and replated in MethoCult GF (Stemcell Technologies). The number of colonies was counted after 4 days.

Luciferase assay

The 293T cells (1.5 x 10^5/well/12-well plate) were incubated overnight. Next day, the cells were transfected with 1.5 μg of ER71 or OVOL2 expression plasmids (pIRES2-ER71-EGFP and pCDNA6-HA-OVOL2, respectively), 100 ng of pGL3-*Flk1*promoter, and 20 ng of pRL-null by $CaCl_2$ precipitation. After 48 hours, the luciferase activity was measured using the Dual luciferase reporter system (Promega) according to the product instructions. Firefly luciferase values were normalized with Renilla luciferase values.

Immunohistochemistry

Embryos were fixed with 4% paraformaldehyde for 1 hr and washed with PBS. Samples were soaked in 30% sucrose and embedded in OCT compound (Tissue-Tek). Samples were sectioned (8 μm) and stored at −80 °C for immunohistochemistry. Frozen sections were washed with PBS and blocked with 0.1% triton X-100 and 0.5% goat serum. Sections were incubated with primary antibodies (Goat anti-ER71, Santa Cruz Biotechnology and Rabbit anti-OVOL2, Abcam) in a humidified chamber overnight at 4 °C. Sections were then washed and incubated with secondary antibodies for 1 h at room temperature. Samples were washed, coverslipped with Vectashield Mounting Media (Vector lab), and photographed using a Zeiss LSM 700 confocal microscope.

Immunofluorescence assay

293T cells were seeded in cover glass containing 6-well culture dish and co-transfected with ER71-MYC and HA-OVOL2-wt. The transfected cells were then rinsed with phosphate-buffered saline (PBS) at 24 hr post-transfection and fixed with fixation and permeabilization buffer solution (BD Cytofix/CytopermTM, BD biosciences) according to manufacturer's protocol. After blocking with PBS containing 1 % BSA, cells were incubated with anti-MYC and anti-HA antibodies for 2 hrs at room temperature, followed by washing with PBS, and further incubated with Alexa Fluor® 488 dye conjugated anti-rabbit for anti-HA and Alexa Fluor® 546 dye conjugated anti-mouse IgG for anti-mouse (Invitrogen). Subsequently, cells were rinsed with PBS and nucleus was stained with DAPI. Cover glasses were then mounted with Fluorescent Mounting Medium (DaKo). Images were examined by confocal laser scanning microscopy (FluoView, Olympus). All confocal images were imported using the FV1000 Viewer software (Olympus).

RNA interference

Lentiviral plasmids of shRNAs against *Ovol2* (TRCN0000085914 and TRCN0000421364 for shRNA#1 and shRNA#2, respectively) and *GFP* (SHC004) were purchased from Sigma-Aldrich (MISSION® shRNA, Sigma-Aldrich). Viral particles were produced in 293T cells by co-transfecting pCMV-dR8.2 and pCMV-VSVG (Addgene plasmids #8455 and #8454, respectively).[8] After 48 hours, viral supernatant were harvested and concentrated with Lenti-X concentrator (Clontech) according to the manufacturer's instructions. ESCs were then infected with lentiviral particles in an MOI (multiplicity of infection) of 5 for 12 hrs in the presence of polybrene (4μg/ml, Sigma-Aldrich), and then subjected to in vitro differentiation for 3 days for FACS or qRT-PCR analysis.

Quantitative RT-PCR

RNA extraction and quantitative RT-PCR were performed as described (Park et al., 2004). RNAs were extracted by Trizol (Invitrogen) according to the manufacturers' instructions, and the resulting RNA was subjected to cDNA synthesis by using SuperScript III reverse transcriptase (Life Technologies). Primer sequences for qRT-PCR are available in supplemental Table S2 and the previous studies (Lee et al., 2008a; Park et al., 2004).

Statistical analysis

The results of luciferase assay, in vitro binding, peptide inhibition, qRT-PCR, FACS analysis, and hematopoietic replating assay were analyzed by Student *t* test. P value less than 0.05 was regarded significant.

Results

In this study we investigated whether ER71 could interact with other regulatory proteins to regulate $FLK1^+$ cell generation in mouse ESC differentiation. To this end, a GST-ER71 fusion protein was incubated with lysates prepared from day (D) 3-3.5 embryoid bodies (EBs), a time at point which the expression of ER71 reached its peak (Lee et al., 2008b). Pull-down fractions were then subjected to LC-MS/MS proteomic analysis. Among candidates, priority was given to OVOL2 (Figure 1A, supplemental Table 1), a member of the zinc finger (ZF) transcription factor family, because *Ovol2* deficient mouse embryos show several developmental defects including abnormal vessel formation (Mackay et al., 2006; Unezaki et al., 2007). Subsequent pull-down assays between GST-ER71 and EB cell lysates identified OVOL2 (Figure 1B). The interaction of ER71 and OVOL2 was

further validated by co-immunoprecipitation in 293T cells (Figure 1C, supplemental Figure 1). Interestingly, OVOL2 did not interact with ETS1 or ETS2 (Figure 1C), which have been reported to activate the *Flk1* promoter (Elvert et al., 2003; Kappel et al., 2000). This finding indicates that the binding of OVOL2 is specific to ER71. We also confirmed the co-localization of ER71 and OVOL2 in the nucleus of 293 T cells by immunostaining (Figure 1E, supplemental Figure 2). To further characterize the interaction between ER71 and OVOL2, a series of deletion mutant forms of OVOL2 (Figure 1A) were subjected to in vitro pull-down with the GST-ER71 fusion protein. As shown in Figure 1F-G, in vitro translated wild type OVOL2 (full-length, WT) were precipitated with GST-ER71, indicating direct interaction. Interestingly, OVOL2 mutants lacking ZF domains, especially Δ6 and Δ8, showed reduced binding to GST-ER71. The pull-down experiment with a GST protein control failed to precipitate OVOL2 (supplemental Figure 3). In agreement with these results, a binding inhibition assay showed that the peptides corresponding to each ZF domain of OVOL2 efficiently inhibited binding between ER71 and OVOL2 (Figure 1H-I). Collectively, these results suggest that ER71 can directly bind with OVOL2 partly through the ZF domains.

As reported previously (Lee et al., 2008a), the expression of *Er71* reached its peak at D3 followed by a sharp decrease in ESC differentiation, while that of *Ovol2* increased steadily up to D6 (Figure 2A). The *Flk1* message was detectable after the induction of *Ovol2* or *Er71.* Further, *Ovol2*, as well as *Flk1* message, was enriched in ER71-VENUS$^+$ cells and ER71-VENUS$^+$FLK1$^+$ from E8.5 mouse embryos, in which VENUS expression is controlled by the endogenous *Er71* locus (Figure 2B, supplemental Figure 4) (Kataoka et

al., 2011b). Taken together with the finding that ER71 and OVOL2 are co-expressed in the blood islands at E8.5 (Figure 2C), these results suggest a functional significance of ER71-OVOL2 interaction in regulating FLK1$^+$ cell generation and differentiation. To further test this, we performed a luciferase-based promoter assay and found that co-expression of OVOL2 and ER71 doubled the *Flk1* promoter activity compared to ER71 alone (Figure 2D). OVOL2 itself did not increase the transcriptional activity of the *Flk1* promoter used in this assay. Next, we generated doxycycline (DOX) inducible ESCs expressing: 1) FLAG-tagged ER71 (iER71), 2) HA-tagged OVOL2 (iOVOL2), 3) both FLAG-tagged ER71 and HA-tagged OVOL2 (iER71-P2A-OVOL2) (supplemental Figure 5) (Iacovino et al., 2009; Kim et al., 2011). We first confirmed the interaction between ER71 and OVOL2 in iER71-P2A-OVOL2 ESCs by co-immunoprecipitation (Figure 1D). Next, upon differentiation in a serum-free media (Lee et al., 2008a), overexpression of ER71 significantly induced the generation of FLK1$^+$ cells (Figure 2E). However, such de novo generation of FLK1$^+$ cells was not observed in iOVOL2, iETS1 or iETS2 (Figure 2E, supplemental Figure 6). Consistent with the analysis of the *Flk1* promoter (Figure 2D), the percentage of FLK1$^+$ cells was higher in iER71-P2A-OVOL2 than in iER71 (73.4 ± 3.35% v.s. 50.2 ± 4.08%, Figure 2E, E'). We also found such a cooperative effect under differentiation conditions in the presence of serum (Figure 2F, F'). Interestingly, we found that the levels of ER71 were increased in cells overexpressing OVOL2-HA, which may also contribute to such a cooperative effect (supplemental Figure 7). Intriguingly, OVOL2 induction alone did not stimulate the *Flk1* promoter nor did it generate FLK1$^+$ cells in a serum free differentiation condition (Figure 2E, E'), while in a serum condition, OVOL2 generated FLK1$^+$ cells to a level comparable to that induced by ER71 (Figure 2F,F'). This

indirectly suggests that OVOL2 might depend on other transcriptional regulators (e.g., ER71) present in a serum condition to generate FLK1^{+} cells. Consistent with this, *Er71* message was approximately 5 fold higher in serum compared to serum free differentiation conditions (supplemental Figure 8). In a subsequent study, we found that the generation of endothelial cells (CD31^{+}VECadherin^{+}) was increased by ER71-OVOL2 co-expression (11.3 ± 1.35%), compared to iER71 (6.1 ± 1.90%) or iOVOL2 ES cells (2.0 ± 1.69%) (Figure 2G, G'). Also, co-expression of ER71 and OVOL2 led to a further increase in the number of erythroid colonies, compared to iER71 or iOVOL2 (Figure 2H). qRT-PCR analysis (Figure 2I) showed that the expression level of the genes critical for endothelial cell development (*Flk1, VE-Cadherin, Cd31, Mef2c, Tie2)* (De Val et al., 2008a; Lee et al., 2008a) were significantly higher when ER71 and OVOL2 were co-induced, compared to cells induced with either ER71 or OVOL2. *Gata1*, a critical gene for erythropoiesis (Fujiwara et al., 1996), was also upregulated in iER71-P2A-OVOL2, compared to iER71 or OVOL2. In contrast, both *Islet1* and *Gata4*, critical genes for cardiac development (Bondue et al., 2011) were downregulated in iER71-P2A-OVOL2. *Pdgfrβ* and *Rgs5*, smooth muscle cell markers, were further reduced in iER71-P2A-OVOL2 cells. *MyoD*, *Myogenin*, skeletal muscle markers, *Runx2* and *Bglap*, osteteoblast markers, were not significantly changed in the three cell lines. While other germ layer markers such as *NeuroD and Pax6* (neuroectoderm) were similar or slightly enhanced upon co-expression of ER71 and OVOL2, *Hinf4, Sox17 and Sox7* (endoderm) were similar in iER71 and iER71-P2A-OVOL2 cells and were reduced in iOVOL2 cells. The expression of posterior primitive streak genes (*T*, *Fgf8*) were also not significantly changed in any of the cell lines (see below).

To further determine whether ER71-OVOL2 interaction is functional in FLK1$^+$ cell generation, we infected *Ovol2* lentiviral shRNA particles into iER71 cells and found that the FLK1$^+$ cells induced by ER71 were significantly decreased in *Ovol2* shRNAs-infected EBs compared with the *Gfp* shRNA-infected control (Figure 2J-K, supplemental Figure 9). Also, qRT-PCR analysis showed that *Ovol2* knockdown led to a greater reduction of expression of the genes known to be induced by ER71 (Figure 2L). Other markers representing non-hemo/endo mesoderm derivatives (*Isl1, Gata4, Pdgfrb, Rsg5, MyoD, Myogenin, Runx2, Bglap)* were slightly upregulated or not affected in *Ovol2* shRNA-infected EBs. While the expression of neuroectoderm markers (*NeuroD, Pax6*) appeared augmented in *Ovol2* shRNA-infected EBs, messages of endodermal markers (*Hinf4a, Sox17*) were decreased. Thus, these results suggest that ER71-mediated FLK1$^+$ cell generation is partly dependent upon OVOL2.

In summary, we demonstrate that ER71 interacts with OVOL2 and that such interaction cooperatively enhances the generation of FLK1$^+$ cells, as well as endothelial and hematopoietic cells. A recent study reported that OVOL2 acting downstream of BMP signaling can expand mesendoderm at the expense of neuroectoderm (Zhang et al., 2013). However, our analysis clearly showed that OVOL2 in a serum free condition failed to induce FLK1$^+$ cell generation, suggesting that *Ovol2* is not sufficient for FLK1$^+$ mesoderm formation. Rather, OVOL2 in collaboration with ER71 directly activated FLK1 promoter activity and was required for optimal endothelial and hematopoietic cell generation without altering the formation of the mesoderm.

Acknowledgements

This work was supported by the March of Dimes Foundation, 5-FY12-44 (to C.P.), the American Heart Association, 11SDG7390074 (to C. P.), NIH HL119291 (to C.P.), NIH HL105732 (to D.M.O) and the NRF Stem Cell Program (NRF-2011-0019509), Republic of Korea (to J-I. C.). We also thank Dr. Novina for providing lentiviral packaging and envelope plasmids.

Author contributions

J.Y.K., R.H.L., T.M.K., performed experiments and analyzed data; D-W.K., Y-J.J., S-H.H., S-Y.O., performed experiments; M.K., H.K., K.C., D.M.O., provided experimental materials; J-I.C., conceived, designed research, analyzed data, and wrote the manuscript; C.P., conceived, designed and performed experiment, analyzed and interpreted data and wrote the manuscript.

Disclosure of Conflicts of Interest

The authors declare no conflict of interests.

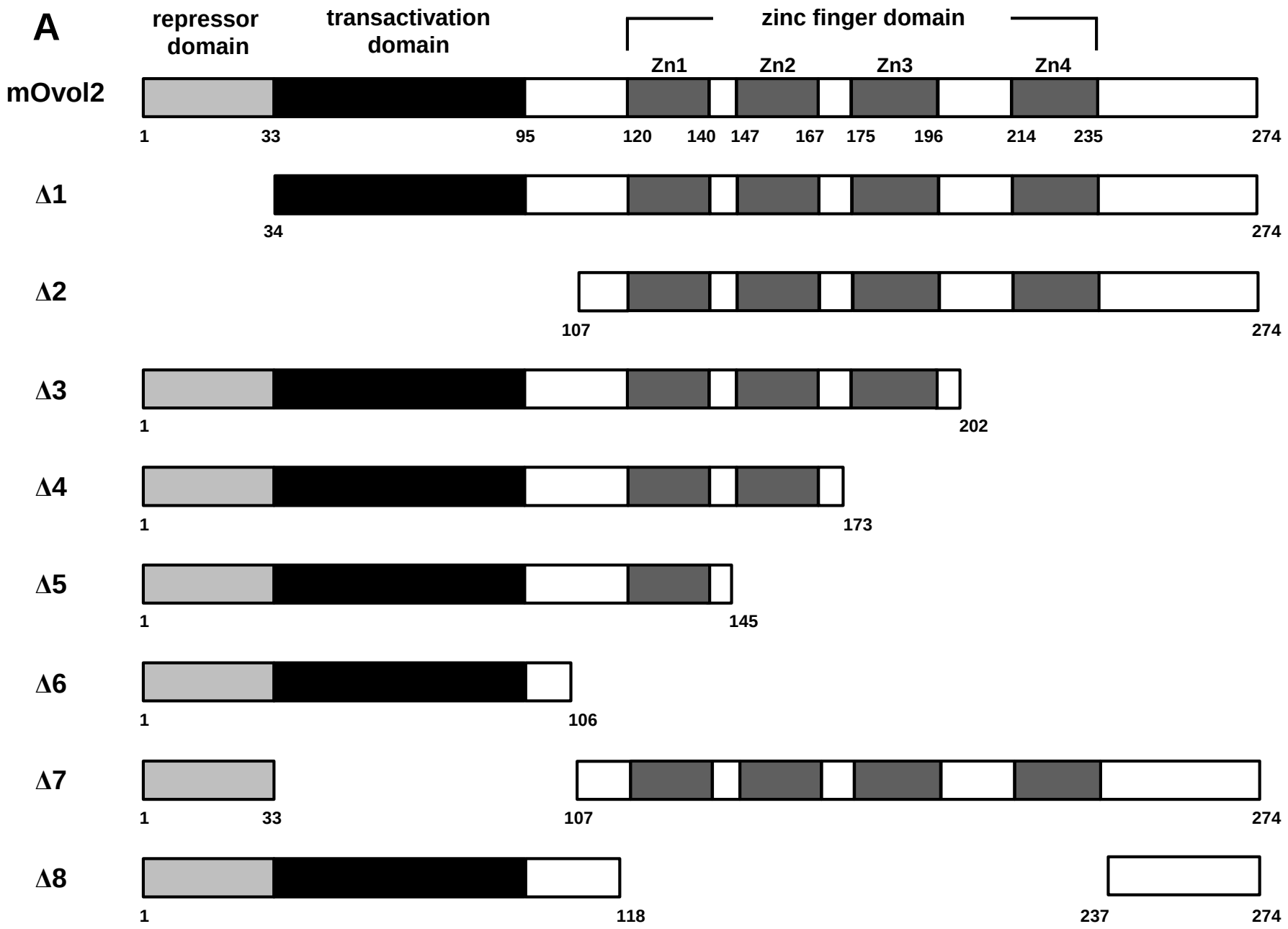
A
repressor domain
transactivation domain
zinc finger domain
Zn1
Zn2
Zn3
Zn4
mOvol2
1
33
95
120
140
147
167
175
196
214
235
274
Δ1
34
274
Δ2
107
274
Δ3
1
202
Δ4
1
173
Δ5
1
145
Δ6
1
106
Δ7
1
33
107
274
Δ8
1
118
237
274

Figure 1A

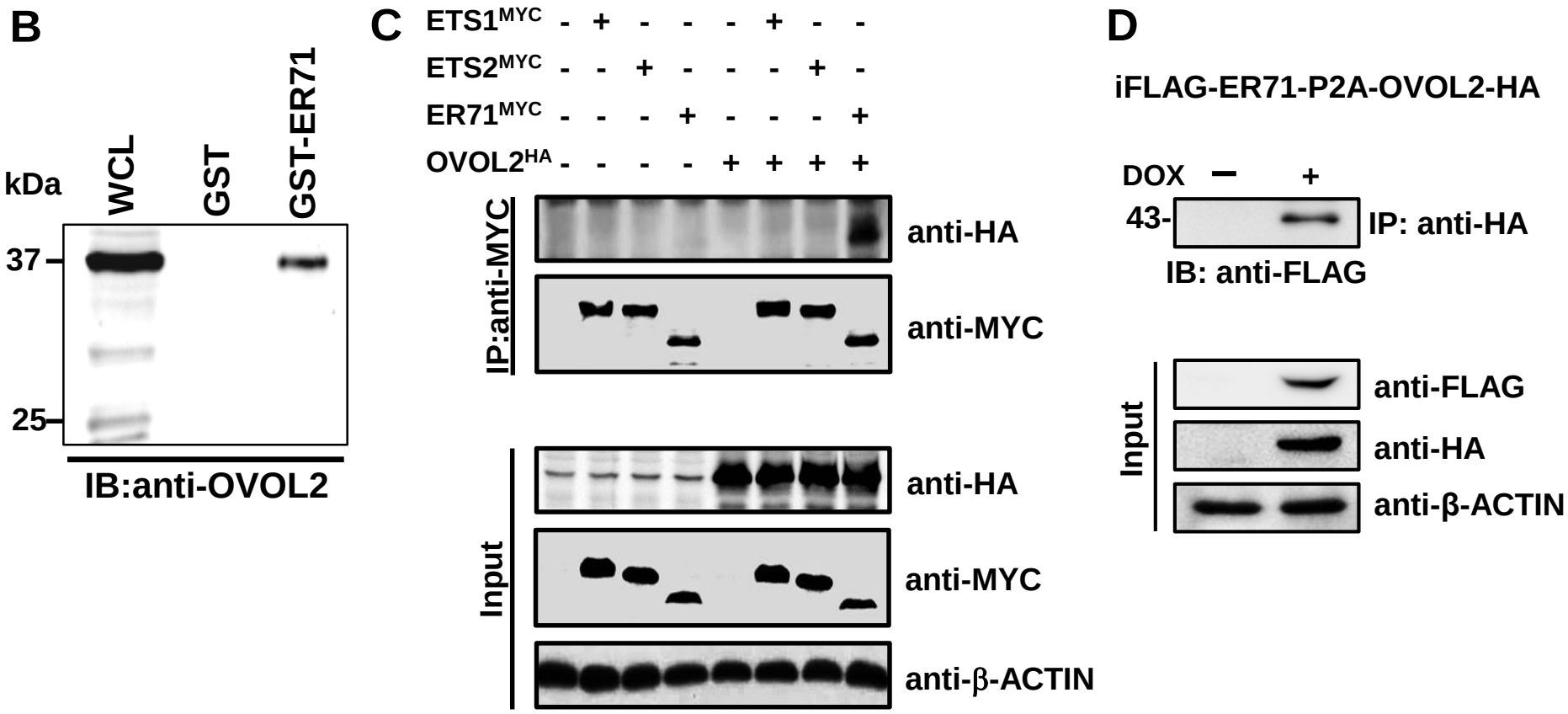
B
kDa
WCL
GST
GST-ER71
37
25
IB:anti-OVOL2
C
ETS1MYC - + - - - + - -
ETS2MYC - - + - - - + -
ER71MYC - - - + - - - +
OVOL2HA - - - - + + + +
IP:anti-MYC
anti-HA
anti-MYC
Input
anti-HA
anti-MYC
anti-β-ACTIN
D
iFLAG-ER71-P2A-OVOL2-HA
DOX – +
43-
IP: anti-HA
IB: anti-FLAG
Input
anti-FLAG
anti-HA
anti-β-ACTIN

Figure 1B-D

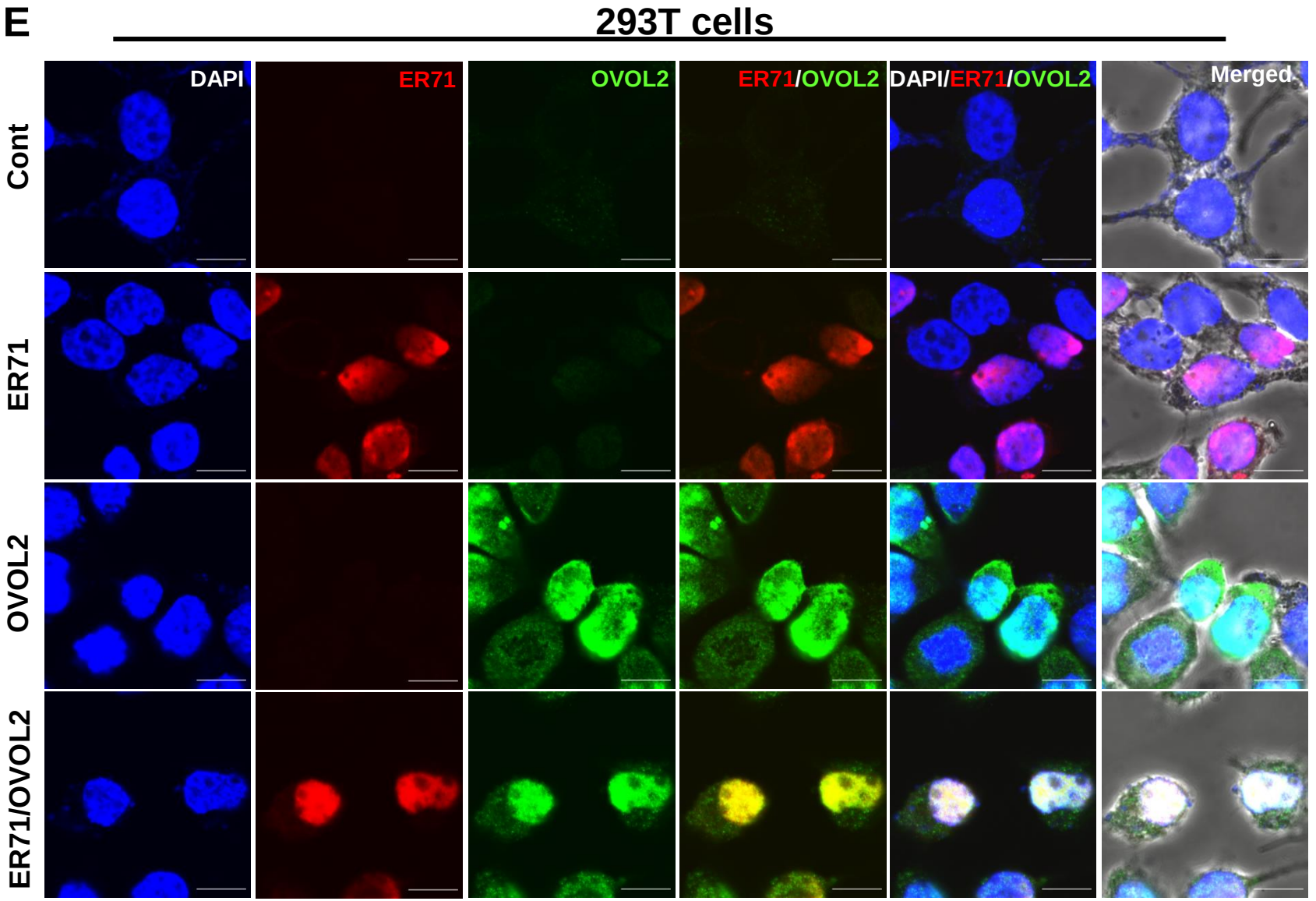
E
293T cells
DAPI
ER71
OVOL2
ER71/OVOL2
DAPI/ER71/OVOL2
Merged
Cont
ER71
OVOL2
ER71/OVOL2

Figure 1E

F

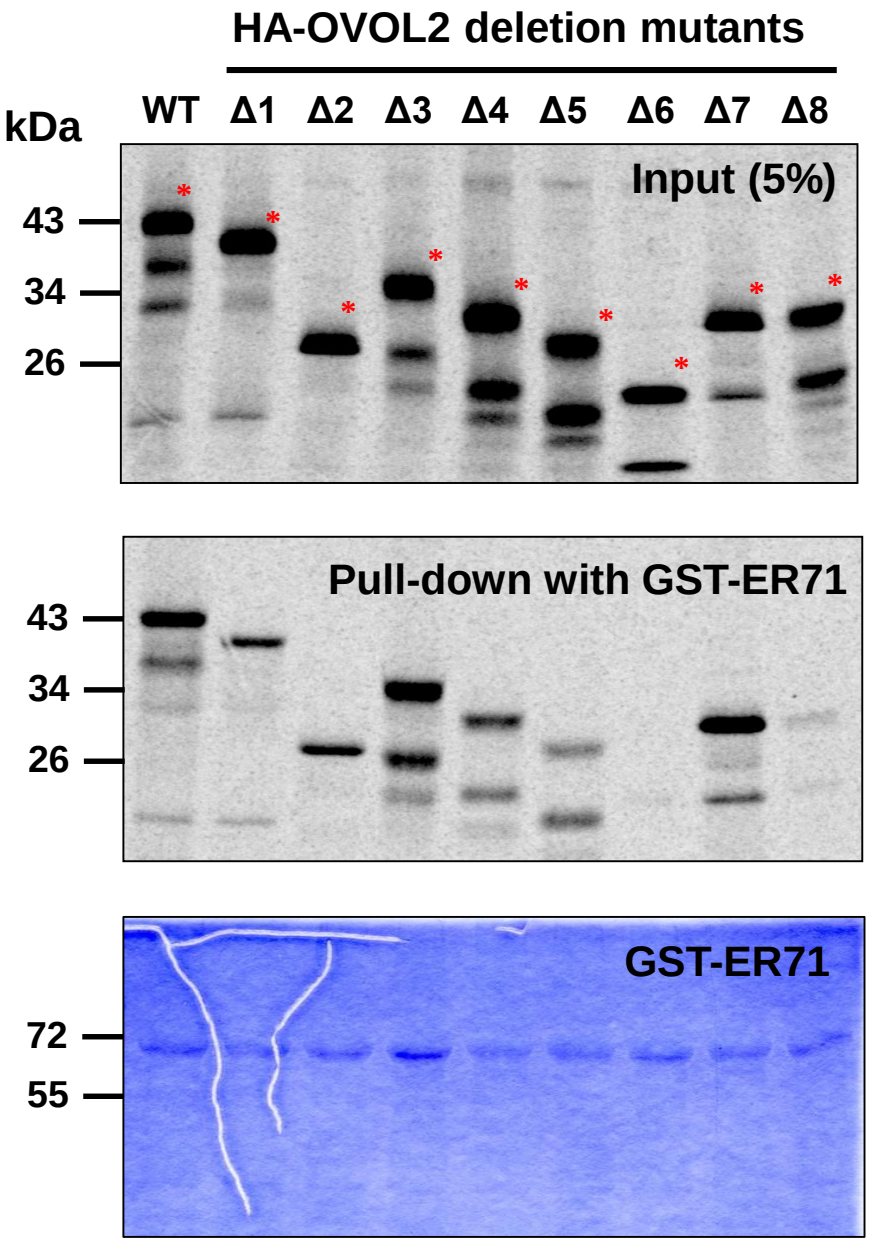

G

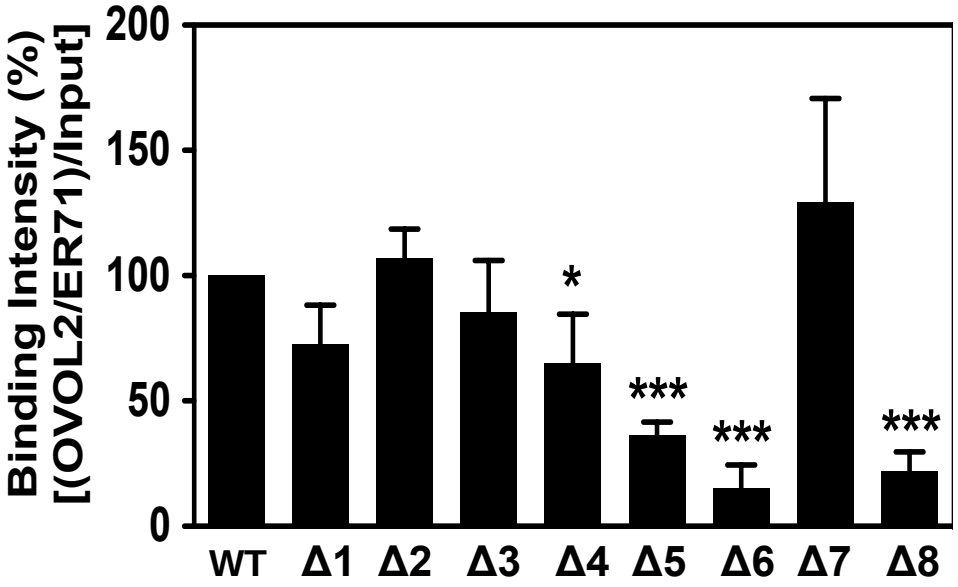

Figure 1F-G

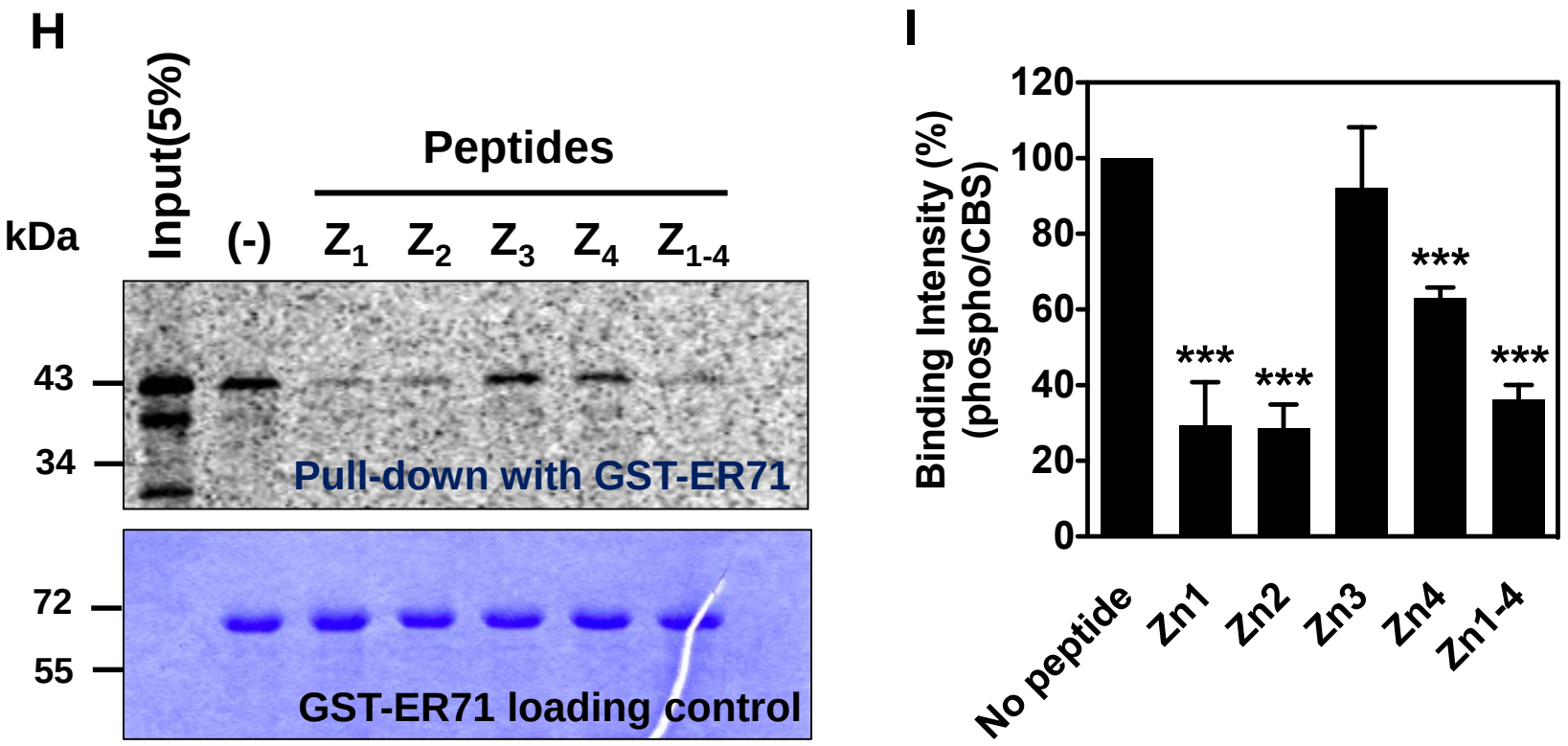
H
Input(5%)
Peptides
kDa
(-)
Z1
Z2
Z3
Z4
Z1-4
43
34
Pull-down with GST-ER71
72
55
GST-ER71 loading control
I
Binding Intensity (%)
(phospho/CBS)
120
100
80
60
40
20
0
***
***
***
No peptide
Zn1
Zn2
Zn3
Zn4
Zn1-4

Figure 1H-I

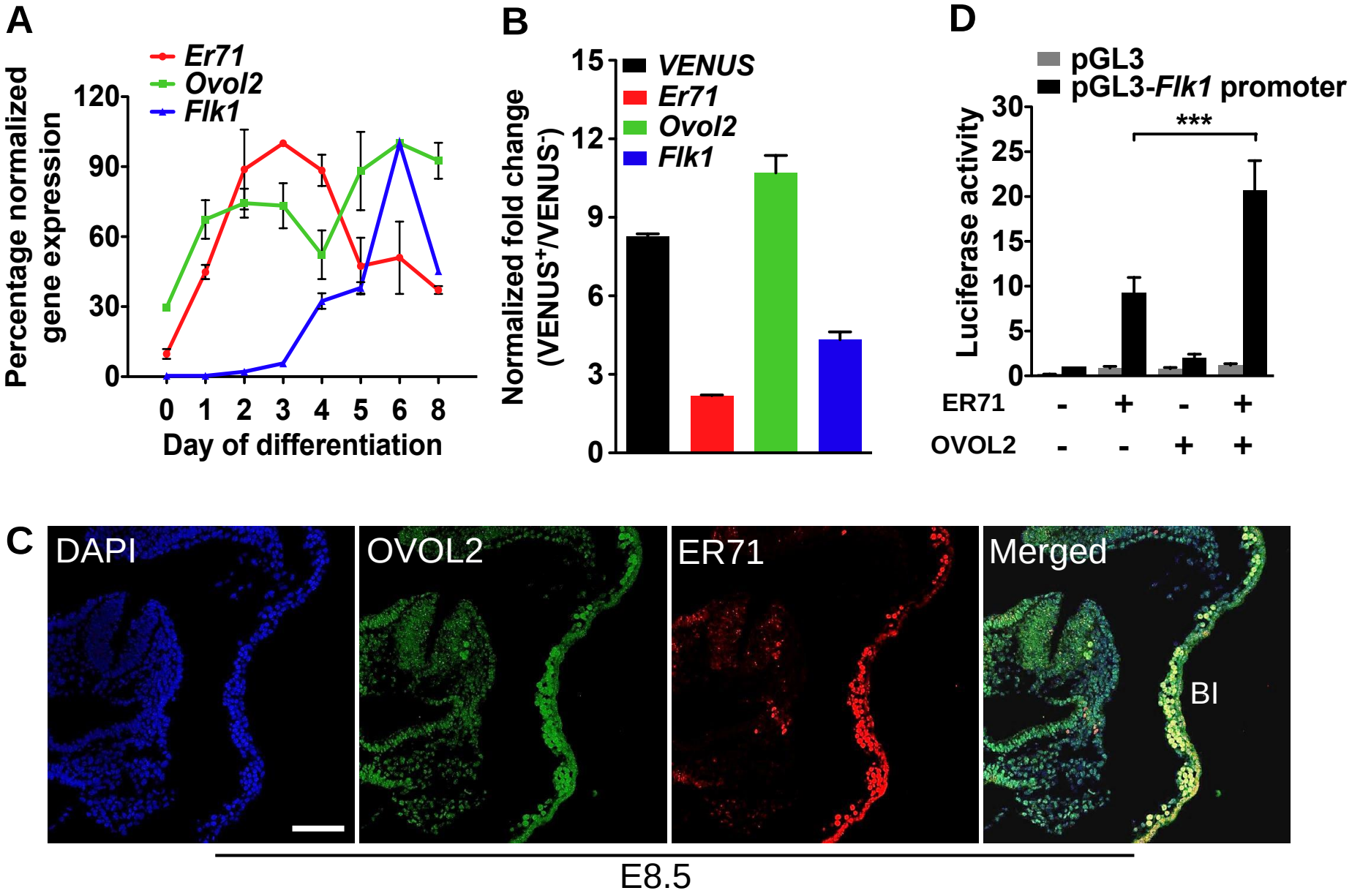
A
Er71
Ovol2
Flk1
Percentage normalized gene expression
120
90
60
30
0
0 1 2 3 4 5 6 8
Day of differentiation
B
VENUS
Er71
Ovol2
Flk1
Normalized fold change (VENUS+/VENUS-)
15
12
9
6
3
0
D
pGL3
pGL3-Flk1 promoter
Luciferase activity
30
25
20
15
10
5
0
***
ER71 - + - +
OVOL2 - - + +
C
DAPI
OVOL2
ER71
Merged
BI
E8.5

Figure 2A-D

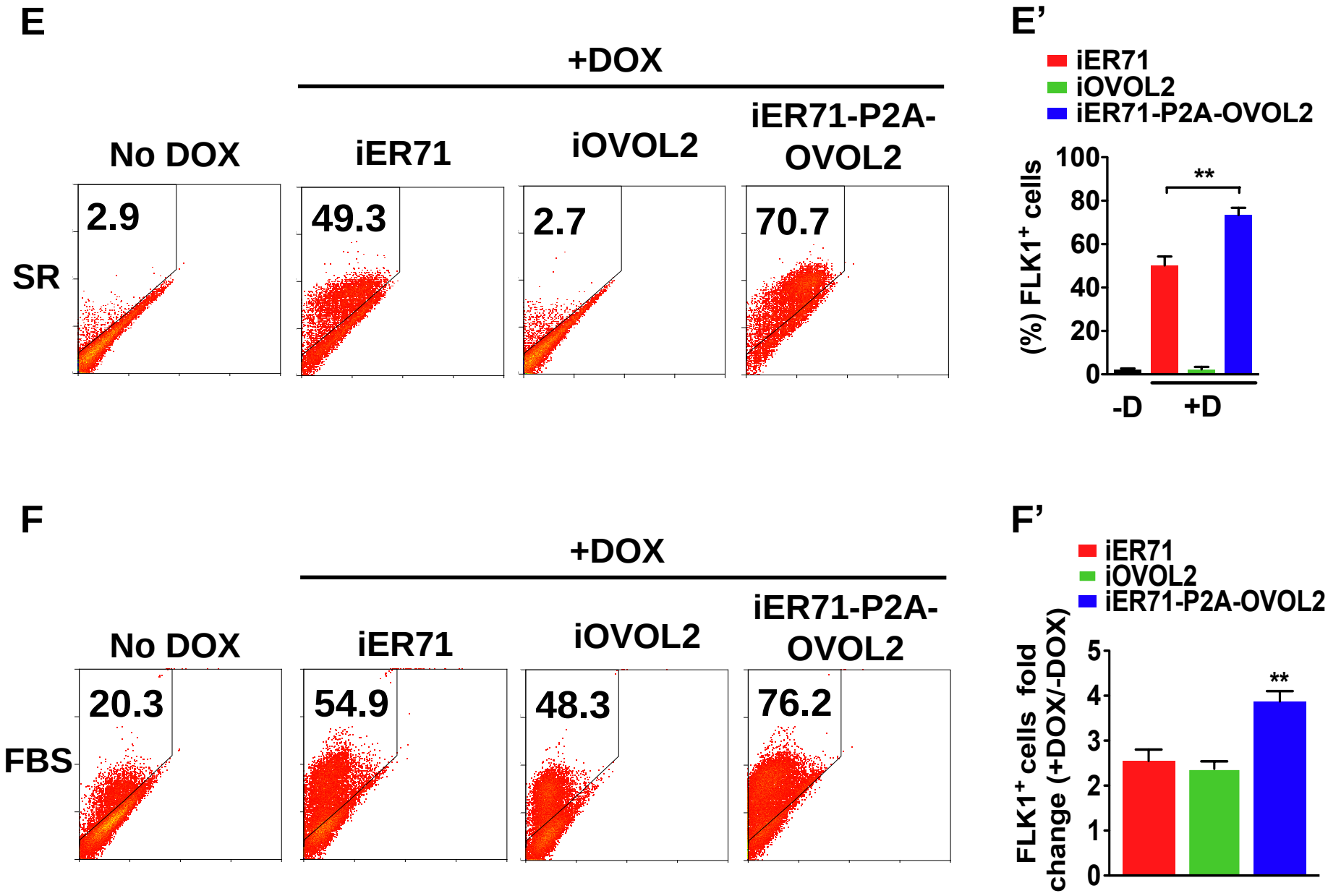
E
+DOX
No DOX
iER71
iOVOL2
iER71-P2A-OVOL2
SR
2.9
49.3
2.7
70.7
E'
iER71
iOVOL2
iER71-P2A-OVOL2
(%) FLK1+ cells
100
80
60
40
20
0
**
-D
+D
F
+DOX
No DOX
iER71
iOVOL2
iER71-P2A-OVOL2
FBS
20.3
54.9
48.3
76.2
F'
iER71
iOVOL2
iER71-P2A-OVOL2
FLK1+ cells fold change (+DOX/-DOX)
5
4
3
2
1
0
**

Figure 2E-F

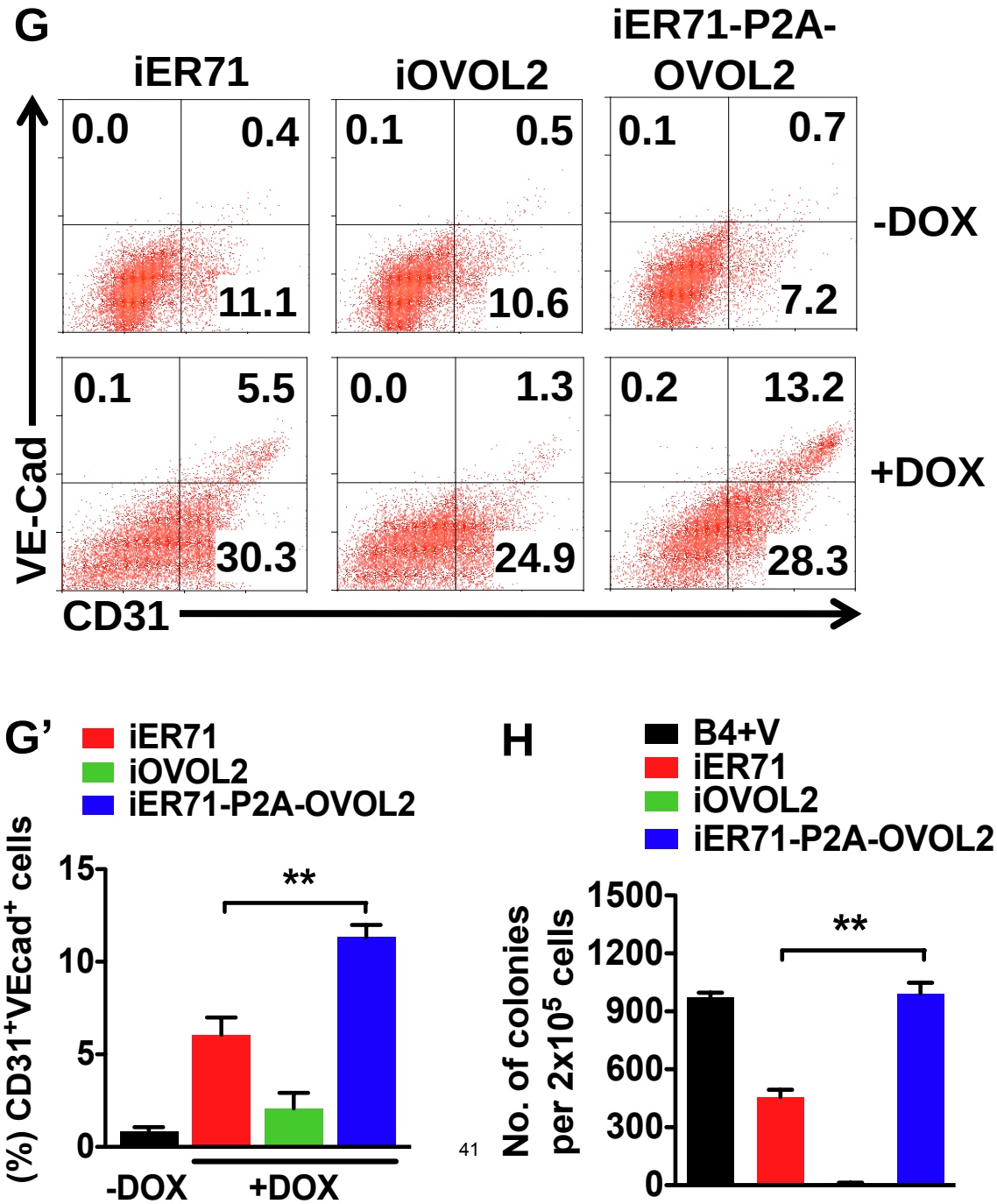
G
iER71
iOVOL2
iER71-P2A-OVOL2
0.0
0.4
11.1
0.1
0.5
10.6
0.1
0.7
7.2
-DOX
0.1
5.5
30.3
0.0
1.3
24.9
0.2
13.2
28.3
+DOX
VE-Cad
CD31
G'
iER71
iOVOL2
iER71-P2A-OVOL2
(%) CD31+VEcad+ cells
15
10
5
0
**
-DOX
+DOX
H
B4+V
iER71
iOVOL2
iER71-P2A-OVOL2
No. of colonies per 2x10^5 cells
1500
1200
900
600
300
0
**

Figure 2G-H

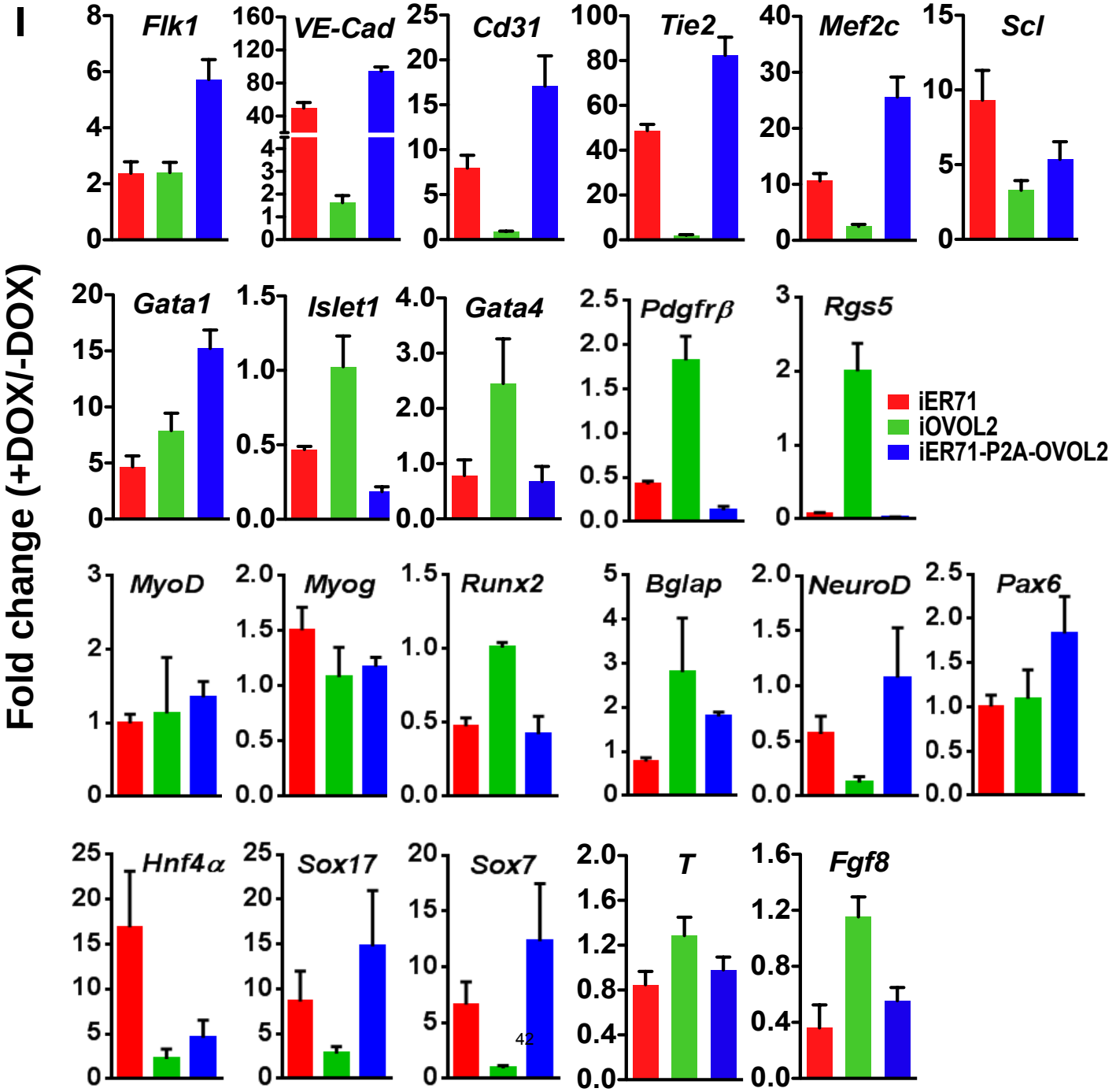
I
Flk1
VE-Cad
Cd31
Tie2
Mef2c
Scl
Gata1
Islet1
Gata4
Pdgfrβ
Rgs5
MyoD
Myog
Runx2
Bglap
NeuroD
Pax6
Hnf4α
Sox17
Sox7
T
Fgf8
Fold change (+DOX/-DOX)
iER71
iOVOL2
iER71-P2A-OVOL2

Figure 2I

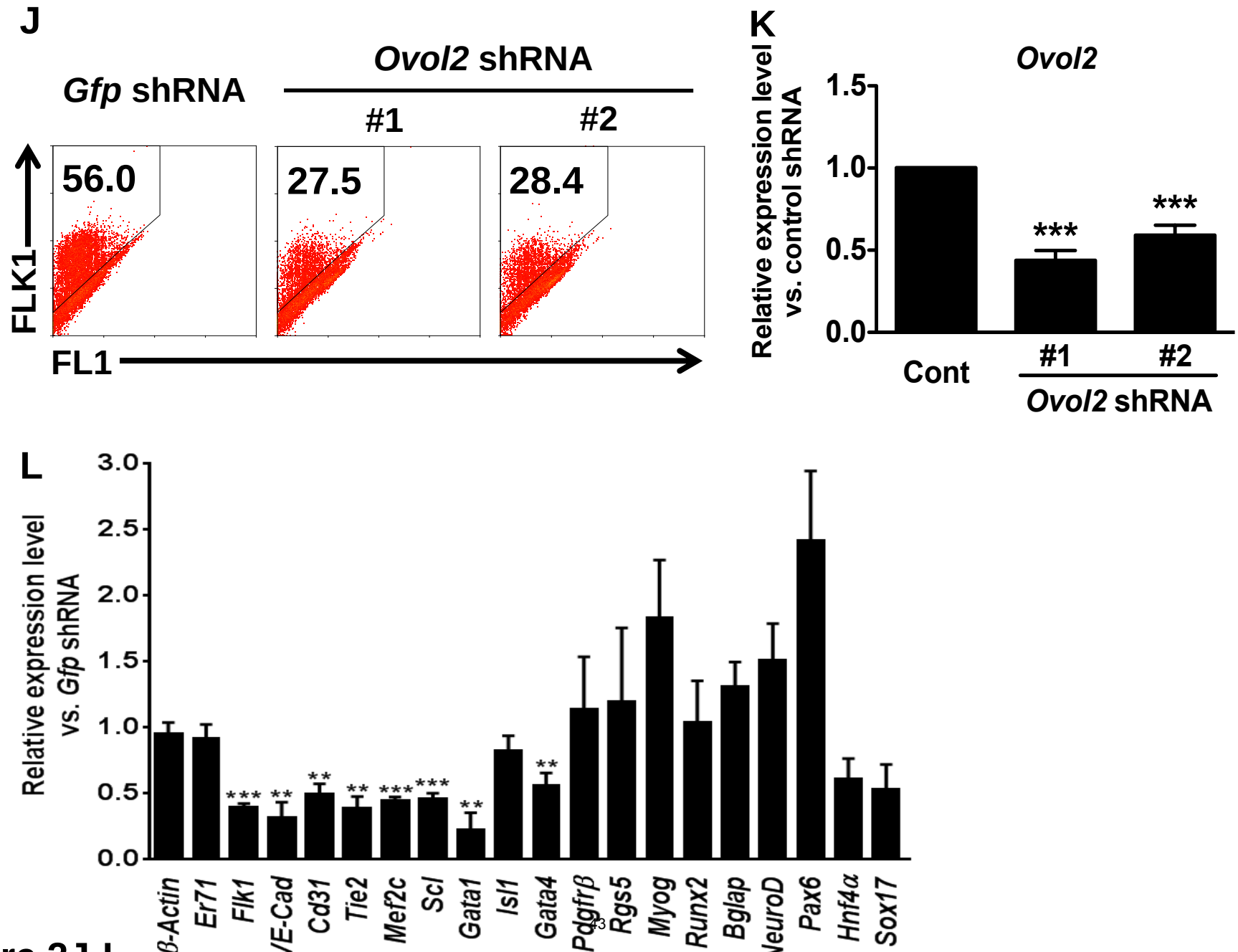
J
Gfp shRNA
Ovol2 shRNA
#1
#2
56.0
27.5
28.4
FLK1
FL1
K
Ovol2
Relative expression level vs. control shRNA
1.5
1.0
0.5
0.0
***
***
Cont
#1
#2
Ovol2 shRNA
L
Relative expression level vs. Gfp shRNA
3.0
2.5
2.0
1.5
1.0
0.5
0.0
β-Actin
Er71
Flk1
VE-Cad
Cd31
Tie2
Mef2c
Scl
Gata1
Isl1
Gata4
Pdgfrβ
Rgs5
Myog
Runx2
Bglap
NeuroD
Pax6
Hnf4α
Sox17

Figure 2J-L

Figure legends

Figure 1. ER71 directly interacts with OVOL2. (A) A schematic diagram of OVOL2 and its deletion mutants. (B) GST-ER71 interacts with OVOL2. Binding between recombinant GST-ER71 and OVOL2 from D3.5 EB was determined by immunoblotting by anti-OVOL2 antibody. (C) Coimmunoprecipitation between ER71 and OVOL2. Cell lysates of 293T cells that were transfected with the control or expression plasmid of ER71-MYC, ETS1-MYC, ETS2-MYC and/or HA-OVOL2 were immunoprecipitated (IP) with anti-MYC antibodies and immunoblotted with anti-MYC and anti-HA antibodies, respectively. β-ACTIN was used for loading control. (D) iFLAG-ER71-HA-OVOL2 embryonic stem cells (ESCs) in which the expression of ER71 and OVOL2 is dependent upon DOX (Doxycycline) were differentiated in a serum-containing media, treated DOX at D1 and harvested at D3.5 of differentiation. Subsequently, cell lysate was subjected to immunoprecipiation with anti-HA antibody, followed by immunoblotting with anti-FLAG antibodies. β-ACTIN was used for loading control. (E) Co-localization of ER71 and OVOL2. 293T cells transiently transfected with ER71-MYC or/and HA-OVOL2 were immunostained with antibodies against MYC or HA and then analyzed by confocal microscopy. Red and green denote ER71 and OVOL2, respectively. DAPI was used for visualization of nucleus (blue), and all fluorescent images were overlaid with phase contrast images (Merge, last column of panels). All Images are magnified view of the original ones in Figure S2. Scale bars; 10 μm. (F) GST-ER71 pull-down with in vitro translated OVOL2. Purified GST-ER71 was incubated with each ^{35}S-labeled wild type or mutants OVOL2. Subsequently, pull-down products were subjected to SDS-PAGE followed by analysis of radioactive signals by phosphor imager. (Top) The phosphor image of input amount of mutants OVOL2 given for binding. (Middle) The phosphor image of mutant OVOL2 that were precipitated by GST-ER71. (Bottom) Coomassie blue staining for GST-mER71 that was used for each binding. (G) Quantification of radioactive signals from in vitro pull-down assays. Binding affinity between GST-ER71 and ^{35}S-labeled OVOL2 mutants were analyzed and presented in the graph. The density of ^{35}S-labeled OVOL2 was normalized against that of

GST-ER71, after which re-normalized against OVOL2 input signal. Value from wild type OVOL2 was given 100%. Results are mean ± S.E.M from three replications. (*P < 0.05 and ***P < 0.001 compared to wild type). (H, I) Peptide competition assay. (H) The phosphor image of ^{35}S-labeled OVOL2 precipitated with GST-ER71 in the absence or presence of ZF peptide. (I) Quantification of radioactive signals from peptide competition assays. Binding affinity between GST-ER71 and ^{35}S-labeled OVOL2 were analyzed. The density of OVOL2 was normalized against that of GST-ER71. Results are means ± S.E.M from three replications (***P < 0.001 compared to no peptide control).

Figure 2. OVOL2 enhances ER71-mediated FLK1$^+$ cell generation as well as hematopoietic and endothelial cell lineage development. (A) Expression of *Er71*, *Ovol2* and *Flk1* in ESC differentiation. The expression in each day point was normalized against *Gapdh*. 100% denotes the level where its maximum expression was reached. (B) VENUS$^+$ cells and VENUS$^-$ cells from E8.5 ER71-VENUS embryos were subjected to qRT-PCR analysis. (C) E8.5 embryos were sectioned and subjected to immunohistochemical analysis of OVOL2 (green) and ER71 (red). DAPI (blue) for nucleus staining. Scale bar: 100 μm, BI: blood islands. (D) Synergistic activation of *Flk1* promoter by ER71 and OVOL2. Expression constructs were transfected into 293T cells with *pGL3* or *pGL3-Flk1* promoter-luciferase reporter plasmids. The relative luciferase activity was gained by normalizing Firefly luciferase activity to Renilla luciferase activity at 48 hours post-transfection (***P < 0.001). (E, F) iER71, iOVOL2 and iER71-OVOL2 ESCs were differentiated either in a serum-free medium for 4 days (E) or in a serum-containing media for 3.5 days (F), and subjected to FACS analysis. Numbers in the plots denote the percentages of FLK1$^+$ cells. DOX (Doxycycline) was added at D2 and D1 in a serum-free or a serum-containing differentiation medium, respectively. (E') The percentage of FLK1$^+$ cells in iER71, iOVOL2 and iER71-OVOL2 differentiated in a serum free condition in the absence (-D) or presence (+D) of DOX. Results are means ± S.E.M from three replications (**P < 0.01). (F') Fold change of the generation of FLK1$^+$ cells in ESCs after DOX treatment (+DOX/-DOX) in a serum-containing media. Results are means ± S.E.M from three

replications (**P < 0.01). (G, G') FACS analysis for CD31/PECAM1 and VECadherin (VE-Cad) in D6.5 EBs. iER71, iOVOL2 and iER71-OVOL2 ESCs differentiated in a serum-containing medium were treated with DOX at D3.5, followed by FACS analysis for CD31 and VE-Cad at D6.5 (** P < 0.01). (H) Hematopoietic replating assay. iER71, iOVOL2 and iER71-P2A-OVOL2 ESCs differentiated in a serum-free condition were treated with DOX at D3 and subjected to hematopoietic replating assay at D6. Colonies were counted 4 days later. B4 and V denote BMP4 and VEGF-A, respectively. Results are means ± S.E.M from three replications (**P < 0.01). (I) Gene expression profiling in D3.5 EBs overexpressing either ER71 (iER71) or OVOL2 (iOVOL2), or both ER71 and OVOL2 (iER71-P2A-OVOL2) in a serum-containing medium. DOX was added at D1 and RNA was prepared at D3.5. Expression of each gene was normalized against *Gapdh*, and the fold change of its expression level (+DOX/-DOX) was calculated. (J-L) iER71 ESCs infected with lentiviral shRNA particles against *Ovol2* or *Gfp* control were differentiated in a serum-containing medium and subjected to FACS analysis for FLK1 (J) and qRT-PCR for *Ovol2* (K) (***P < 0.001). (L) Gene expression analysis in D3.5 EBs that had been infected with lentiviral particles of *Ovol2* shRNAs (**P < 0.01, ***P < 0.001).

Table S1. Identification of OVOL2 as an ER71-interacting protein by LC/MS

Accession No.	Description	mW (Da)	pI[a]	PLGS score[b]	Peptides	Coverage[c]	Products[d]
Q8CIV7-2	Isoform 2 of transcription factor Ovo-like 2	26875	8.3	38.927	2	2.9	14

a: The pH at which a protein carries no net charge, **b:** PLGS Score is calculated by the Protein Lynx Global Server (PLGS 2.2.5) software using a Monte Carlo algorithm to analyze all available mass spec. data and is a statistical measure of accuracy of assignation. A higher score implies greater confidence of protein identity.[10] **c:** Coverage represents the percentage of the protein's sequence represented by the peptides identified in the MS run. **d:** Fragment ions (product ions).

Table S2. Primer sequences used for qRT-PCR

Genes		Sequence(5'-3')	Reference
β-Actin	Forward	GCTACAGCTTCACCACCACAG	
	Reverse	GGTCTTTACGGATGTCAACGTC	
Bglap	Forward	ACCCTGGCTGCGCTCTGTCTCT	
	Reverse	GATGCGTTTGTAGGCGGTCTTCA	
Gata4	Forward	CCCTACCCAGCCTACATGG	primer bank ID: 6679953a1
	Reverse	ACATATCGAGATTGGGGTGTCT	
Myf5	Forward	GGAGATCCTCAGGAATGCCATCCGC	
	Reverse	TGCTGTTCTTTCGGGACCAGACAGG	
MyoD1	Forward	TACAGTGGCGACTCAGATGC	
	Reverse	CGGTGTCGTCGCCATTCTG	
Myog	Forward	CAACCAGGAGGAGCGCGATCTCCG	
	Reverse	AGGCGCTGTGGGAGTTGCATTCACT	
Ovol2	Forward	CCTTTGTGGCAAGAGCTTCC	
	Reverse	CGTACGTGCCTCTTCAGGT	
Pax6	Forward	TACCAGTGTCTACCAGCCAAT	primer bank ID : 1405745a1
	Reverse	TGCACGAGTATGAGGAGGTCT	
Pdgfrβ	Forward	CTGGGTGAAGGCTATAAAAAGAAGTACCAG	
	Reverse	CTTCATCAGCAACGTCAGGCTTG	
Rgs5	Forward	CGCACTCATGCCTGGAAAG	primer bank ID : 29336055a1
	Reverse	TGAAGCTGGCAAATCCATAGC	
Runx2	Forward	TTTAGGGCGCATTCCTCATC	
	Reverse	TGTCCTTGTGGATTAAAAGGACTTG	
Sox7	Forward	CCTTACTCACCGGAGTTCACA	primer bank ID : 6755611c3
	Reverse	GAAACCCCTGGGGATTGGC	

Sox17	Forward	CGAGCCAAAGCGGAGTCTC	
	Reverse	TGCCAAGGTCAACGCCTTC	
	Reverse	TGGCACAGATGCGTTGAATAC	
Venus	Forward	ACCCTGAAGCTGATCTGCAC	
	Reverse	GGTCTTGTAGTTGCCGTCGT	

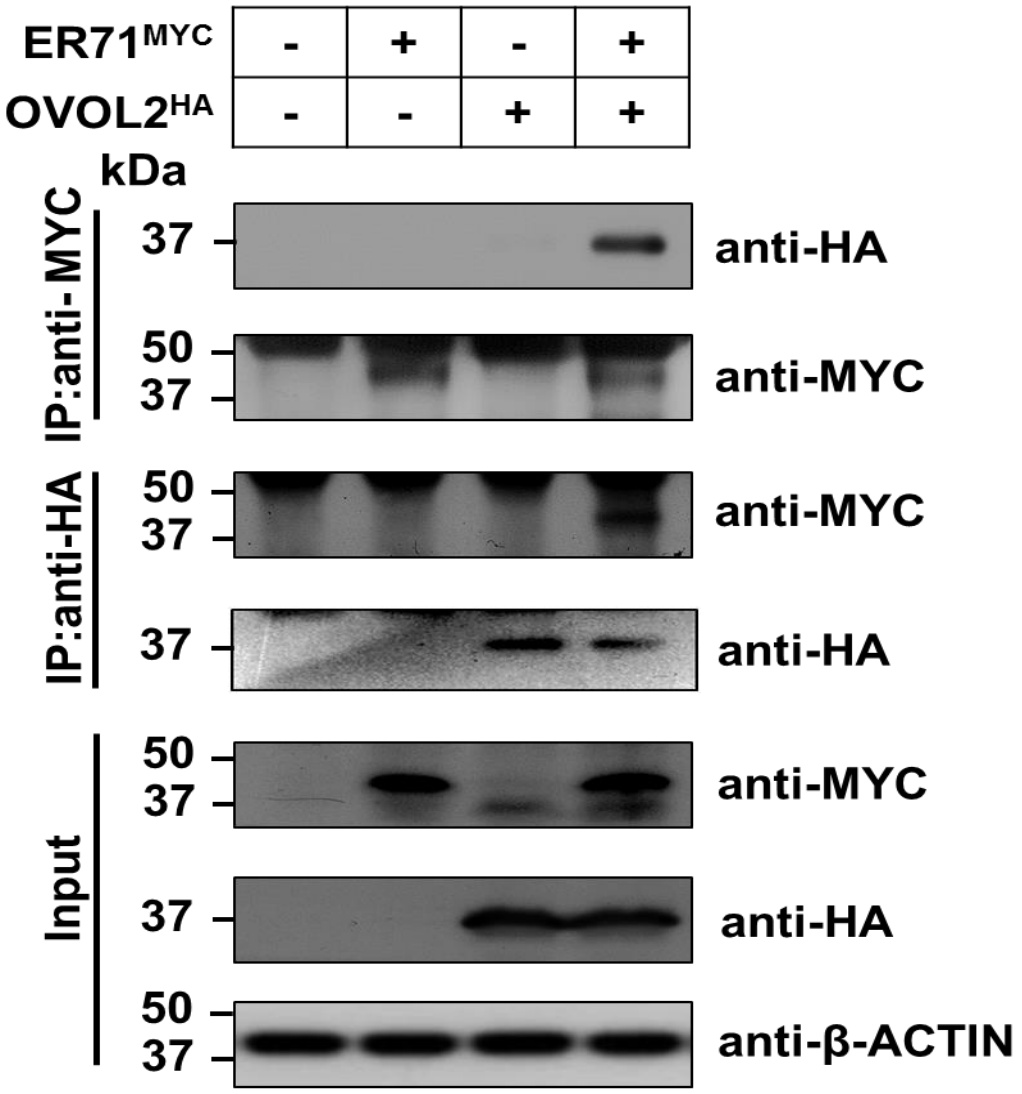

Figure S1. Interaction between ER71 and OVOL2. Cell lysates of 293T cells that were transfected with the control or expression plasmid of ER71-MYC and/or HA-OVOL2 were immunoprecipitated (IP) with anti-MYC antibodies or anti-HA antibodies, followed by immunoblot with anti-HA and anti-MYC antibodies, respectively. β-ACTIN was used for loading control.

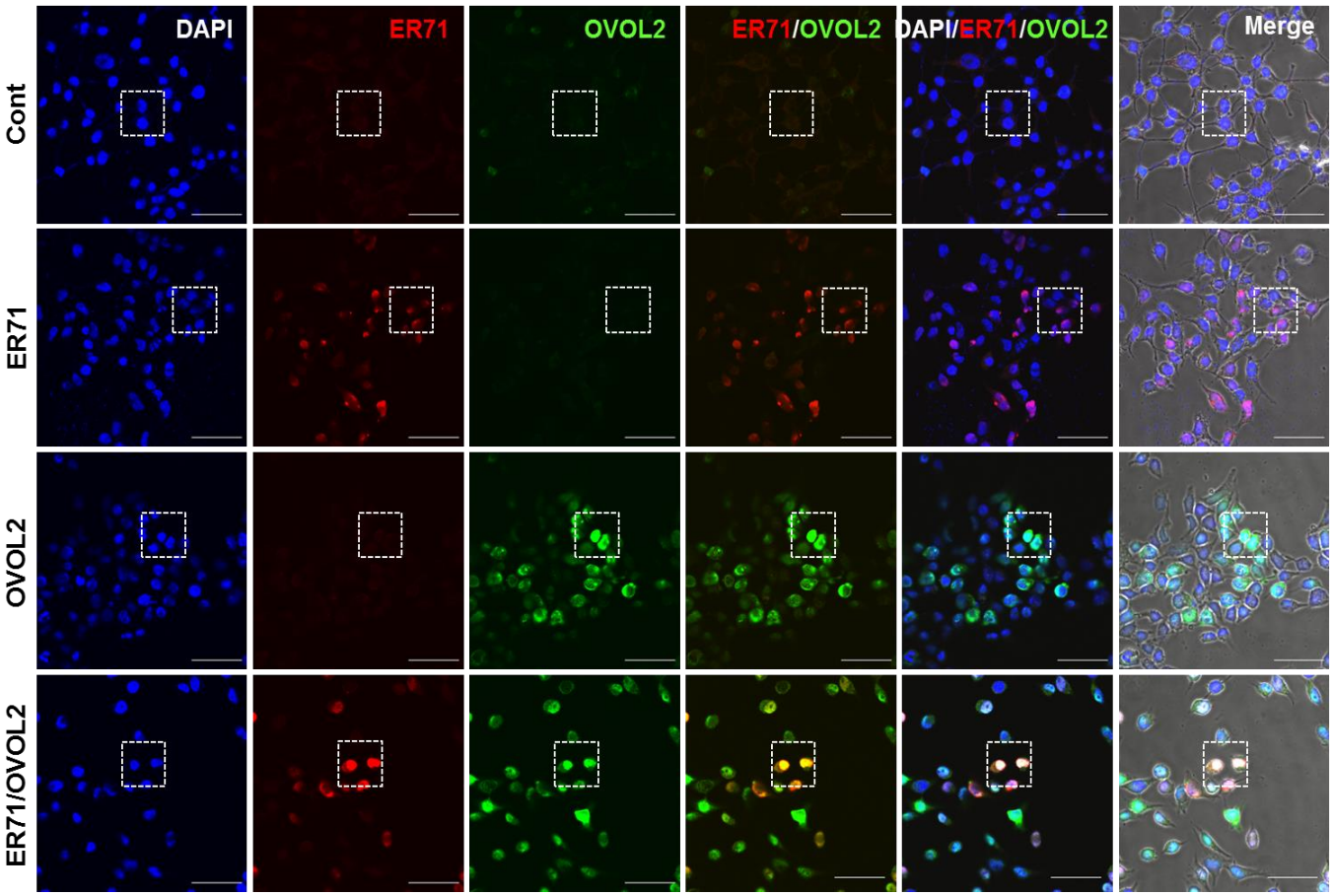

Figure S2. ER71 and OVOL2 co-localize in the nucleus. 293T cells transiently transfected with ER71-MYC or/and HA-OVOL2 were immunostained with antibodies against MYC or HA and then analyzed by confocal microscopy. Red and green denote ER71 and OVOL2, respectively. DAPI was used for visualization of nucleus (blue), and all fluorescence images were overlaid with phase contrast images (Merge, last column of panels). The magnified images marked by dotted square are shown in Figure 1D in the main text. Scale bars = 50 μm.

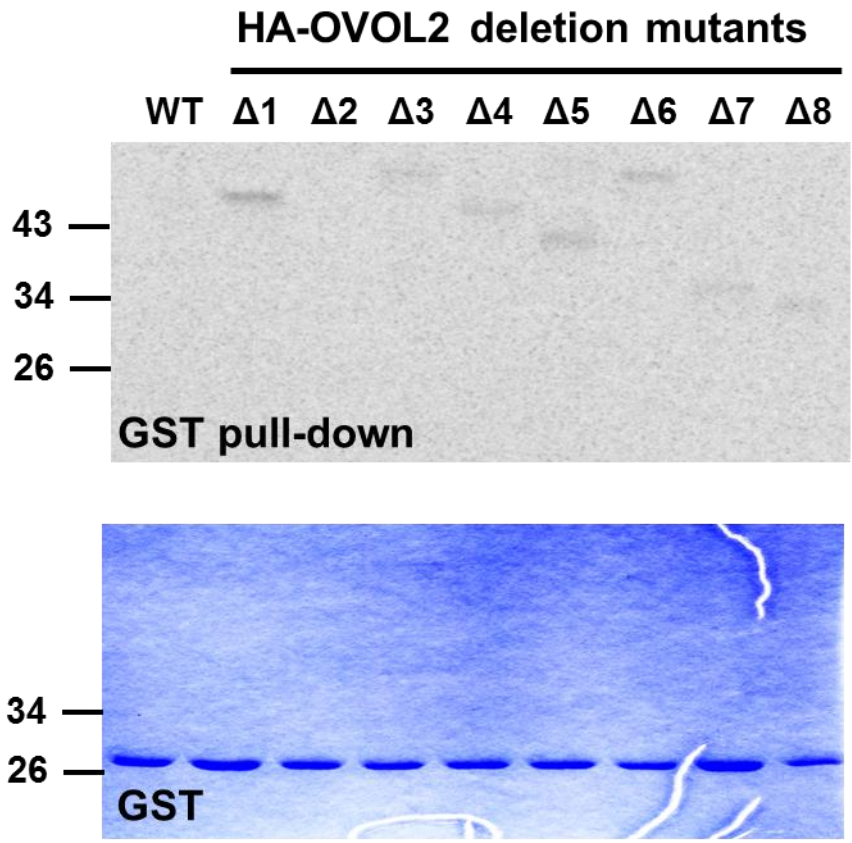

Figure S3. GST pull-down with in vitro translated OVOL2. Purified GST was incubated with each ^{35}S-labeled wild type or mutant OVOL2. Subsequently, pull-down products were subjected to SDS-PAGE followed by analysis of radioactive signals by phosphor imager. (Top) The phosphor image of mutant OVOL2 that were precipitated by GST. (Bottom) Coomassie blue staining of the amounts of GST that were given for each reaction.

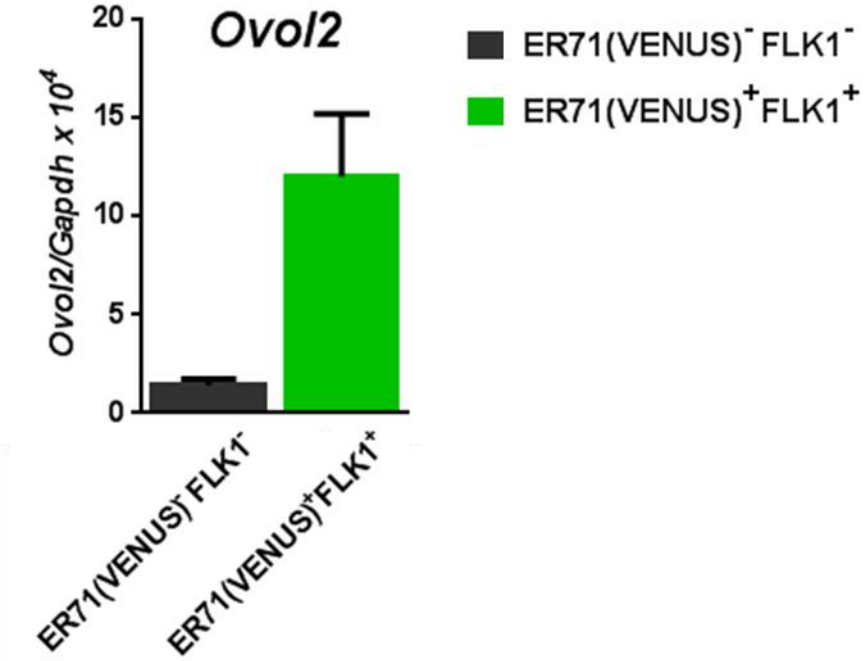

Figure S4. OVOL2 expression in ER71(VENUS)$^{+}$FLK1^{+} cells. VENUS^{+}FLK1^{+} cells and VENUS^{-}FLK1^{-} cells from E8.5 ER71-VENUS embryos were subjected to qRT-PCR analysis. Due to limited number of cells, the sorted cells were pooled for the analysis.

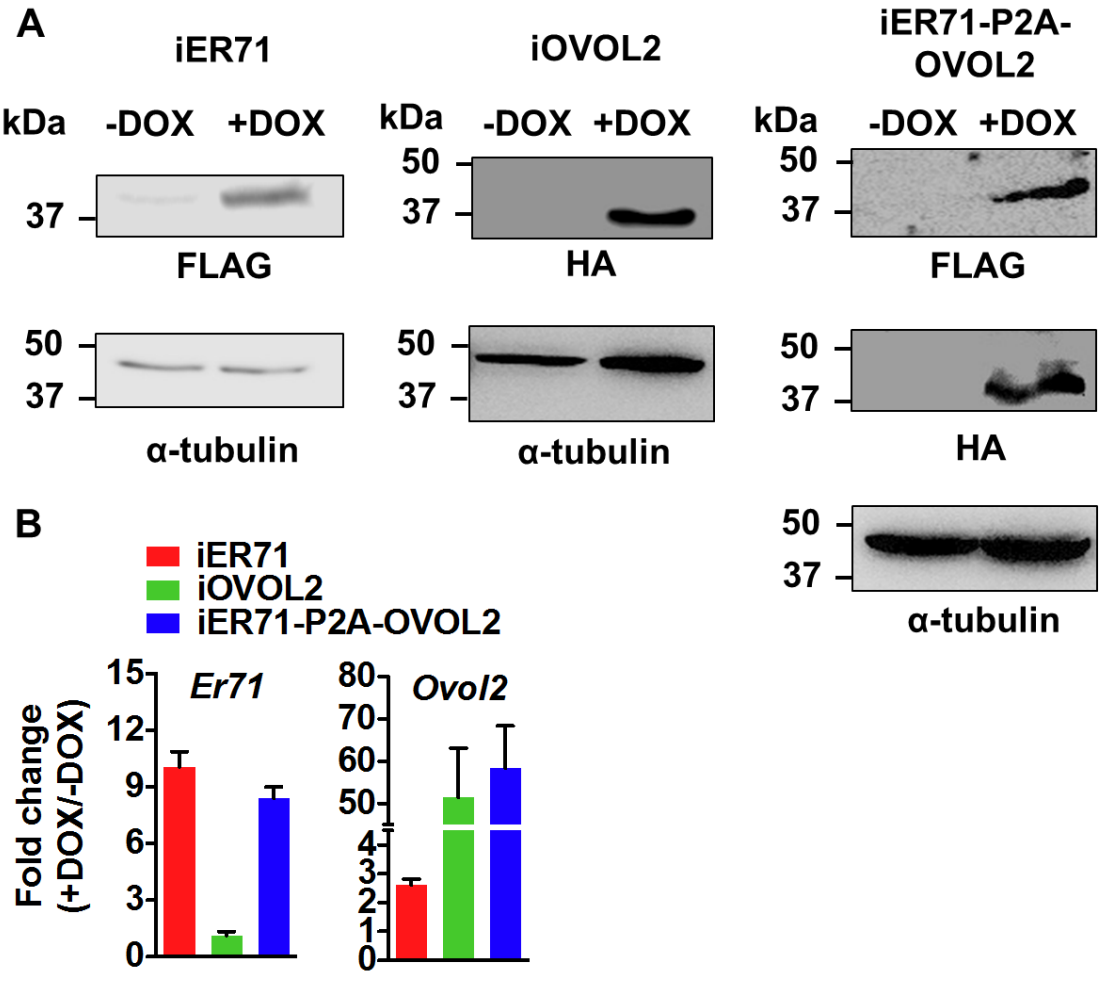

Figure S5. Confirmation of the DOX-inducible ESCs by immunoblotting. (A) Western blot analysis for the induction of FLAG-ER71, HA-OVOL2, and FLAG-ER71-P2A-HA-OVOL2. ESC were differentiated for 4 days in serum-containing medium and the whole cell lysates were used for immunoblotting with anti-FLAG tag or anti-HA tag antibody. DOX was added at D2 for gene induction. Anti-α-tubulin antibody blot was used for loading control. (B) Verification of gene induction by DOX in inducible ESCs by qRT-PCR. ESCs differentiated in serum-containing medium for 3.5 days were used for analysis. DOX was added at D1.

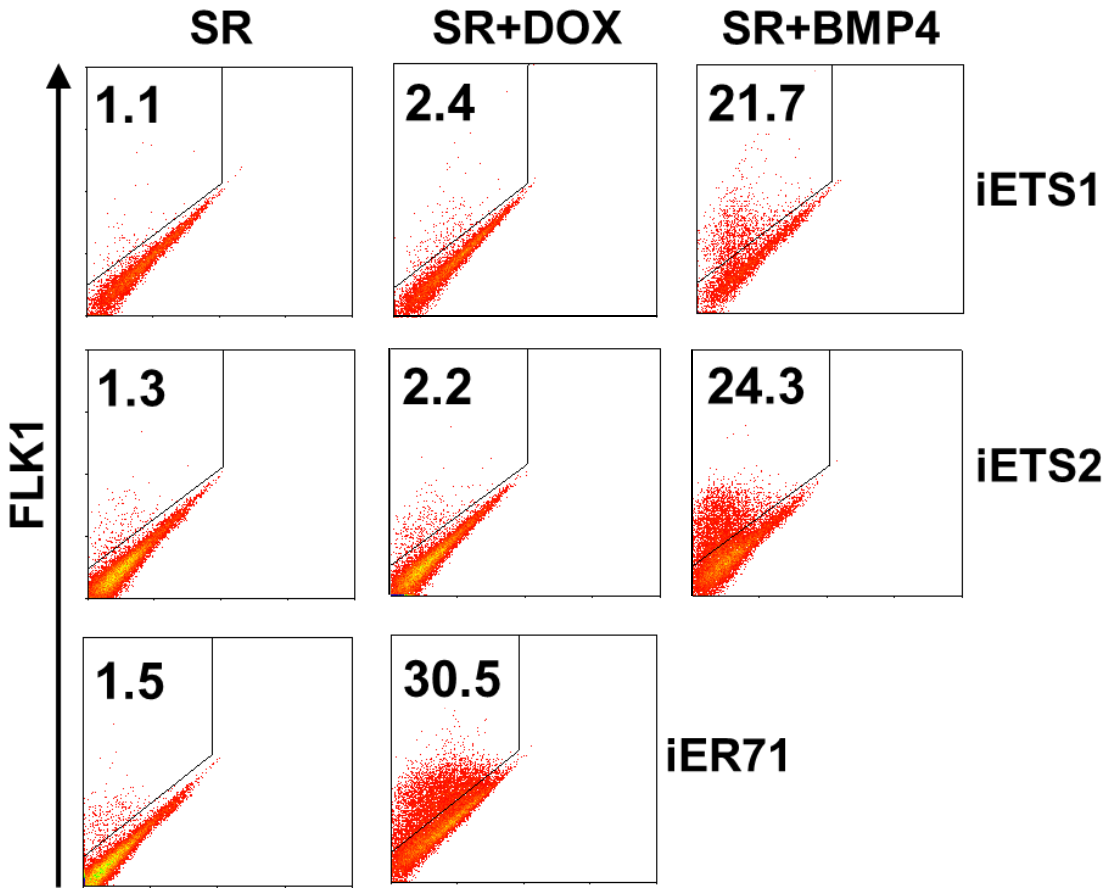

Figure S6. ETS1 and ETS2 fail to induce the generation of FLK1^{+} cells in differentiating ESCs. iETS1, iETS2 or iER71 were differentiated, treated with DOX at D2 in serum-free medium. At D4, cells were subjected to FACS analysis for FLK1. Numbers in the plots denote the percentages of FLK1^{+} cells among live cells.

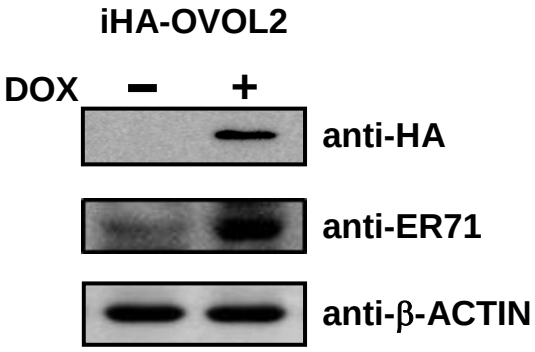

Figure S7. Expression of ER71 is upregulated upon OVOL2 induction. iHA-OVOL2 ESCs were differentiated for 4 days in serum-containing medium and the whole cell lysates were used for immunoblotting with anti-HA tag or anti-ER71 antibody. DOX was added at D1 and Anti-β-ACTIN antibody blot was used for loading control.

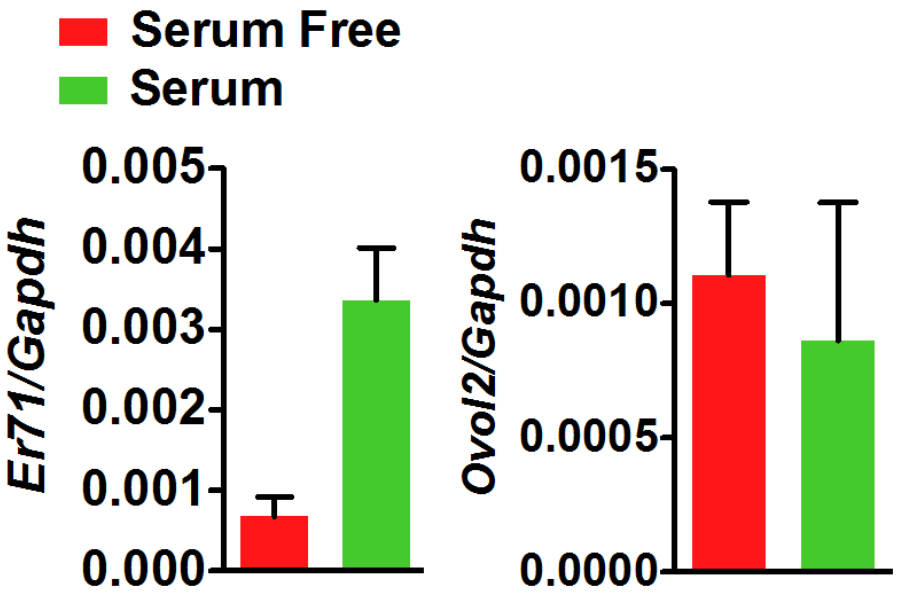

Figure S8. Comparison of *Er71* and *Ovol2* in serum and serum free conditions. A2 ESCs (parental ESCs for generating DOX inducible cell lines) were differentiated in either in a serum-free media for 4 days or in a serum-containing media for 3.5 days, and subjected to qRT-PCR analysis.

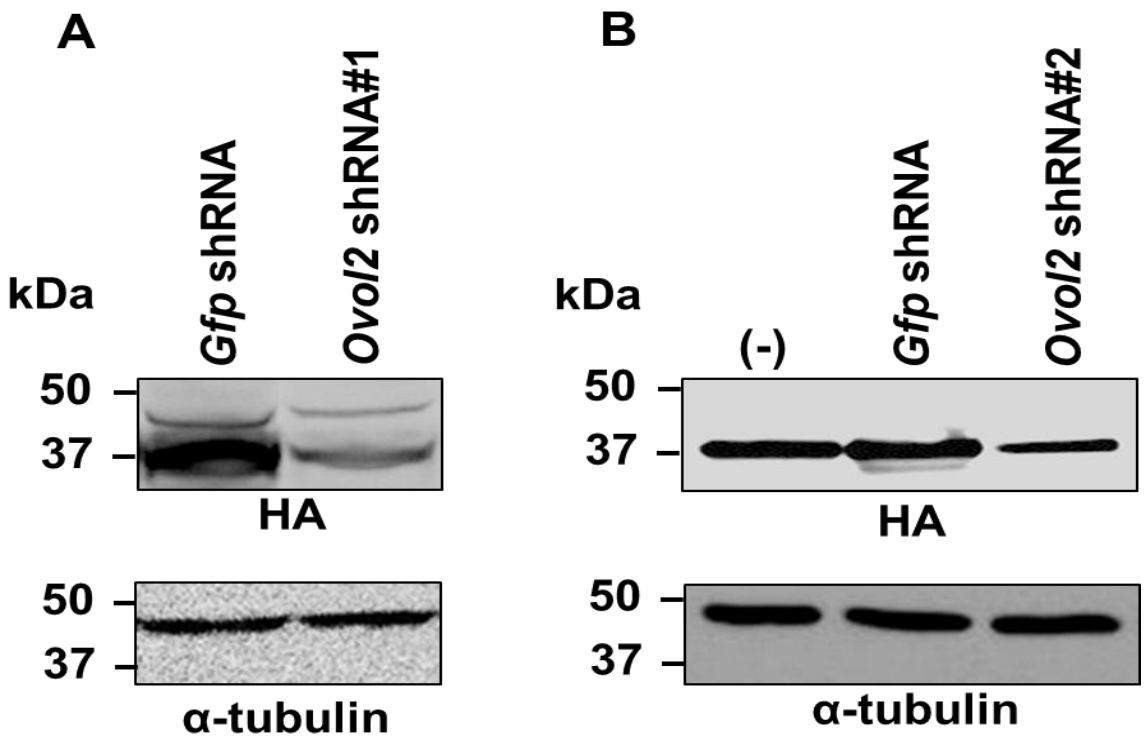

Figure S9. Confirmation of *Ovol2* knockdown in 293T cells. 293T cells infected with shRNAs against either coding region of OVOL2 (A, shRNA#1) or 3'UTR (B, shRNA#2) were transfected with HA-tagged OVOL2 and the expression of OVOL2 was examined by immunoblotting with anti-HA tag antibody. *Gfp* shRNA denotes sham infection with shRNA against *Gfp*. (-) in (B) denotes HA-OVOL2 transfection control without any shRNA infection

CHAPTER III

ETV2/ER71 regulates the generation of FLK1^{+} cells from mouse embryonic stem cells through miR-126-MAPK signaling

The results are being assembled for submission.

ETV2/ER71 regulates the generation of FLK1^{+} cells from mouse embryonic stem cells through miR-126-MAPK signaling

Ju Young Kim,[1,2,3] Dong Hun Lee,[1,2] Heesang Song,[1,6] Joo Kyung Kim,[1,2] Kanghyuck Kwon,[1] Christina Chang,[1] Manali Rupji,[5] Bhakti Dwivedi,[5] Jeanne Kowalski,[5] Tae-Min Kim,[7] and Changwon Park[1,2,3,4,#]

[1]Department of Pediatrics, [2]Children's Heart Research and Outcomes Center, [3]Molecular and Systems Pharmacology Program, [4]Biochemistry, Cell Biology and Developmental Biology Program, [5]Winship Cancer Institute, Emory University School of Medicine, [6]Department of Biochemistry and Molecular Biology, Chosun University School of Medicine, Gwangju, Republic of Korea, [7]Graduate School of International Agricultural Technology, Seoul National University, Pyeongchang-gun, Gangwon-do, Republic of Korea

[#]Correspondence: Changwon Park, Ph.D. Department of Pediatrics, Emory University School of Medicine, 2015 Uppergate Dr. Atlanta, GA, 30322, USA. Email:cpark23@emory.edu, Tel:404-727-7143, Fax:404-727-5737

Running Title: FLK1^{+} cell generation via ETV2-miR126-MAPK

Abstract

Previous studies including ours have demonstrated a critical function of the transcription factor ETV2 (also known as ER71) in determining the fate of cardiovascular lineage development. However, the underlying mechanisms of ETV2 remains largely unknown. In this study, we demonstrated the novel function of miR-126-MAPK pathway in ETV2-mediated $FLK1^+$ cell generation from mouse embryonic stem cells (mESCs). By performing a series of experiments including miRNA-sequencing and ChIP-PCR, we found that miR-126 is directly induced by ETV2. Further, miR-126 positively regulates the generation of $FLK1^+$ cells by activating the MAPK pathway through SPRED1 targeting and JUN/FOS activate the enhancer region of FLK1 through AP1 binding sequences. Therefore, our findings provide a novel molecular mechanism of ETV2 function in regulating cardiovascular development.

Introduction

ETV2, a member of the ETS transcription factor family, has been reported as an indispensable factor in establishing cardiovascular system (Oh et al., 2015; Sumanas and Choi, 2016). We previously demonstrated that deficiency in *Etv2* led to embryonic lethality due to a complete lack of both vascular and hematopoietic compartments (Lee et al., 2008b; Liu et al., 2012b). We also showed that ETV2 can directly bind the promoters/enhancers present on endothelial and hematopoietic genes including *Flk1* (Lee et al., 2008b; Liu et al., 2012b; Liu et al., 2015). Together with the findings that ETV2 can induce de novo generation of $FLK1^+$ cells, the multipotent progenitor for blood, endothelial and cardiac lineages from mouse embryonic stem cells (mESCs) (Lee et al., 2008b), these results strongly suggest the critical function of ETV2 for the establishment of the circulatory system. Reports from other groups further support the importance of ETV2 in this process (Ferdous et al., 2009b; Kataoka et al., 2011a; Neuhaus et al., 2010a; Sumanas and Lin, 2006). Regarding the regulatory mechanisms of ETV2 functions, several studied dealing with ETV2 binding proteins have been reported. For example, some reports show that the interaction between ETV2 and FOXC2 plays an important role in regulating several key genes of endothelial and hematopoietic lineages (De Val et al., 2008b; Veldman and Lin, 2012). Also, our recent study revealed the functional significance of ETV2-OVOL2 interaction in generating $FLK1^+$ cells and its further differentiation into hematopoietic and endothelial cells (Kim et al., 2014). However, the detailed molecular insight into ETV2 function remains largely unknown.

Micro RNAs (miRNAs) are short noncoding RNAs that target mRNAs for degradation or translational repression (Bartel, 2009). Transcribed by RNA polymerase II in the

nucleus, pri-miRNAs are processed into pre-miRNAs by microprocessor complex, which include RNase III enzyme Drosha, and other factor DGCR-8. Then, pre-miRNA exported into cytosol through Exportin-5. Transported pre-miRNA further processed as mature miRNAs via another RNase III enzyme Dicer, and TRBP, and other factor. This mature miRNAs are approximately 20-22 base pair duplexes. In the cytoplasm, the mature miRNA duplex is incorporated into the RNA-induced silencing complex (RISC), where the unwound duplex binds to the 30 bp untranslated regions through a complementary match. Studies have demonstrated the importance of miRNAs in cardiovascular system development and function (Liu and Olson, 2010). Among them, miRNA-126 has been an active target for investigation due to its diverse and important role in biological processes (Chistiakov et al., 2016). In addition to well-known function of miR-126 in post-natal hematopoiesis and angiogenesis (Chistiakov et al., 2016), several studies reported embryonic function of miR-126 in hematopoietic and endothelial cell development. Sturgeon et al showed that mesenchymal miR-126 can regulate primitive erythropoiesis by a VCAM1-Src kinase axis (Sturgeon et al., 2012). However, inhibitory function of miR-126 in erythropoiesis has been revealed in zebrafish and human ESCs. Knockdown of miR-126 in zebrafish enhances erythropoiesis with concomitant reduction of thrombopoiesis (Grabher et al., 2011). hESCs that overexpress miR-126, generated reduced number of erythrocyte colonies upon differentiation (Huang et al., 2011), suggesting context-dependent functions of miR-126 in embryonic hematopoiesis. Vascular function of miR-126 is conserved in different experimental settings. It was shown that depletion of miR-126 in developing mouse embryos results in embryonic lethality and showed defective vascular integrity as well as hemorrhaging (Kuhnert et al., 2008; Wang et al., 2008). A similar vascular defects were observed in zebrafish received miR-126 morpholino (Fish et al., 2008).

Taken together, these results suggest the important role of miRNA-126 in blood and endothelial cell development.

During embryonic development, various developmental processes are mediated by growth factor-induced signaling pathways via the receptor tyrosine kinase (RTK)-MAPK pathway (Basson, 2012). Studies indicate important function of the RTK-MAPK pathway during the development of the mesoderm and its derivatives including hematopoietic and endothelial cells. For example, MAPK activity is closely associated with the mesoderm induction in Xenopus (Hartley et al., 1994). In subsequent studies, the mesoderm inductive role of MAPK was reported from Xenopus with constitutive forms of MEK or MAPK as well as MAPK specific phosphatase (Gotoh et al., 1995; Umbhauer et al., 1995). In mouse embryos, activated ERK1/2 is detected in the blood islands, the first sites of blood and endothelial cell development and later in the dorsal aorta and intersomatic vessels (Corson et al., 2003). Further, *Erk2* deficient mouse embryos are incompatible with proper mesoderm formation (Saba-El-Leil et al., 2003; Yao et al., 2003). Sprouty/Spred proteins, the negative effectors for Ras/MAPK pathway (Casci et al., 1999; Wakioka et al., 2001), have inhibitory functions in generating mesoderm and blood as well as vessel development (Muhl et al., 2015; Nobuhisa et al., 2004; Sivak et al., 2005; Taniguchi et al., 2007). Taken together, these results suggest that the MAPK pathway performs an important function for mesoderm formation and thereafter in the development of its downstream lineages including blood and endothelial cells. However, mechanisms by which MAPK can regulate emergence of mesoderm with hematopoietic and endothelial potential remains elusive.

In an effort to investigate the machinery of ETV2 that regulates $FLK1^+$ cell generation from mESCs, we initially profiled miRNAs that are differentially regulated by ETV2 expression and found miR-126 as one of the key players of ETV2 function. Further, we showed that ETV2 directly induces the expression of miR-126, which in turn activates MKK1/ERK1/2 by targeting SPRED1, a negative regulator of the MAPK pathway. ETV2-mediated $FLK1^+$ cell generation was significantly decreased by inhibiting MAPK activity or by overexpressing SPRED1. Further, we showed Flk1 enhancer activation by AP1 via AP1 binding elements. These findings suggest a novel insight into ETV2's molecular mechanism; ETV2 regulates the generation of $FLK1^+$ cells partly through miR126/MAPK pathway in addition to its direct transcriptional activation function.

Materials and Methods

Cell culture and ES cell differentiation

Inducible Flag-mouse ETV2 ES cells (iETV2) (Kim JY et al. 2014), and *Etv2*$^{-/-}$ mouse ES cells (kindly provided by Dr. Kyunghee Choi at Washington University School of Medicine, St. Louis, MO) were maintained on mitomycin C treated MEF feeder cells in DMEM (Cellgro) containing 15% FBS (Atlanta Biologics), 50 units/50 µg/ml penicillin/streptomycin (Invitrogen), 1% MEM non-essential amino acids solution (Invitrogen), 2 mM L-glutamine (Invitrogen), 10^3 units/ml mouse Leukemia inhibitory Factor (LIF) (Millipore), 1.5 X 10^{-4} M 1-Thioglycerol (MTG) (Sigma). HEK 293T cells cultured in DMEM containing 10% FBS, 1% L-glutamine and 50 units/50 µg/ml penicillin/streptomycin. For serum differentiation, ES cells were cultured in IMDM (Invitrogen) containing 15% FBS (Atlanta Biologics), 2 mM L-glutamine (Invitrogen), 50 µg/ml Ascorbic acid (Sigma), 4.5X10^{-4} M MTG solution and 50 units/50 ug/ml

penicillin/streptomycin (Invitrogen). During the differentiation, 1 μg/ml Doxycyclin (Dox) was treated at day 1, and U0126 (5 μM, Tocris), and inactive analog of U0126, U0124 (5 μM, Tocris) treated at day 1.5. For serum free differentiation, ES cells were induced to differentiation in serum free conditioned medium (15% serum replacement (Invitrogen), 2mM L-glutamine, 50 μg/ml Ascorbic acid (Sigma), $4.5X10^{-4}$ M MTG in IMDM. The resulting cells were harvested at indicated times for the subsequent analysis as described below.

Cell sorting and flow cytometry analysis

Cells were dissociated with StemPro Accutase (Invitrogen) and the resulting single cell suspension was incubated for 20~30 minutes with PE-conjugated anti-mouse FLK1 monoclonal antibodies (1:200) (Biolegend) in FACS solution (4% FCS in PBS), followed by cell sorting with FACS ARIA II (Becton-Dickinson). For flow cytometry analysis, samples were prepared as the same way as the cell sorting and subjected to flow cytometry analysis with a BD LSRII (Beckton-Dickinson). Data were analyzed with FlowJo ver.10.

Construction of small RNA libraries

Samples were prepared in the same manner as for cell sorting. RNA were isolated from the cells by using Trizol (Invitrogen). Construction of libraries and sequencing on the Illumina HiSeq2500 were performed at the W. M. Keck Center for Comparative and Functional Genomics at the University of Illinois at Urbana-Champaign. Small RNA libraries were constructed from the RNA isolated from sorted $FLK1^{+}$ cells using the TruSeq small RNA Sample Preparation Kit (Illumina). The individually-barcoded libraries were mixed into a pool, which was size, selected on a Novex 10% TBE gel

(LifeTechnologies) to enrich for small RNAs 17nt to 30nt in length. The final libraries were quantitated by Qubit (Life Technologies) and the average size was determined on an Agilent Bioanalyzer High Sensitivity DNA chip (Agilent Technologies) and diluted to 10 nM. The pooled libraries were further quantitated by qPCR on an ABI 7500 (Life Technologies).

Sequencing on an Illumina HiSeq 2000/2500

The pooled libraries were loaded onto one lane and two lanes of an 8-lane flowcell for cluster formation and sequenced on an Illumina HiSeq 2000 and HiSeq 2500. One of the lanes was loaded with a PhiX Control library that provides a balanced genome for calculation of matrix, phasing and prephasing. The libraries were sequenced from one end of the molecules to a total read length of 50 nt. The raw .bcl files were converted into demultiplexed fastq files with Casava 1.8.2 (Illumina).

miRNA sequencing data analysis

The quality of the single-ended miRNA sequencing data was assessed using FastQC (Andrews, 2010). The 3'-adaptor and low-quality sequences were trimmed using cutadapt (v 1.4.2) (Martin, 2011) with the command options: cutadapt -a TGGAATTCTCGGGTGCCAAGGAACTCCAGTCAC -O 5 -m 16 -q 30 --discard-untrimmed <raw_reads_fastq_file> <trimmed_reads_fasta_file>. The length distribution of resulting reads was centered around 22nt and 32nt suggesting a reliable miRNA sequencing. The trimmed reads were mapped to the mouse reference genome (GRCm38/mm10; https://genome.ucsc.edu/index.html) and analyzed using miRDeep2 package (v2.0.0.8) (Friedlander et al., 2012). The reads were preprocessed using mapper module of miRDeep2 with the command options: perl

mapper.pl <trimmed_collapsed_reads_fasta_file> -e -h -j -k TGGAATTCTCGGGTGCCAAGGAACTCCAGTCAC -l 17 -m -p <mm10_cluster> -s <reads_fasta_file> -t <trimmed_collapsed_vs_genome.arf> –v. The miRNA expression levels of known mature miRNAs were measured using the quantifier module with command options: perl quantifier.pl -p <mm10_hairpin.fa> -m <mm10_mature.fa> -r <trimmed_collapsed_reads_fasta_file> -t Mouse -y <output_file>. The novel miRNAs were also predicted using the miRDeep2 module with command options: perl miRDeep2.pl <trimmed_collapsed_reads_fasta_file> <mm10_chromFa_1_22.fa> <trimmed_collapsed_vs_genome.arf> <mm10_mature.fa> none <mm10_hairpin.fa> -t Mouse. Novel miRNAs with significant randfold p-value were kept for further analysis. All published mature miRNA precursors and hairpins for the mouse genome were downloaded from miRBase release 21 (http://www.mirbase.org/). The raw expression counts from both known and novel miRNAs for all four samples were normalized using DESeq package (Love et al., 2014) and log2 transformed. A total of 2240 known and 119 novel miRNAs were detected.

Differential expression analysis of miRNAs

Differentially expressed miRNAs were identified using the Moderated t-test available in ‘limma’ R package (Ritchie et al., 2015). An FDR adjusted p-value was calculated and applied. The miRNAs with ≥ 1.5 fold change and an FDR ≤ 0.05 were considered to be significantly differentially expressed, resulting in a total of 67 miRNAs (30 up-regulated and 37 down-regulated). Unsupervised hierarchical clustering was performed with 1-pearson correlation distance and average linkage clustering method as implemented in NOJAH (http://bbisr.shinyapps.winship.emory.edu/NOJAH/).

Functional annotation analysis of significant known miRNAs

Predicted miRNA target genes and interactions were identified using the DIANA-microT-CDS algorithm (v3.0) (Vlachos et al., 2015). KEGG and GO analyses were conducted on the predicted targets of known 22 up-regulated and known 33 down-regulated differentially expressed miRNAs.

Real time quantitative reverse transcription PCR

One μg of total RNA prepared using Trizol (Invitrogen) was treated with DNase I (Invitrogen), then reverse transcribed with Superscript IV cDNA synthesis kit according to the manufacture's protocol (Invitrogen). Each gene expression was amplified and detected by using IQ-SYBR Green (Biorad) with ABI 7500Fast (ABI). The result was normalized by *Gapdh* expression. cDNA generation and measurement of miRNA-126-3p and -5p expression were performed by using miScript PCR starter kit (Qiagen) with ABI 7500Fast. Each miRNA expression was normalized by snRNA RNU6B (RNU6-2, Qiagen). Each experiment with duplicates was performed at least three times. Primers in Table 1.

Plasmid constructs and Luciferase assay

The PCR amplified *Egfl7* promoter fragment from mouse ES cell was inserted into the pGL3-Basic (Promega) using primers described in Table1. *Flk1* promoter/enhancer in pGL3-basic was a gift from Dr. Kyunghee Choi (Washington University School of Medicine, St. Louis, MO). The *Egfl7* promoter mutant constructs were generated by site direct mutagenesis to mutate ETS DNA binding site. HEK/293T cells in 12 wells (4×10^4 cells/well) were co-transfected with 40 ng of p-RL-null (Promega), 200 ng of each Firefly reporter construct, and 1.2 μg of ETV2, MKK 8E, c-JUN, c-FOS or c-JUN

dominant negative in mammalian expression vector using Lipofectamine 2000 (Invitrogen). Cells were collected after 48 hours of transfection and renilla and firefly luciferase activity were measured by using Dual-Luciferase reporter assay system according to manufacturer's instruction (Promega). Firefly luciferase activity was normalized to Renilla luciferase activity to control to transfection efficiency. Each experiment with duplicates was performed at least three times.

Chromatin Immunoprecipitation Assay (buffer contents as well)

The procedure was previously described (Lee et al., 2008b). Briefly, iFLAG-ETV2 ES cells at day 3.5 of differentiation were cross-linked with 1% formaldehyde and lysed with cell membrane lysis buffer [5 mM PIPES, 85 mM KCl, 0.5% NP-40, Protease inhibitors cocktail (SIGMA)]. The resulting nuclear fraction was further lysed with nuclear membrane lysis buffer (10 mM EDTA, 1% SDS in Tris-HCl) and subjected to sonication on ice (Bioruptor, Diagenode). The solution containing sonicated chromatin was precleared with agarose A/G beads (Santacruz) and the supernatant was subsequently incubated with 5 µg of anti-FLAG monoclonal antibody (Sigma). Immunoprecipitated DNA fragments were isolated and subjected to qRT-PCR to measure protein binding on *Egfl7* promoter. Primers listed in Table1. Mouse IgG (SantaCruz) was used for negative control.

Western Blot analysis

Briefly, cells at day 4 of differentiation were lysed by RIPA buffer with phosphatase inhibitor (Sigma) and protease inhibitor (Sigma-Aldrich), 0.1M PMSF and the cell lysates was subjected to SDS-PAGE, followed by a western analysis with rabbit anti-

phospo-ERK1/2 (1:1000) (Cell signaling), rabbit anti-ERK1/2 (1:1000) (cell signaling), rabbit anti-SPREAD1 (1:1000) (Millipore), or mouse anti-β-ACTIN (Sigma)

Lentivirus generation and transduction

All lentiviral particles were generated by calcium phosphate transfection methods and concentrated as described previously (blood and nature protocol). pCMV- Lenti-III-miR-126 premature or pCMV-Lenti-III-empty control plasmid (Abm) was co-transfected with pCMV-dr8.2-dvpr and pCMV-VSV-G, ratio as 10:5:1. Forty-eight hours later, supernatant was collected, centrifuged, filtered using 0.45 μm PES filter, and precipitated with 22.5% PEG 6000 (Sigma) and 9.9% 4M NaCl for 90 minutes at 4 ^{o}C. Following centrifugation at 3500g for 60 minutes, the resulting pellets were resuspended with PBS, and stored -80 ^{o}C. The titer of viral particles was determined by qPCR lentivirus titration kit (Abm). For the transduction, *Etv2*$^{-/-}$ ESCs in 6 well plates (1 x 10^5 cells/well)) were incubated with control or miR-126 viral particles (25 moiety of infection) by centrifugation at 2250 rpm for 90 minutes. Subsequently, the cells were differentiated for further analysis.

Statistics

The results of luciferase assay, ChIP-PCR, Western blot, qRT-PCR and FACS analysis were analyzed by Student *t* test. P value less than 0.05 was regarded significant.

Results

ETV2 mediated miRNA sequencing profiling

Since miRNAs known to be critical for cardiovascular system development (Liu and Olson, 2010), we performed miRNA profiling analysis to better understand the function of ETV2 in the generation of hematopoietic and endothelial lineage cells. To this end, doxycycline inducible ETV2 in mESC (herein, iFLAG-ETV2 ESCs) were differentiated and treated with or without Dox at day 1 of differentiation. $FLK1^+$ cells at day 3.5 were FACS-sorted and subjected to miRNA sequencing (**Fig. 1A**). Differentially expressed miRNAs were identified using the Moderated t-test available in 'limma' R package (Ritchie et al., 2015). The miRNAs with ≥ 1.5 fold change and an FDR ≤ 0.05 were considered to be significantly differentially expressed, resulting in a total of 67 miRNAs of interest (30 up-regulated and 37 down-regulated), which were subsequently subjected to unsupervised hierarchical clustering (**Fig. 1B-C**). KEGG analysis shows that the ETV2-mediated miRNAs regulate the MAPK pathway and the WNT pathway, all of which are critical for cardiovascular development (**Fig. 1D**). Also, GO term analysis shows that 15 miRNAs among 67 miRNAs are involved in vasculogenesis and 46 miRNAs regulate embryo development (**Fig. 1E**).

Among the differentially regulated miRNAs was miRNA-126 that drew our attention as an important player of ETV2-mediated $FLK1^+$ cell generation. As discussed, miR126 has been involved in vascular and hematopoiesis as well as in angiogenesis by targeting various genes such as *Spred1, Vcam1,* and *Pik3r2* (Fish et al., 2008; Sturgeon et al., 2012; Wang et al., 2008). Independently, our previous reports showed that *Egfl7*, host gene of *miR-126*, is one of the most upregulated genes upon ETV2

overexpression (Liu et al., 2012b). Accordingly, we sought to determine the functional consequence of miR126 in regulating ETV2-mediated FLK1$^+$ cell generation.

ETV2 directly activate the expression of miR-126 through *Egfl7* promoter.

First, we compared the expression of *miR-126* and *Egfl7*, the gene containing *miR-126* in the 7th intron (Kuhnert et al., 2008), to that of ETV2 in differentiating mESCs. We found that *Egfl7* and *miR-126* (both 3p and 5p) were significantly upregulated in response to Dox treatment (i.e., *Etv2* overexpression) (data not shown). FLK1$^+$ cells sorted from day 3.5 of differentiation in the presence of Dox also showed a greater expression of both genes, compared to FLK1$^+$ cells in the absence of Dox (**Fig. 2A**). These results suggest functional links between ETV2 and miR-126 in the generation of FLK1$^+$ cells from mouse ESCs.

Next, we examined whether ETV2 can directly activate the promoter of *Egfl7*, thus inducing the expression of miR126. We performed a luciferase-based promoter assay. From the literature search and our own investigation, we found the highly conserved upstream region of the transcription start site in mouse and human EGFL7 in which has two conserved potential ETS binding sites (**Fig. 2B**). By performing the promoter assay we discovered that the overexpression of *Etv2* significantly increased the activity of the *Egfl7* promoter. However, the *Egfl7* promoter construct with mutations on one putative ETS site failed to respond to ETV2, suggesting ETV2 as a direct upstream regulator of *Egfl7* (**Fig. 2C**). Next, to validate the luciferase results and determine the in vivo occupancy of ETV2 on the upstream region of *Egfl7*, we first analyzed the ETV2-chromatin immunoprecipiation (ChIP) sequencing results (Liu et al., 2015) and found ETV2 binding peaks in the upstream region of *Egfl7* that we

determined for the luciferase assay (data not shown). Importantly, the binding of ETV2 in the genomic region of *Egfl7* was validated by ChIP-PCR with day 3.5 EBs (embryoid bodies, cell aggregates of differentiating ESCs) of iFLAG-ETV2 ESCs (**Fig. 2D**). Taken together, we conclude that the expression of *Egfl7* and thus *miR-126* is directly regulated by ETV2 in differentiating mESCs.

The miR-126/MAPK pathway plays an important role for ETV2-induced FLK1$^+$ cell generation.

To get the functional consequence of miR126 in ETV2-mediated FLK1$^+$ cell generation, we first performed a rescue experiment by introducing miR-126 into *Etv2*$^{-/-}$ ESCs and confirmed transgenic expression of *miR-126* (data not shown). As shown in **Fig, 2E**, *Etv2*$^{-/-}$ ESCs overexpressing miR-126 generated increased number of FLK1$^+$ cells, compared to control (*Etv2*$^{-/-}$ ESCs transfected with empty vector) as demonstrated with differentiation and flow cytometry analysis, suggesting an important function of miR-126 in ETV2-induced FLK1$^+$ cell generation. Next, to investigate how miR-126 regulates development of FLK1$^+$ cells in response to ETV2, we first investigated the downstream targets of miR-126. From previous findings, it was shown that miR-126 controls angiogenesis by regulating the MAPK pathway through the suppression of the expression of SPRED1, a negative regulator of the MAPK pathway (Casie Chetty et al., 2017; Wakioka et al., 2001). Together with the report that bFGF treatment increases the generation of FLK1$^+$ cells from mESCs (Faloon et al., 2000), we hypothesized that ETV2 induces FLK1$^+$ cells partly through the miR-126-MAPK pathway by suppressing the expression of SPRED1. To test the hypothesis, we first differentiated iFLAG-ETV2 ESCs in the presence or absence of DOX and performed a western blot analysis for MAPK phosphorylation and SPRED1. As shown in **Fig. 3A-**

B, while SPRED1 was significantly reduced in response to ETV2, augmented phospho-ERK1/2 level was evident upon ETV2 overexpression. Interestingly, *Etv2*$^{-/-}$ ESCs showed increased level of SPRED1 expression with concomitant decrease of phosphorylated ERK1/2, further validating ETV2-dependent regulation of SPRED1 and MAPK activity in differentiating ESCs.

To understand the functional significance of the MAPK/SPRED regulation by ETV2, we sought to determine whether MAPK activity is critical for ETV2-mediated FLK1^{+} cell generation. To this end, iFLAG-ETV2 ESCs differentiated with Dox were treated with U0126, a MAPK inhibitor, and subjected to flow cytometry for FLK1 expression. U0124 served as a negative control for U0126. As shown in **Fig. 3C-C',** ETV2-induced FLK1^{+} cell generation at day 3.5 of differentiation was significantly reduced in the U0126 treated group (+DOX vs. +DOX+U0126, Serum: 44.5 % vs. 26.3, Serum Free: 38.3% vs. 24.4%). To corroborate the findings, we generated iETV2-MKK1 8E in which both ETV2 and a catalytically inactive form of MKK1 (Mansour et al., 1994) are co-overexpressed upon Dox treatment. In agreement with the inhibitor treatment (**Fig. 3C**), overexpression of MKK1 8E together with ETV2 led to decreased generation of FLK1^{+}, compared to the group in which ETV2 is overexpressed (**Fig. 3D**). Additionally, we went on to show that overexpression of SPRED1 was able to inhibit the generation of FLK1^{+} cells induced by overexpression of ETV2 (**Fig. 3D**). These results clearly suggest that the MAPK-SPRED1 pathway plays an important role for ETV2-induced FLK1^{+} cell generation from mESCs.

Direct activation of FLK1 gene expression by the MAPK pathway

Next, to get a detailed insight into how the MAPK pathway activated by ETV2 regulates the generation of FLK1^{+} cells, we examined the regulatory elements such as promoter and enhancer of *Flk1* gene (Kappel et al., 1999) and found several potential AP1 binding sequences in *Flk1* enhancer (**Fig. 4A**). To examine if the MAPK pathway can directly activate *Flk1* gene expression, we performed a series of luciferase-based promoter assay. MKK1R4F, a constitutively active form of MKK1 (Mansour et al., 1994), significantly activated the *Flk1*-promoter/enhancer (*Flk1-p/e*)-driven luciferase activity, but the kinase dead mutant of MKK1, MKK1 8E failed to activate it (**Fig. 4B**). In line with the results (Fig xx), ETV2-induced activation of *Flk1-p/e* was significantly impaired upon expression of MKK1 8E, further supporting the importance of the MAPK pathway in ETV2-incuded *Flk1* expression (**Fig. 4B**). To further determine whether the activity of the *Flk1-p/e* was increased in response to c-JUN/FOS, the downstream effectors of the MAPK pathway, we again performed the luciferase-based promoter assay and found that overexpression of c-JUN/FOS indeed activated *the Flk1-p/e* (**Fig. 4B**). Also, we showed that JUN dominant negative mutant (Wang et al., 2005b) inhibited ETV2 function in activating *Flk1-p/e* (**Fig. 4B**). Importantly, mutations on the putative AP-1 binding site in the *Flk1-p/e* led to a significantly reduced the luciferase activity induced by c-JUN/FOS (**Fig. 4C**). Collectively, these results suggest that the MAPK pathway activates the expression of *Flk1* gene through c-JUN/FOS.

Acknowledgements

This work was supported by the March of Dimes Foundation, 5-FY12-44 (to C.P.), the American Heart Association, 11SDG7390074 (to C. P.), NIH HL119291 (to C.P.).

Author contributions

J.Y.K., D.H.K., H.S., J.K.K., performed experiments and analyzed data; K.K., C.C., performed experiments; M.R., B.D., J.K., analyzed data, C.P., conceived, designed and performed experiment, analyzed and interpreted data and wrote the manuscript.

Disclosure of Conflicts of Interest

The authors declare no conflict of interests.

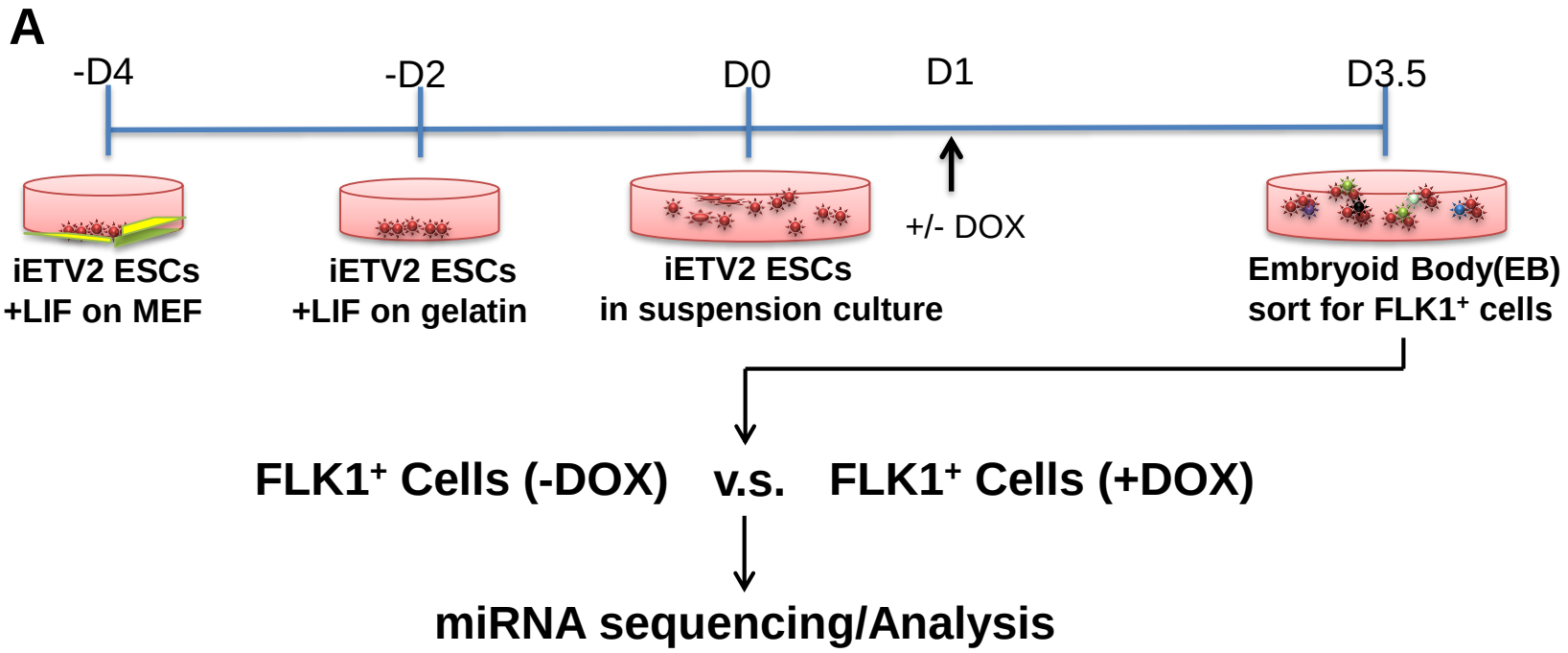
A
-D4
-D2
D0
D1
D3.5
+/- DOX
iETV2 ESCs
+LIF on MEF
iETV2 ESCs
+LIF on gelatin
iETV2 ESCs
in suspension culture
Embryoid Body(EB)
sort for FLK1+ cells
FLK1+ Cells (-DOX) v.s. FLK1+ Cells (+DOX)
miRNA sequencing/Analysis

Figure 1A

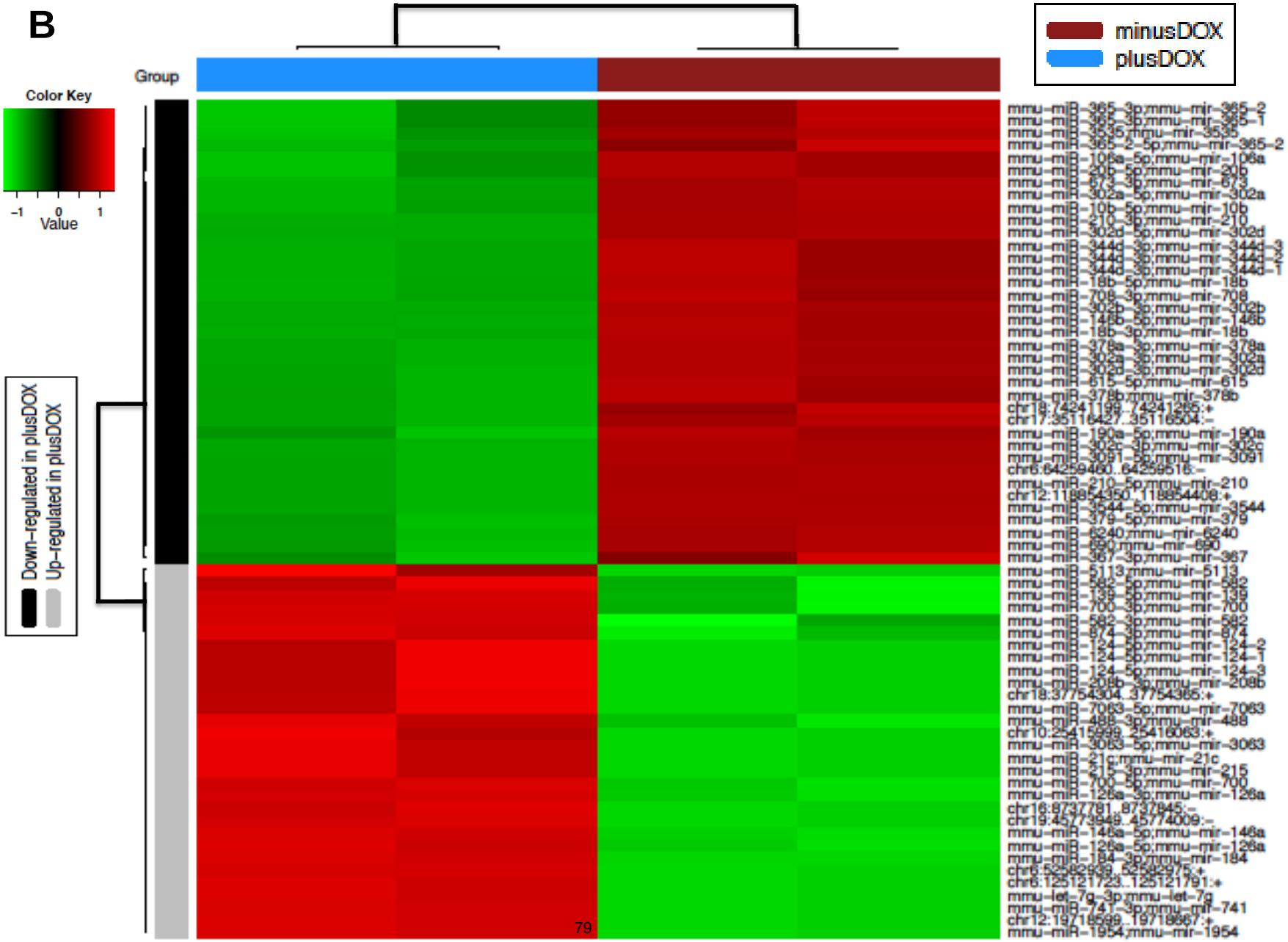
B
Group
minusDOX
plusDOX
Color Key
−1
0
1
Value
Down−regulated in plusDOX
Up−regulated in plusDOX
mmu−miR−365−3p;mmu−mir−365−2
mmu−miR−365−3p;mmu−mir−365−1
mmu−miR−3535;mmu−mir−3535
mmu−miR−365−2−5p;mmu−mir−365−2
mmu−miR−106a−5p;mmu−mir−106a
mmu−miR−20b−5p;mmu−mir−20b
mmu−miR−673−3p;mmu−mir−673
mmu−miR−302a−5p;mmu−mir−302a
mmu−miR−10b−5p;mmu−mir−10b
mmu−miR−210−3p;mmu−mir−210
mmu−miR−302d−5p;mmu−mir−302d
mmu−miR−344d−3p;mmu−mir−344d−3
mmu−miR−344d−3p;mmu−mir−344d−2
mmu−miR−344d−3p;mmu−mir−344d−1
mmu−miR−18b−5p;mmu−mir−18b
mmu−miR−708−3p;mmu−mir−708
mmu−miR−302b−3p;mmu−mir−302b
mmu−miR−146b−5p;mmu−mir−146b
mmu−miR−18b−3p;mmu−mir−18b
mmu−miR−378a−3p;mmu−mir−378a
mmu−miR−302a−3p;mmu−mir−302a
mmu−miR−302d−3p;mmu−mir−302d
mmu−miR−615−5p;mmu−mir−615
mmu−miR−378b;mmu−mir−378b
chr19:7424199..7424285:+
chr17:35116427..35116504:−
mmu−miR−190a−5p;mmu−mir−190a
mmu−miR−302c−3p;mmu−mir−302c
mmu−miR−3091−5p;mmu−mir−3091
chr6:64259460..64259516:−
mmu−miR−210−5p;mmu−mir−210
chr12:118854350..118854408:+
mmu−miR−3544−5p;mmu−mir−3544
mmu−miR−379−5p;mmu−mir−379
mmu−miR−6240;mmu−mir−6240
mmu−miR−690;mmu−mir−690
mmu−miR−367−3p;mmu−mir−367
mmu−miR−5113;mmu−mir−5113
mmu−miR−582−5p;mmu−mir−582
mmu−miR−139−5p;mmu−mir−139
mmu−miR−700−3p;mmu−mir−700
mmu−miR−582−3p;mmu−mir−582
mmu−miR−874−3p;mmu−mir−874
mmu−miR−124−5p;mmu−mir−124−2
mmu−miR−124−5p;mmu−mir−124−1
mmu−miR−124−5p;mmu−mir−124−3
mmu−miR−208b−3p;mmu−mir−208b
chr18:37754304..37754365:+
mmu−miR−7063−5p;mmu−mir−7063
mmu−miR−488−3p;mmu−mir−488
chr10:25415999..25416063:+
mmu−miR−3063−5p;mmu−mir−3063
mmu−miR−21c;mmu−mir−21c
mmu−miR−215−3p;mmu−mir−215
mmu−miR−700−5p;mmu−mir−700
mmu−miR−126a−3p;mmu−mir−126a
chr16:8737781..8737845:−
chr19:45773949..45774009:−
mmu−miR−146a−5p;mmu−mir−146a
mmu−miR−126a−5p;mmu−mir−126a
mmu−miR−184−3p;mmu−mir−184
chr6:52582909..52582975:+
chr6:125121723..125121791:+
mmu−let−7g−3p;mmu−let−7g
mmu−miR−741−3p;mmu−mir−741
chr12:19718599..19718667:+
mmu−miR−1954;mmu−mir−1954
79

Figure 1B

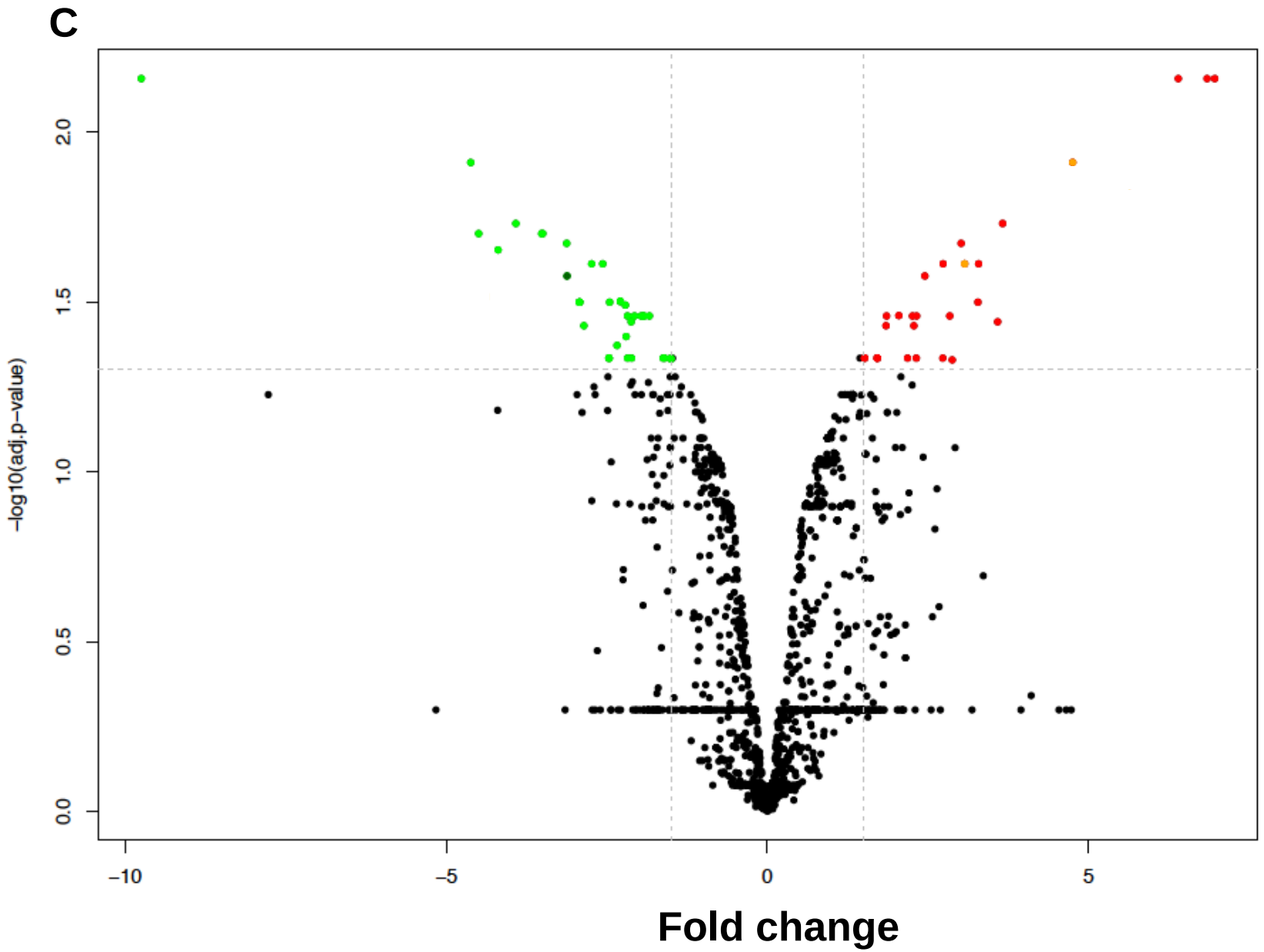

Figure 1C

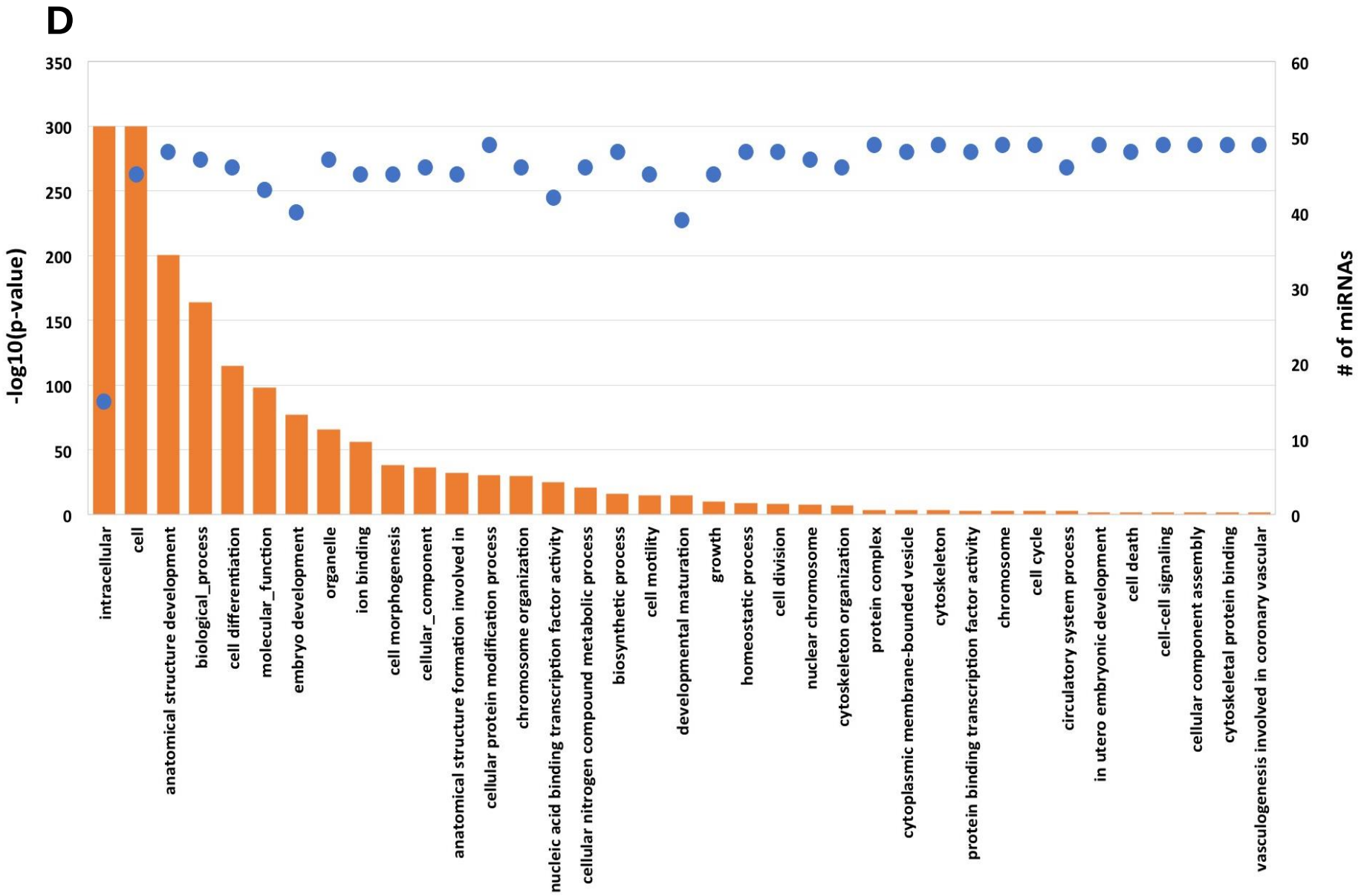
D
-log10(p-value)
# of miRNAs
350
300
250
200
150
100
50
0
60
50
40
30
20
10
0
intracellular
cell
anatomical structure development
biological_process
cell differentiation
molecular_function
embryo development
organelle
ion binding
cell morphogenesis
cellular_component
anatomical structure formation involved in
cellular protein modification process
chromosome organization
nucleic acid binding transcription factor activity
cellular nitrogen compound metabolic process
biosynthetic process
cell motility
developmental maturation
growth
homeostatic process
cell division
nuclear chromosome
cytoskeleton organization
protein complex
cytoplasmic membrane-bounded vesicle
cytoskeleton
protein binding transcription factor activity
chromosome
cell cycle
circulatory system process
in utero embryonic development
cell death
cell-cell signaling
cellular component assembly
cytoskeletal protein binding
vasculogenesis involved in coronary vascular

Figure 1D

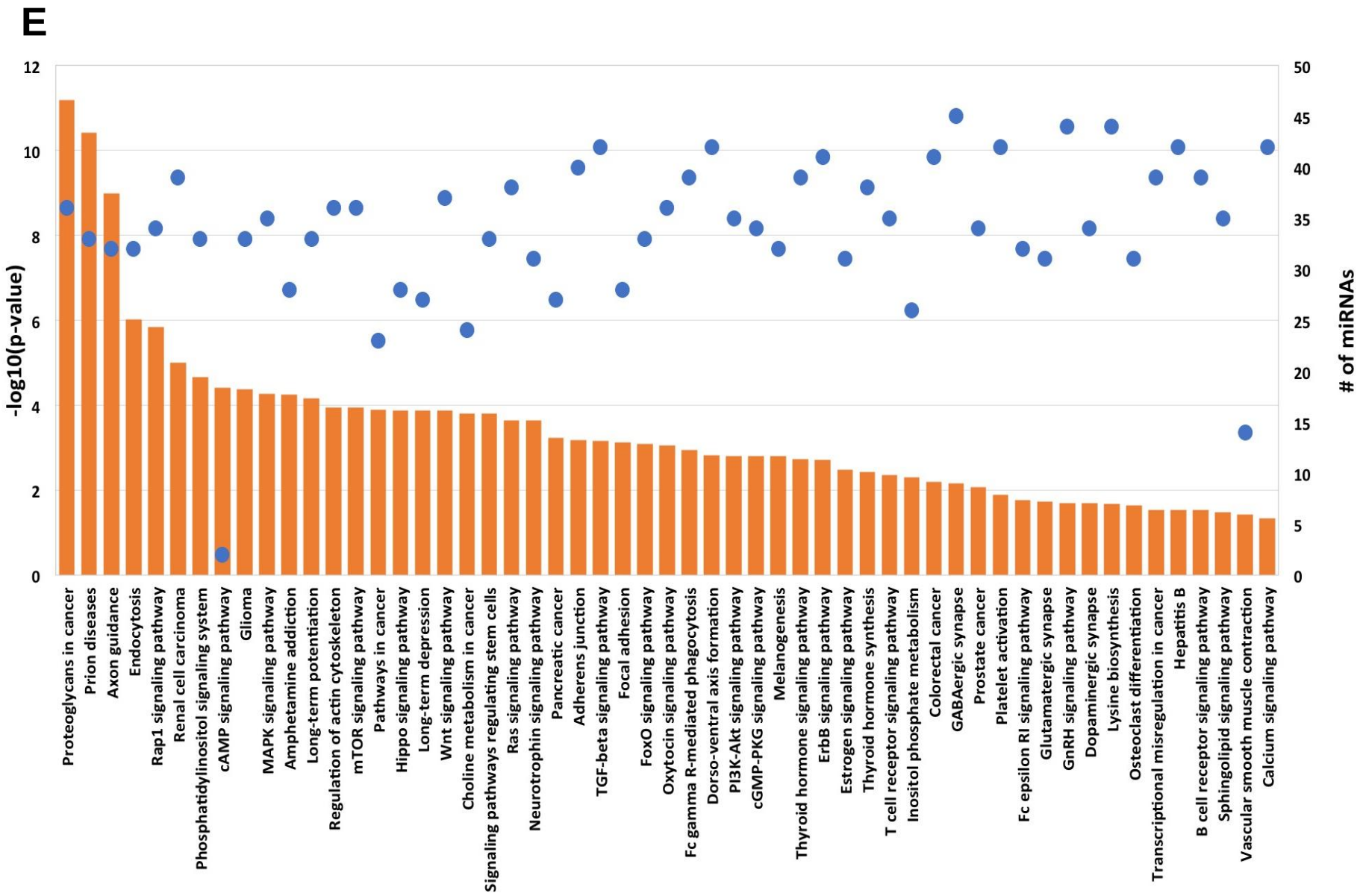
E
-log10(p-value)
# of miRNAs
0
2
4
6
8
10
12
0
5
10
15
20
25
30
35
40
45
50
Proteoglycans in cancer
Prion diseases
Axon guidance
Endocytosis
Rap1 signaling pathway
Renal cell carcinoma
Phosphatidylinositol signaling system
cAMP signaling pathway
Glioma
MAPK signaling pathway
Amphetamine addiction
Long-term potentiation
Regulation of actin cytoskeleton
mTOR signaling pathway
Pathways in cancer
Hippo signaling pathway
Long-term depression
Wnt signaling pathway
Choline metabolism in cancer
Signaling pathways regulating stem cells
Ras signaling pathway
Neurotrophin signaling pathway
Pancreatic cancer
Adherens junction
TGF-beta signaling pathway
Focal adhesion
FoxO signaling pathway
Oxytocin signaling pathway
Fc gamma R-mediated phagocytosis
Dorso-ventral axis formation
PI3K-Akt signaling pathway
cGMP-PKG signaling pathway
Melanogenesis
Thyroid hormone signaling pathway
ErbB signaling pathway
Estrogen signaling pathway
Thyroid hormone synthesis
T cell receptor signaling pathway
Inositol phosphate metabolism
Colorectal cancer
GABAergic synapse
Prostate cancer
Platelet activation
Fc epsilon RI signaling pathway
Glutamatergic synapse
GnRH signaling pathway
Dopaminergic synapse
Lysine biosynthesis
Osteoclast differentiation
Transcriptional misregulation in cancer
Hepatitis B
B cell receptor signaling pathway
Sphingolipid signaling pathway
Vascular smooth muscle contraction
Calcium signaling pathway

Figure 1E

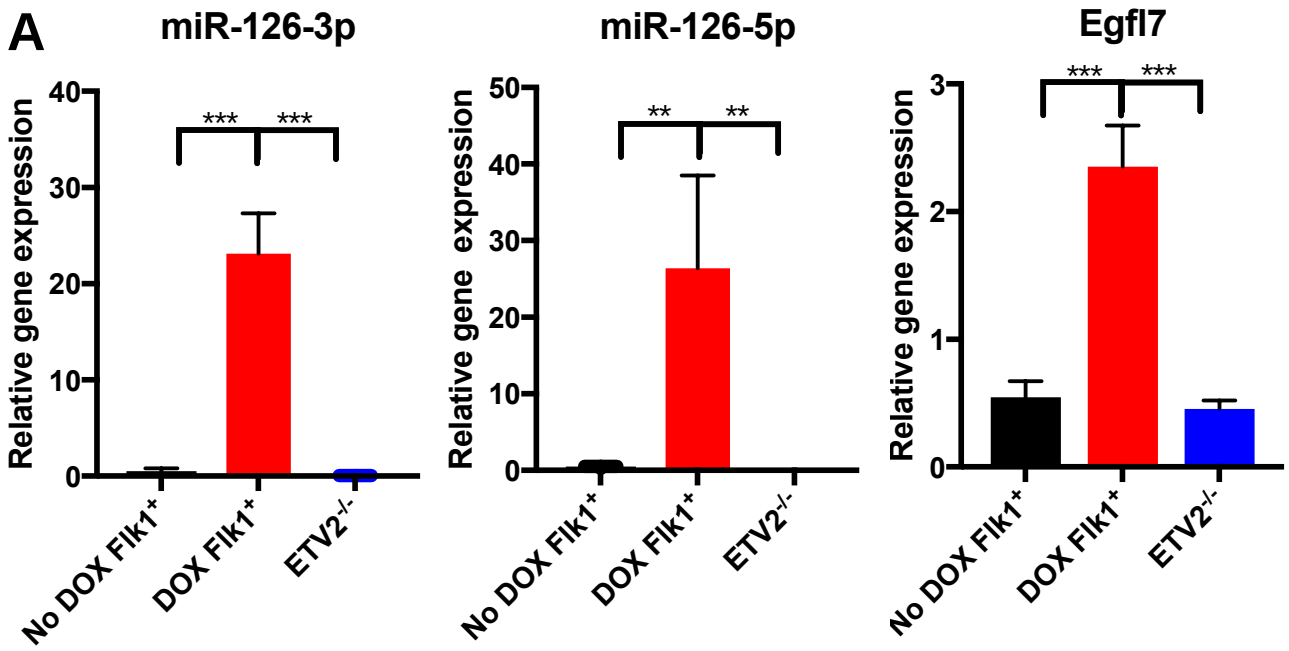
A
miR-126-3p
Relative gene expression
40
30
20
10
0
***
***
No DOX Flk1+
DOX Flk1+
ETV2-/-
miR-126-5p
Relative gene expression
50
40
30
20
10
0
**
**
No DOX Flk1+
DOX Flk1+
ETV2-/-
Egfl7
Relative gene expression
3
2
1
0
***
***
No DOX Flk1+
DOX Flk1+
ETV2-/-

Figure 2A

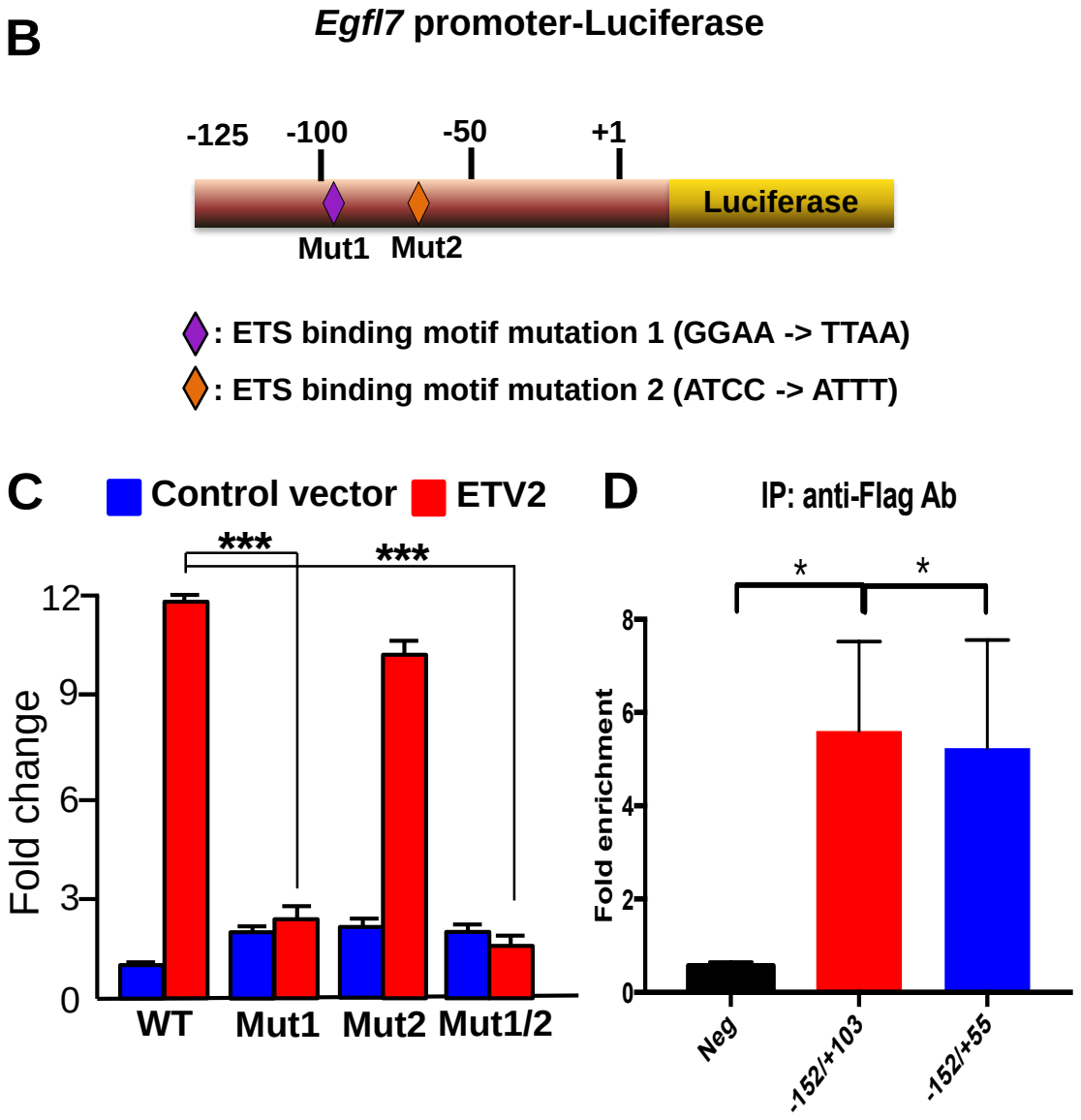
B
Egfl7 promoter-Luciferase
-125
-100
-50
+1
Luciferase
Mut1
Mut2
: ETS binding motif mutation 1 (GGAA -> TTAA)
: ETS binding motif mutation 2 (ATCC -> ATTT)
C
Control vector
ETV2
***
***
Fold change
12
9
6
3
0
WT
Mut1
Mut2
Mut1/2
D
IP: anti-Flag Ab
*
*
Fold enrichment
8
6
4
2
0
Neg
-152/+103
-152/+55

Figure 2B-D

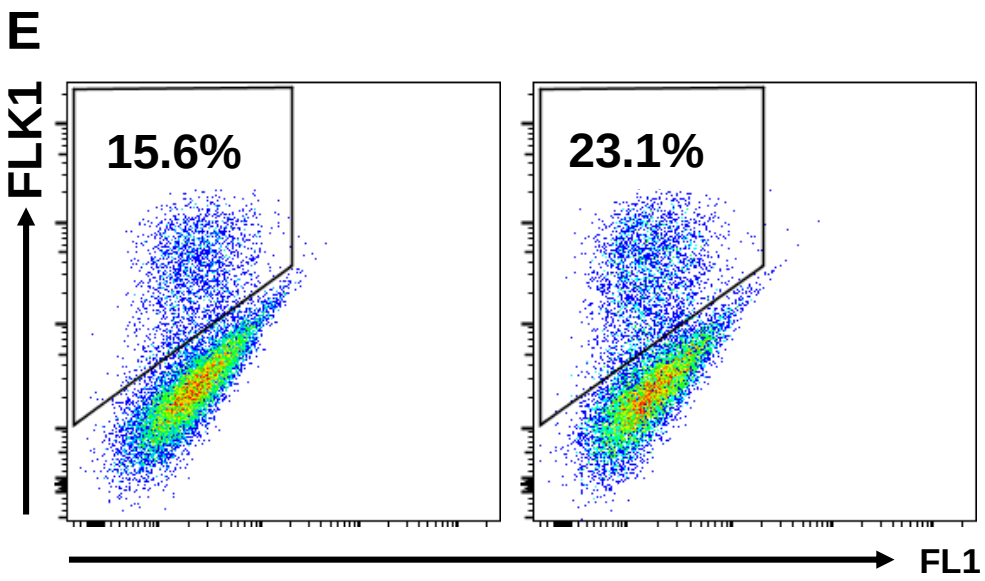

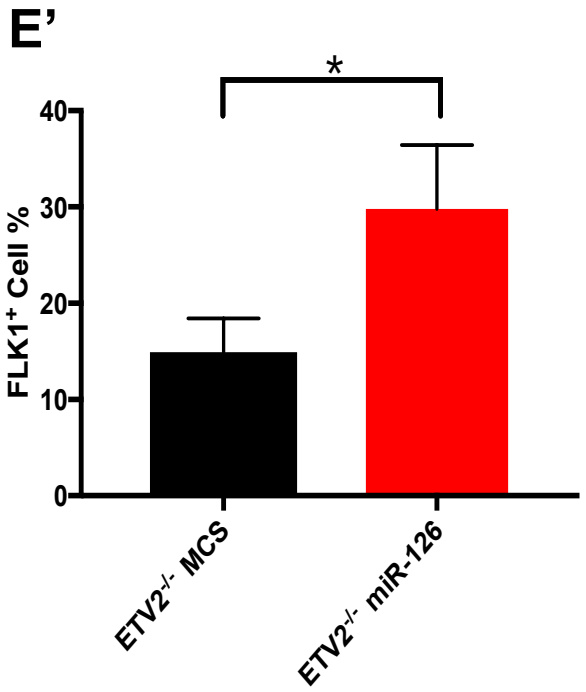

Figure 2E

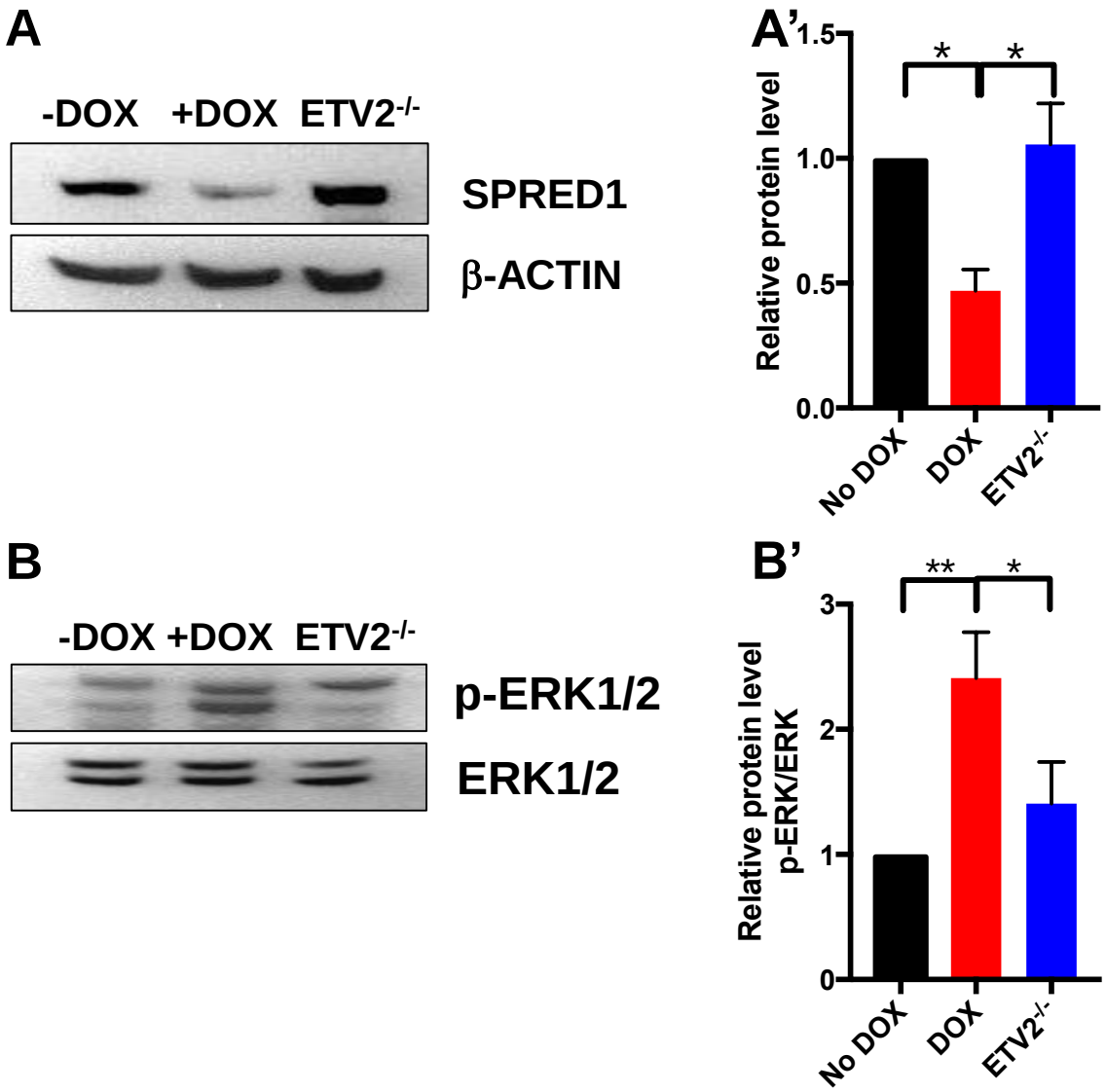
A
-DOX
+DOX
ETV2-/-
SPRED1
β-ACTIN
A'
Relative protein level
1.5
1.0
0.5
0.0
*
*
No DOX
DOX
ETV2-/-
B
-DOX
+DOX
ETV2-/-
p-ERK1/2
ERK1/2
B'
Relative protein level
p-ERK/ERK
3
2
1
0
**
*
No DOX
DOX
ETV2-/-

Figure 3A-B

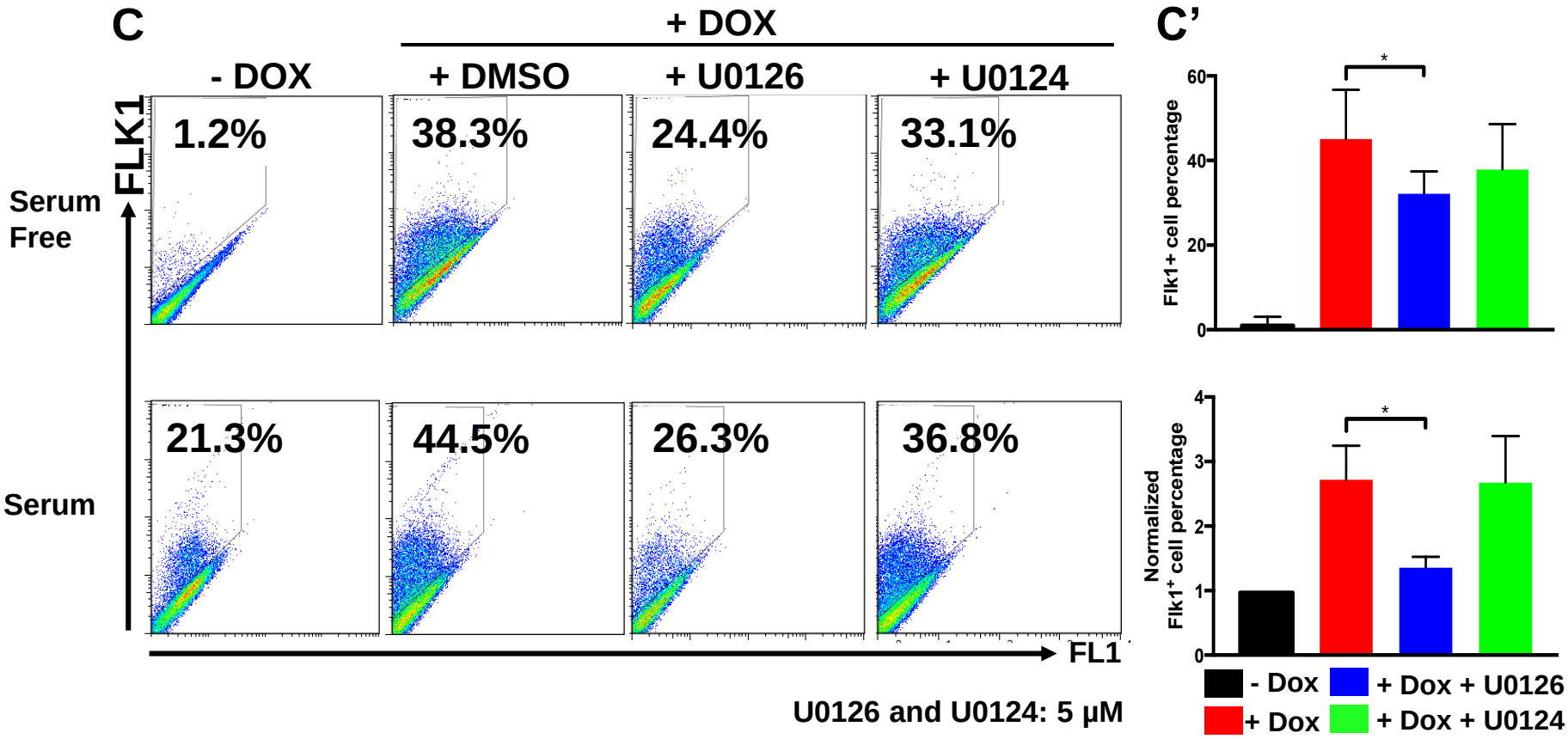
C
+ DOX
- DOX
+ DMSO
+ U0126
+ U0124
FLK1
Serum Free
1.2%
38.3%
24.4%
33.1%
Serum
21.3%
44.5%
26.3%
36.8%
FL1
U0126 and U0124: 5 μM
C'
Flk1+ cell percentage
60
40
20
0
*
Normalized Flk1+ cell percentage
4
3
2
1
0
*
- Dox
+ Dox
+ Dox + U0126
+ Dox + U0124

Figure 3C

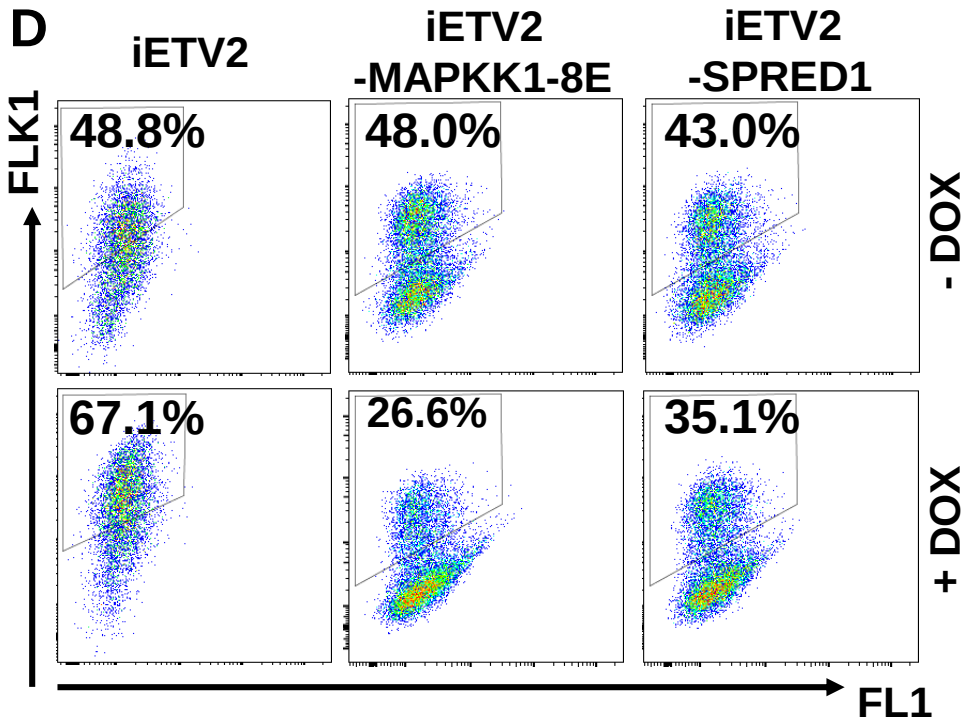
D
iETV2
iETV2
-MAPKK1-8E
iETV2
-SPRED1
FLK1
48.8%
48.0%
43.0%
- DOX
67.1%
26.6%
35.1%
+ DOX
FL1

Figure 3D

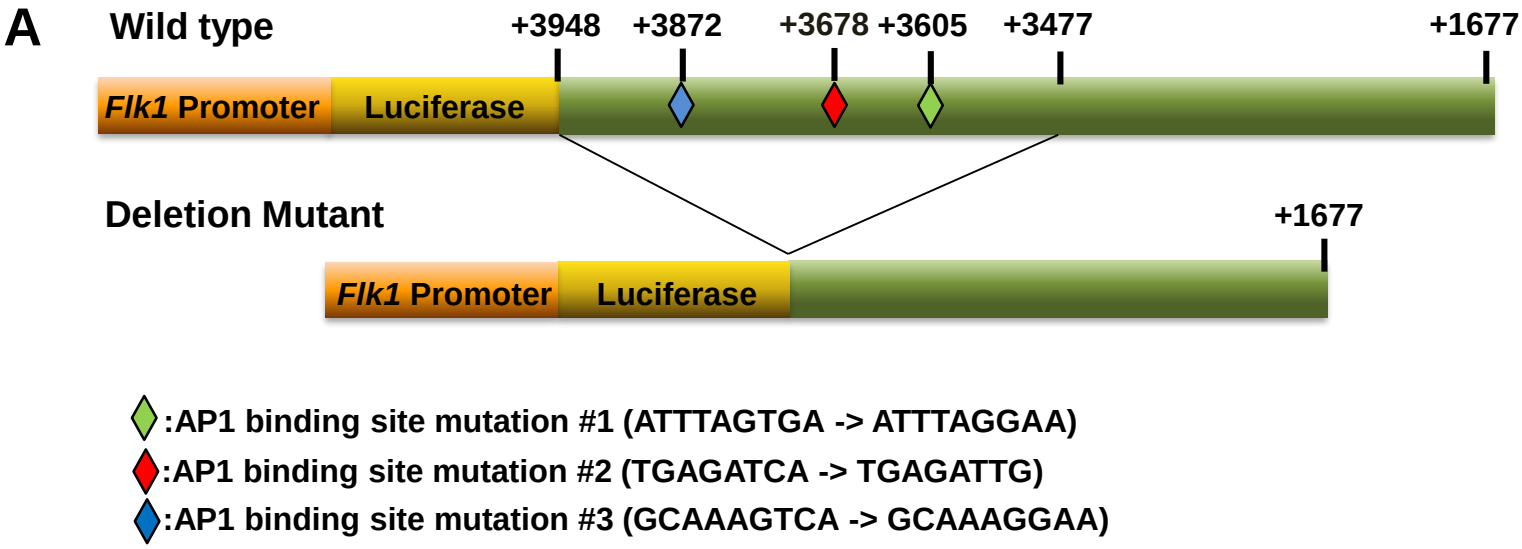
A
Wild type
+3948
+3872
+3678
+3605
+3477
+1677
Flk1 Promoter
Luciferase
Deletion Mutant
+1677
Flk1 Promoter
Luciferase
:AP1 binding site mutation #1 (ATTTAGTGA -> ATTTAGGAA)
:AP1 binding site mutation #2 (TGAGATCA -> TGAGATTG)
:AP1 binding site mutation #3 (GCAAAGTCA -> GCAAAGGAA)

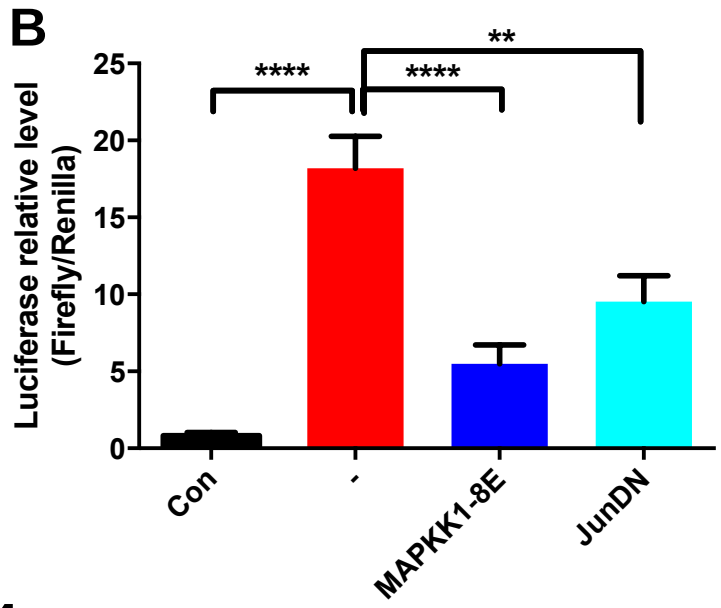
B
Luciferase relative level (Firefly/Renilla)
25
20
15
10
5
0
****
****
**
Con
-
MAPKK1-8E
JunDN

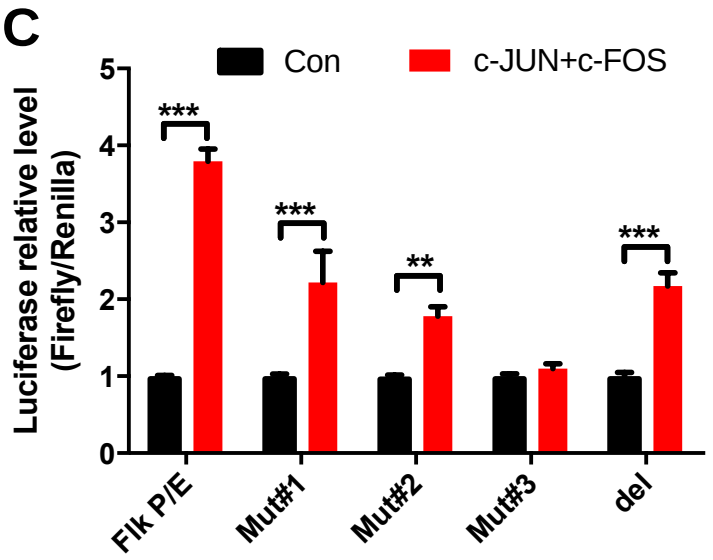
C
Con
c-JUN+c-FOS
Luciferase relative level (Firefly/Renilla)
5
4
3
2
1
0
***
***
**
***
Flk P/E
Mut#1
Mut#2
Mut#3
del

Figure 4

Table 1. Primer list

qPCR		**Sequences (5'-3')**	**Reference**
Egfl7 qRT-PCR	Forward	CGCTGTGTCAATACTGTGGGA	Primer Bank ID :257096015c3
	Reverse	GTTCTAGCACATCAACCCGAG	
Egfl7 ChIP-PCR -152/+103	Forward	CCCTTGGCCTCCTGTTTGTT	
	Reverse	AGCCAACCATGCAATGCAAC	
Egfl7 ChIP-PCR -152/+55	Forward	CCCTTGGCCTCCTGTTTGTT	
	Reverse	AGCCAACCATGCAATGCAAC	
Cloning		**Sequences (5'-3')**	**Reference**
Egfl7 promoter -125/+30	Forward	CATGAGCTAGCGGATCCCCGTTATCAGCAGA	
	Reverse	CATGCAGATCTTTCCTCGTGGACTGCACAG	
Mutation		**Sequences (5'-3')**	**Reference**
Egfl7 mut1	Sense	CAGAGAACACACACAttAAGTCCGGCGGGAAG	
	Antisense	CTTCCCGCCGGAC*TT*aaTGTGTGTGTTCTCTG	
Egfl7 mut2	Sense	GCGGGAAGGGCCC*ATtt*CAGTCCTGATTTACC	
	Antisense	GGTAAATCAGGACTG*aa*ATGGGCCCTTCCCGC	
Flk1 P/E deletion mutant	Sense	CCTTTTCCTCCATTTTTTCCTATTGGATCC	
	Antisense	GGATCCAATAGGAAAAAATGGAGGAAAAGG	
Flk1 P/E mut1	Sense	AATCAGCAATTTAGgaAGATCTGTGCATCC	
	Antisense	GGATGCACAGATCTtcCTAAATTGCTGATT	
Flk1 P/E mut2	Sense	GTCAGTGGGCCTGAGATtgTCAGATGGAGGTTCATC	
	Antisense	GATGAACCTCCATCTGAcaATCTCAGGCCCACTGAC	
Flk1 P/E mut3	Sense	GGACTGGGGCAAAGgaAATCCCACCTTTAT	
	Antisense	ATAAAGGTGGGATTtcCTTTGCCCCAGTCC	

Figure legends

Figure 1. Analysis of ETV2-regualted miRNA expression. (**A**) Schematic diagram of ESC differentiation. Doxycycline inducible (iFLAG-ETV2) ESCs were differentiated, treated with ± Doxycycline (Dox) at day 1 and sorted for $FLK1^+$ cells at day 3.5~4. RNAs from the sorted cells were subjected to miRNA sequencing and analysis. (**B-E**) Selected miRNAs displaying ≥ 1.5 fold change and an FDR ≤ 0.05 in response to overexpression of ETV2 were subjected to heat map analysis (B), volcano analysis (C), KEGG (D) and GO term analysis (E), respectively.

Figure 2. ETV2 up-regulates miR126 expression through direct binding on *Egfl7* promoter. (**A**) Expression analysis. $FLK1^+$ cells from iFLAG-ETV2 ESCs or *Etv2*$^{-/-}$ ESCs at day 3.5~4 of differentiation ± Dox treatment were subjected to gene expression analysis. n=3, $^{**}p>0.01$, $^{***}p>0.001$. (**B**) Schematic diagram of *Egfl7* promoter-luciferase plasmid. Two potential ETS binding elements were marked as diamonds. Purple: sense strand, Brown: anti-sense strand. (**C**) HEK/293T cells were transiently co-transfected with pCMV-*Etv2* and pGL3-*Egfl7* promoter wt, mut1 (mutagenesis on site #1), mut2 (mutagenesis on site #2), or mut1/2 (mutagenesis on site #1 and #2). Firefly luciferase activity was normalized by Renillar luciferase activity. n=3. $^{***}p>0.001$. (**D**l), Differentiated iFLAG-ETV2 ESCs were subjected to ChIP-PCR assay. Anti-FLAG or mouse IgG antibody (Negative control) was used for the immunoprecipitation. Primers for qRT-PCR were used to amplify the *Egfl7* promoter regions. Neg: negative control primer for gene dessert area. n=3, $^{*}p>0.05$. (**E**) *Etv2*$^{-/-}$ ESCs infected with lentiviral miR-126 were differentiated and subjected to FACS analysis for FLK1 expression. Scramble miRNAs were used for control. n=3, $^{*}p>0.05$.

Figure 3. ETV2 increases FLK1^{+} cells through the miR-126/MAPK pathway. (**A, B**) iFLAG-ETV2 ESCs were differentiated, treated with Dox at day 2 and harvested at day 4, followed by western blot analysis. (A) The expression of SPRED1 was reduced upon overexpression of ETV2, but augmented in differentiated *Etv2*$^{-/-}$ ESCs. (A') Quantification. SPRED1 expression was normalized by β-ACTIN. n=3, ***p*<0.05. (B) The level of pERK1/2 was increased in response to ETV2 overexpression, but decreased in differentiated *Etv2*$^{-/-}$ ESCs. (B') Quantification. p-ERK1/2 was normalized by ERK expression, and its quantification. n=3, **p*>0.05, ***p*>0.01. (**C**) iETV2 ESCs differentiated in serum-free (upper) or serum (lower) conditions were treated ± Dox and ± U0126 (5 μM), followed by FACS analysis for FLK1 expression at day 4. (C') Quantification. U0124 (5 μM) was used as negative control. n=3, **p*>0.05. (**D**) Differentiated iETV2, iETV2-MAPK1-8E or iETV2-SPRED1 ESC ± Dox were FACS analyzed for FLK1 expression.

Figure 4. ETV2 activates FLK1 expression through AP-1 binding sites in *Flk1* enhancer region. (**A**) Schematic diagram of *Flk1*-promoter-enhancer (p/e) - luciferase plasmid. Three potential AP-1 binding elements were marked as diamonds. (**B, C**) Luciferase-based promoter assay. (B) pGL3-*Flk1* p/e was transiently co-transfected with pCMV-*Etv2,* + pMCL-MAPK1-8E, or pCMV-Etv2 + pCMV-*c-Jun* ND (dominant negative) into HEK/293T cells. (C) pGL3-*Flk1* p/e (wt), putative AP-1 binding site mutants (Mut #1, Mut #2, Mut #3) or enhancer deletion mutant (del) was co-transfected with pCMV-*c-Jun and c-Fos* into 293FT cells. Firefly luciferase activity was normalized by Renillar luciferase activity. n=3. ** *p*>0.01, *** *p*>0.001.

CHAPER IV

Discussion and Perspective

Discussion

From Chapter II, we demonstrated OVOL2 as an important interacting protein of ETV2 in generating FLK1^{+} cells, endothelial as well as hematopoietic cells. The ETS factors have been shown to interact with other proteins when regulating target genes (Dejana et al., 2007a; Sharrocks, 2001b; Verger and Duterque-Coquillaud, 2002). Furthermore, several studies showed that ETV2 can form a transcription complex with other proteins. In 2008, De Val et al. reported that the interaction of ETV2 and FOXC2 (forkhead transcription factor) synergistically induces the expression of endothelial and hematopoietic genes (De Val et al., 2008b). Recently, we demonstrated that OVOL2, a zinc finger transcription factor, directly binds to ETV2 to cooperatively generate FLK1^{+} mesoderm and vascular endothelial and hematopoietic cell lineages from mouse ESCs (Kim et al., 2014). Interestingly, stability of ETV2 was significantly enhanced upon the overexpression of OVOL2, suggesting a possible mechanism for the cooperative interaction of the two proteins. Additionally, Shi et al (2014) reported Gata2 as the interacting protein of ETV2 (Batta et al., 2014). This interaction was cooperative in activating important genes for vascular endothelial and blood cell development. It is of note that all the identified proteins of ETV2 interacting partners have been implicated in embryonic vessel and blood cell development (Kume et al., 2001; Lugus et al., 2007; Seo et al., 2006; Tsai et al., 1994; Tsai and Orkin, 1997; Unezaki et al., 2007). All in all, it is evident that ETV2 can form a multiprotein transcription complex to control the expression of target genes. Thus, revealing more ETV2 interacting proteins in the regulation of endothelial and hematopoietic genes would be an important next step. Another interesting topic for further studies would be to delineate the relation between OVOL2, GATA2 and FOXC2 with regard to ETV2 function.

Studies in other systems have shown that OVOL2 can directly bind its target genes through the zinc finger domains. De novo motif-binding analysis revealed that zinc finger domains of OVOL2 has ability to bind directly on consensus sequence 5'-CCGTTA-3' present on Myc (Wells et al., 2009). In a subsequent study, Watanabe et al reported key epithelial to mesenchymal transition genes such as Tgfb3, Vim, Zeb1, Zeb2, and Twist as direct downstream targets of OVOL2 by performing ChIP assay. Furthermore, they also proved that OVOL2 directly binds those gene through same consensus sequence which is 5'-CCGTTA-3' and mentioned above (Watanabe et al., 2014). However, our analysis showed that OVOL2 alone failed to induce transcriptional activity of *Flk1* promoter. Rather, the function of OVOL2 is dependent upon ETV2 in ETV2-mediated $FLK1^{+}$ cell generation, suggesting DNA binding-independent role of OVOL2. In agreement with this interpretation, we found that ETV2 interacts with the zinc finger domains of OVOL2.

One of the clues to the potential mechanism of OVOL2 acting on ETV2 came from our findings that protein level of ETV2 was significantly higher upon the overexpression of OVOL2, compared to the condition where OVOL2 was not induced. ETV2 message was comparable regardless of OVOL2 overexpression. Thus, these findings suggest that OVOL2 is able to protect ETV2 protein from degradation, which could explain the cooperative function of the interaction. By examining ePASTfind analysis, we found that a potential PEST domain, which serves as proteolytic signal and leads to rapid degradation (Rechsteiner and Rogers, 1996), is present in the upstream of ETS domain in ETV2. Further, one report show that the ETS domain of ETV2 has a putative ubiquitination site (N terminus-MNYEK*LSR-C terminus) (Potu et al., 2017). Interestingly, we identified several E3 ubiquitin ligases such as Trim21, Nedd4, and

Arih1 as interacting proteins of ETV2 (unpublished data). Therefore, it is tempting to speculate that OVOL2 masks the PEST domain or ubiquitination site on ETV2, thereby increasing stability of ETV2. Investigation of protein modification of ETV2 would provide additional layers of molecular mechanisms of ETV2 in cardiovascular development.

In Chapter III, we demonstrate an important function of miR-126/MAPK pathway in ETV2-mediating FLK1$^+$ cell generation from mouse embryonic stem cells. Due to its potent and unique function, ETV2 has gained extensive attention in investigating cardiovascular system development and post-natal angiogenesis as well as direct cell reprogramming, aiming generating functional ECs from non-ECs. In this study, we demonstrate a novel function of the miR-126/MAPK pathway in ETV2-mediating FLK1$^+$ cell generation from mouse embryonic stem cells. Due to its potent and unique function, ETV2 has gained extensive attention in investigating cardiovascular system development and post-natal angiogenesis as well as direct cell reprogramming, aiming generating functional ECs from non-ECs. In our study, several layers of novel findings on ETV2 function were made. First, we reported genome-wide miRNA profiles in FLK1$^+$ cells generated in response to ETV2, providing a new and detailed insight into the mechanisms of ETV2. Second, we demonstrated the functional significance of the miR-126/MAPK pathway in ETV2-mediated FLK1$^+$ cell generation. Third, we also showed a direct activation of *Flk1* enhancer by JUN/FOS complex. Overall, our results reveals an additional arm of ETV2 function in regulating *Flk1* expression.

Our miRNA profiling results suggest that ETV2 regulates development of FLK1$^+$ cells, hematopoietic and endothelial cell lineages as well as cardiomyocytes through

miRNAs. For example, miR-10b, one of the downregulated genes by ETV2, is a critical regulator for vessel development through targeting FLT-1, which can inhibit VEGF-FLK1 signaling (Hassel et al., 2012). Interestingly, one study showed that ETV2 directly activates the expression of Flt-1 and that the phenotypic defects of *Flt-1* KO embryos characterized by excessive number of ECs forming disorganized vasculature were partly restored upon ETV2 inactivation in $FLK1^+$ cells (*Flk1Cre;Etv2* CKO embryos) (Koyano-Nakagawa et al., 2015). Therefore, it is tempting to speculate that ETV2-mediated downregulation of miR-10b ensures proper vascular development in early embryos. On the other hand, our analysis also found increased expression of miRNAs such as miR-146a upon overexpression ETV2 that could behave as anti-cardiogenic. The function of miR-146a has been mainly implicated in inflammation, immune reaction and cardiovascular disease (Paterson and Kriegel, 2017). Interestingly, miR-146 can target CXCR4, a receptor of SDF1, whose signaling is important during heart development and promotes cardiogenesis from pluripotent stem cells (Chiriac et al., 2010; Ma et al., 1998; Nagasawa et al., 1996; Zou et al., 1998). Another downregulated miRNA by ETV2, mIR-106 has been reported as a critical player for cardiac development as evidenced by in utero lethality displaying severe cardiac defects in compound knockout of mouse miR-106~25 and miR-17~92 cluster (Ventura et al., 2008). Thus, revealing link between ETV2 and ETV2-dependent miRNAs for cardiovascular lineage development would be an interesting topic for further studies.

Unlike the requirement of miR-126 in vessel formation mainly regulating vessel integrity and in erythropoiesis (Fish et al., 2008; Sturgeon et al., 2012; Wang et al., 2008), we demonstrated the unknown function of miR-126 in generating the first

emerging FLK1^{+} cells. From the miRNA profiling regulated by ETV2, miR-126 was identified as one of the most upregulated miRNAs by ETV2. In addition, we show that ETV2 via a direct binding on the *Egfl7* promoter induces the expression of miR-126 by performing the promoter based luciferase assay and a ChIP assay. In the subsequent studies, inhibition of the miR-126/MAPK pathway leads to impairment of ETV2 mediated FLK1^{+} cell generation. Although EGFL7 is co-transcribed with miR-126 upon ETV2 expression, we rule out the potential contribution of EGFL7 to inducing FLK1^{+} cell generation due to the dispensable function of EGFL7 in early stages of embryogenesis and embryonic vasculature formation as demonstrated by knock-out studies in mice and knock-down experiments in differentiating ESCs (Durrans and Stuhlmann, 2010; Kuhnert et al., 2008). Taken together along with the finding that introduction of miR-126 into *Etv2*$^{-/-}$ ES cells increases the generation of FLK1^{+} cells, it is evident that miR-126 acting downstream of ETV2 plays important roles in the establishment of the cardiovascular system.

The molecular insights into *Flk1* gene expression (i.e., upstream regulators) has not been an active research area, although it's a critical function in hematopoietic and vascular system. Regarding this, we for the first time demonstrate that the defects of *Etv2* knockout mice phenocopy those seen in *Flk1* knockout mice, namely complete absence of both vascular endothelial and hematopoietic cells (Lee et al., 2008b). Mechanistically, ETV2 directly binds ETS binding elements present on both promoter and enhancer of *Flk1* and activates its expression. The subsequent ChIP-sequencing analysis demonstrated that a wide range of genes critical for endothelial cell and blood cells are direct downstream targets of ETV2 (Liu et al., 2015). In this current study, we revealed an important function of MAPK activity in regulating *Flk1* gene expression.

Overexpression of ETV2 activates the MAPK activity, while inhibition of the MAPK pathway with inhibitor and genetic studies leads to decrease of the generation of ETV2-mediated FLK1^{+} cells. Further, we showed that the MAPK pathway is able to directly upregulates the expression of Flk1 via a direct binding of JUN/FOS on *Flk1* enhancer. Thus, we envision that ETV2 activates *Flk1* gene expression by activating the miR-126/MAPK pathway in addition to its direct binding on *Flk1* gene regulatory elements. Since ETV2 and JUN/FOS acts on *Flk1* promoter and enhancer, it would be interesting to determine interaction of ETV2 and JUN/FOS. In addition, ETS1, a closely related member to ETV2, has been known as a target of MAPK where phosphorylated ETS1 becomes transcriptionally active, raising the possibility that activated MAPK by ETV2 can in turn phosphorylate ETV2, establish a positive feedback loop to further substantiate the function of ETV2. However, ETV2 shows very limited sequence identity compared to ETS1 and other ETS factors besides the ETS domain (Brown and McKnight, 1992). Further, in vitro kinase assay show that ETV2 is not phosphorylated by MAPK (Selvaraj et al., 2015), making the regulatory loop between ETV2 and MAPK unlikely and suggesting a linear relationship between ETV2 and MAPK (at least ERK1/2) in regulating FLK1^{+} cell generation.

In summary, we report miRNA profiles regulated by ETV2 in generating FLK1+ cells from mouse embryonic stem cells. We further demonstrate the functional significance of the miR-126/MAPK pathway in ETV2-mediated FLK1^{+} cell generation. These findings could provide novel insight into the mechanisms of how ETV2 regulates the development of the cardiovascular system, which potentially provide a novel research venue for the basic and translational aspects of endothelial cell biology.

Perspective

By virtue of extensive studies over the past few years, we have a better understanding on the critical function of ETV2 in the genesis of the vessel, blood and heart in developing mouse embryos. As discussed, one of the salient observations in ETV2 biology is its transient expression in vessel and blood cells (Ferdous et al., 2009b; Kataoka et al., 2011a; Lee et al., 2008b). The intricate interplay between ETV2 and FLI1, an ETS factor, is proposed as a means to maintain functional vessels and hematopoietic cells throughout embryogenesis and perhaps in adults (Abedin et al., 2014; Liu et al., 2015). However, the mechanisms, in which the ETV2 expression is off, remain to be determined. The switch-off of the proposed upstream signals as previously discussed could be one possible explanation. Additional means of regulation would be active ways to restrict the expression of ETV2 in a certain narrow window of time to ensure proper development of vessel and hematopoietic cells. Indeed, *let7-a* miRNA is capable of targeting *zebrafish etsrp*, resulting in the reduction of expression of both vascular endothelial and hematopoietic markers (Moore et al., 2013). Given the recent report that *Kdm1a*, histone demethylase, in *zebrafish* promotes hematopoietic cell development by suppressing *etsrp* function (Takeuchi et al., 2015), epigenetic modifications of the ETV2 genomic loci would be another possible mechanism. In addition, it was reported that the sustained expression of ETV2 in endothelial and hematopoietic cells caused abnormal development and endothelialization, respectively (Hayashi et al., 2012). Thus, future studies on the safe-guard mechanisms of the ETV2 expression are warranted.

We and others unequivocally proved the potent vasculogenic function of ETV2 in developing mouse embryogenesis. As previously stated, the message becomes

extinct once the vessel and hematopoietic cells develop. This raised a question as to the functional significance of ETV2 in post-natal life. In this regard, Lee et al., (2011) found the enriched expression of ETV2 in BM HSCs and reported that *Mx1-cre* driven deletion of *Etv2* led to the decrease in the number and repopulating capacity of BM HSCs (Lee et al., 2011). The authors claimed the increased death of BM HSC in the absence of *Etv2* as an etiology of the observed phenotypes. Mechanistically, they showed that ETV2 can directly regulate *Tie2* expression, but failed to link how the reduced *Tie2* expression is related to the death of BM HSCs. Recently, we have found that the endothelial ETV2 acts as a critical regulator in neovascularization in response to injury (Park et al., 2016). The *Etv2* expression in endothelial cells is reactivated after injury. Mice deficient in *Etv2* in endothelial cells exhibited a significant impairment of new vessel formation upon injury such as wounding, eye injury and hindlimb ischemia. Interestingly, single delivery of lentiviral *Etv2* not only promotes the recovery of blood perfusion, but also augments proliferation of endothelial cells as well as smooth muscle cells, leading to neovascularization and tissue repair in the ischemic hindlimbs. These results suggest that ETV2 in adults plays an important role in vessel and blood construction systems under physiological conditions. Extending from these findings (Park et al., 2016), investigation of the function of ETV2 in pathological settings such as tumor angiogenesis and diabetics related vessel defects would be of significant interest from a therapeutic stand point. Interestingly, upregulated level of *Etv2* in tumor associated endothelial cells has been reported (Kabir et al., 2018). In this study, the authors demonstrate that deletion of *Etv2* in endothelial cells or systemic delivery of siETV2 into tumor bearing mice impairs the development of tumor and angiogenesis. As ETV2 function is conserved in other vertebrates, the vascular expression of *etsrp* in *zebrafish* that becomes greatly reduced by 2-4 dpf (days post fertilization) is

significantly induced in tumor blood vessel and in embryonic vasculatures upon transplantation of tumor cells (Baltrunaite et al., 2017). While wild type *zebrafish* injected with tumor cells induces tumor-associated angiogenesis, blocking the function of *etsrp* using *etsrp* null mutant and photoactivatable *etsrp* morpholino leads to severe impairment of the angiogenesis. Last, but not least, ETV2 alone or together with other endothelial transcription factors were reported to directly convert non-endothelial cells into endothelial cells (Ginsberg et al., 2012; Han et al., 2014; Lee et al., 2017; Morita et al., 2015; Veldman et al., 2013), suggesting a potent determinant function of ETV2 in converting non-endothelial cells into endothelial cells, which could be useful for treating CVDs. However, the use of lentiviral or retroviral delivery systems in these studies, which can alter the genomic integrity, is not compatible with clinical use. Therefore, to design novel tools with non-integrating materials such as modified mRNA, small molecules or chemicals is an imperative need in the field of direct reprogramming. Additional efforts should be made to generate specific types of endothelial cells such as arterial, venous and lymphatic ECs.

In summary, ETV2 is an indispensable transcription factor and plays a crucial role in vessel development and function. Throughout my thesis, I reveal detailed and unknown regulatory functions of ETV2 in this process. Recent findings have demonstrated additional capabilities of ETV2 in direct cell reprogramming. Thus, deciphering the mechanisms by which ETV2 is regulated in governing vascular development and neovascularization in pathophysiological conditions would provide a novel research venue for the basic and translational aspects of endothelial cell biology.

References

Abedin, M.J., Nguyen, A., Jiang, N., Perry, C.E., Shelton, J.M., Watson, D.K., and Ferdous, A. (2014). Fli1 acts downstream of Etv2 to govern cell survival and vascular homeostasis via positive autoregulation. Circulation research *114*, 1690-1699.

Baltrunaite, K., Craig, M.P., Palencia Desai, S., Chaturvedi, P., Pandey, R.N., Hegde, R.S., and Sumanas, S. (2017). ETS transcription factors Etv2 and Fli1b are required for tumor angiogenesis. Angiogenesis *20*, 307-323.

Bartel, D.P. (2009). MicroRNAs: target recognition and regulatory functions. Cell *136*, 215-233.

Bartel, F.O., Higuchi, T., and Spyropoulos, D.D. (2000). Mouse models in the study of the Ets family of transcription factors. Oncogene *19*, 6443-6454.

Barton, K., Muthusamy, N., Fischer, C., Ting, C.N., Walunas, T.L., Lanier, L.L., and Leiden, J.M. (1998). The Ets-1 transcription factor is required for the development of natural killer cells in mice. Immunity *9*, 555-563.

Basson, M.A. (2012). Signaling in cell differentiation and morphogenesis. Cold Spring Harb Perspect Biol *4*.

Batta, K., Florkowska, M., Kouskoff, V., and Lacaud, G. (2014). Direct Reprogramming of Murine Fibroblasts to Hematopoietic Progenitor Cells. Cell reports *9*, 1871-1884.

Behrens, A.N., Zierold, C., Shi, X., Ren, Y., Koyano-Nakagawa, N., Garry, D.J., and Martin, C.M. (2014). Sox7 is regulated by ETV2 during cardiovascular development. Stem cells and development *23*, 2004-2013.

Berman, H.M., Westbrook, J., Feng, Z., Gilliland, G., Bhat, T.N., Weissig, H., Shindyalov, I.N., and Bourne, P.E. (2000). The Protein Data Bank. Nucleic acids research *28*, 235-242.

Bertrand, J.Y., Chi, N.C., Santoso, B., Teng, S., Stainier, D.Y., and Traver, D. (2010). Haematopoietic stem cells derive directly from aortic endothelium during development. Nature *464*, 108-111.

Boisset, J.C., van Cappellen, W., Andrieu-Soler, C., Galjart, N., Dzierzak, E., and Robin, C. (2010). In vivo imaging of haematopoietic cells emerging from the mouse aortic endothelium. Nature *464*, 116-120.

Bondue, A., Lapouge, G., Paulissen, C., Semeraro, C., Iacovino, M., Kyba, M., and Blanpain, C. (2008). Mesp1 acts as a master regulator of multipotent cardiovascular progenitor specification. Cell stem cell *3*, 69-84.

Bondue, A., Tannler, S., Chiapparo, G., Chabab, S., Ramialison, M., Paulissen, C., Beck, B., Harvey, R., and Blanpain, C. (2011). Defining the earliest step of cardiovascular progenitor specification during embryonic stem cell differentiation. J Cell Biol *192*, 751-765.

Brown, T.A., and McKnight, S.L. (1992). Specificities of protein-protein and protein-DNA interaction of GABP alpha and two newly defined ets-related proteins. Genes Dev *6*, 2502-2512.

Caprioli, A., Koyano-Nakagawa, N., Iacovino, M., Shi, X., Ferdous, A., Harvey, R.P., Olson, E.N., Kyba, M., and Garry, D.J. (2011). Nkx2-5 represses Gata1 gene expression and modulates the cellular fate of cardiac progenitors during embryogenesis. Circulation *123*, 1633-1641.

Carmeliet, P., Ferreira, V., Breier, G., Pollefeyt, S., Kieckens, L., Gertsenstein, M., Fahrig, M., Vandenhoeck, A., Harpal, K., Eberhardt, C.*, et al.* (1996). Abnormal blood vessel development and lethality in embryos lacking a single VEGF allele. Nature *380*, 435-439.

Carmeliet, P., and Jain, R.K. (2011). Molecular mechanisms and clinical applications of angiogenesis. Nature *473*, 298-307.

Casci, T., Vinos, J., and Freeman, M. (1999). Sprouty, an intracellular inhibitor of Ras signaling. Cell *96*, 655-665.

Casie Chetty, S., Rost, M.S., Enriquez, J.R., Schumacher, J.A., Baltrunaite, K., Rossi, A., Stainier, D.Y., and Sumanas, S. (2017). Vegf signaling promotes vascular endothelial differentiation by modulating etv2 expression. Developmental biology *424*, 147-161.

Chiriac, A., Terzic, A., Park, S., Ikeda, Y., Faustino, R., and Nelson, T.J. (2010). SDF-1-enhanced cardiogenesis requires CXCR4 induction in pluripotent stem cells. J Cardiovasc Transl Res *3*, 674-682.

Chistiakov, D.A., Orekhov, A.N., and Bobryshev, Y.V. (2016). The role of miR-126 in embryonic angiogenesis, adult vascular homeostasis, and vascular repair and its alterations in atherosclerotic disease. Journal of molecular and cellular cardiology *97*, 47-55.

Choi, K. (2002). The hemangioblast: a common progenitor of hematopoietic and endothelial cells. Journal of hematotherapy & stem cell research *11*, 91-101.

Chung, Y.S., Zhang, W.J., Arentson, E., Kingsley, P.D., Palis, J., and Choi, K. (2002). Lineage analysis of the hemangioblast as defined by FLK1 and SCL expression. Development *129*, 5511-5520.

Ciau-Uitz, A., Wang, L., Patient, R., and Liu, F. (2013). ETS transcription factors in hematopoietic stem cell development. Blood cells, molecules & diseases *51*, 248-255.

Corson, L.B., Yamanaka, Y., Lai, K.M., and Rossant, J. (2003). Spatial and temporal patterns of ERK signaling during mouse embryogenesis. Development *130*, 4527-4537.

Craig, M.P., Grajevskaja, V., Liao, H.K., Balciuniene, J., Ekker, S.C., Park, J.S., Essner, J.J., Balciunas, D., and Sumanas, S. (2015). Etv2 and fli1b function together

as key regulators of vasculogenesis and angiogenesis. Arteriosclerosis, thrombosis, and vascular biology *35*, 865-876.

De Haro, L., and Janknecht, R. (2002). Functional analysis of the transcription factor ER71 and its activation of the matrix metalloproteinase-1 promoter. Nucleic acids research *30*, 2972-2979.

De Haro, L., and Janknecht, R. (2005). Cloning of the murine ER71 gene (Etsrp71) and initial characterization of its promoter. Genomics *85*, 493-502.

De Val, S., Chi, N.C., Meadows, S.M., Minovitsky, S., Anderson, J.P., Harris, I.S., Ehlers, M.L., Agarwal, P., Visel, A., Xu, S.-M.*, et al.* (2008a). Combinatorial regulation of endothelial gene expression by Ets and Forkhead transcription factors. Cell *135*, 1053-1064.

De Val, S., Chi, N.C., Meadows, S.M., Minovitsky, S., Anderson, J.P., Harris, I.S., Ehlers, M.L., Agarwal, P., Visel, A., Xu, S.M.*, et al.* (2008b). Combinatorial regulation of endothelial gene expression by ets and forkhead transcription factors. Cell *135*, 1053-1064.

Dejana, E., Taddei, A., and Randi, A.M. (2007a). Foxs and Ets in the transcriptional regulation of endothelial cell differentiation and angiogenesis. Biochimica et biophysica acta *1775*, 298-312.

Dejana, E., Taddei, A., and Randi, A.M. (2007b). Foxs and Ets in the transcriptional regulation of endothelial cell differentiation and angiogenesis. Biochim. Biophys. Acta *1775*, 298-312.

Drake, C.J., and Fleming, P.A. (2000). Vasculogenesis in the day 6.5 to 9.5 mouse embryo. Blood *95*, 1671-1679.

Durrans, A., and Stuhlmann, H. (2010). A role for Egfl7 during endothelial organization in the embryoid body model system. J Angiogenes Res *2*, 4.

Elvert, G., Kappel, A., Heidenreich, R., Englmeier, U., Lanz, S., Acker, T., Rauter, M., Plate, K., Sieweke, M., Breier, G.*, et al.* (2003). Cooperative interaction of hypoxia-inducible factor-2alpha (HIF-2alpha) and Ets-1 in the transcriptional activation of vascular endothelial growth factor receptor-2 (Flk-1). J Biol Chem *278*, 7520-7530.

Ema, M., Faloon, P., Zhang, W.J., Hirashima, M., Reid, T., Stanford, W.L., Orkin, S., Choi, K., and Rossant, J. (2003). Combinatorial effects of Flk1 and Tal1 on vascular and hematopoietic development in the mouse. Genes Dev *17*, 380-393.

Ema, M., Takahashi, S., and Rossant, J. (2006). Deletion of the selection cassette, but not cis-acting elements, in targeted Flk1-lacZ allele reveals Flk1 expression in multipotent mesodermal progenitors. Blood *107*, 111-117.

Faloon, P., Arentson, E., Kazarov, A., Deng, C.X., Porcher, C., Orkin, S., and Choi, K. (2000). Basic fibroblast growth factor positively regulates hematopoietic development. Development *127*, 1931-1941.

Ferdous, A., Caprioli, A., Iacovino, M., Martin, C.M., Morris, J., Richardson, J.A., Latif, S., Hammer, R.E., Harvey, R.P., Olson, E.N.*, et al.* (2009a). Nkx2-5 transactivates the Ets-related protein 71 gene and specifies an endothelial/endocardial fate in the developing embryo. PNAS *106*, 814-819.

Ferdous, A., Caprioli, A., Iacovino, M., Martin, C.M., Morris, J., Richardson, J.A., Latif, S., Hammer, R.E., Harvey, R.P., Olson, E.N.*, et al.* (2009b). Nkx2-5 transactivates the Ets-related protein 71 gene and specifies an endothelial/endocardial fate in the developing embryo. Proceedings of the National Academy of Sciences of the United States of America *106*, 814-819.

Findlay, V.J., LaRue, A.C., Turner, D.P., Watson, P.M., and Watson, D.K. (2013). Understanding the role of ETS-mediated gene regulation in complex biological processes. Advances in cancer research *119*, 1-61.

Fish, J.E., Santoro, M.M., Morton, S.U., Yu, S., Yeh, R.F., Wythe, J.D., Ivey, K.N., Bruneau, B.G., Stainier, D.Y., and Srivastava, D. (2008). miR-126 regulates angiogenic signaling and vascular integrity. Developmental cell *15*, 272-284.

Flamme, I., Frolich, T., and Risau, W. (1997). Molecular mechanisms of vasculogenesis and embryonic angiogenesis. Journal of cellular physiology *173*, 206-210.

Friedlander, M.R., Mackowiak, S.D., Li, N., Chen, W., and Rajewsky, N. (2012). miRDeep2 accurately identifies known and hundreds of novel microRNA genes in seven animal clades. Nucleic acids research *40*, 37-52.

Frum, T., and Ralston, A. (2015). Cell signaling and transcription factors regulating cell fate during formation of the mouse blastocyst. Trends in genetics : TIG *31*, 402-410.

Fujiwara, Y., Browne, C.P., Cunniff, K., Goff, S.C., and Orkin, S.H. (1996). Arrested development of embryonic red cell precursors in mouse embryos lacking transcription factor GATA-1. PNAS *93*, 12355-12358.

Ginsberg, M., James, D., Ding, B.S., Nolan, D., Geng, F., Butler, J.M., Schachterle, W., Pulijaal, V.R., Mathew, S., Chasen, S.T.*, et al.* (2012). Efficient direct reprogramming of mature amniotic cells into endothelial cells by ETS factors and TGFbeta suppression. Cell *151*, 559-575.

Gotoh, Y., Masuyama, N., Suzuki, A., Ueno, N., and Nishida, E. (1995). Involvement of the MAP kinase cascade in Xenopus mesoderm induction. The EMBO journal *14*, 2491-2498.

Grabher, C., Payne, E.M., Johnston, A.B., Bolli, N., Lechman, E., Dick, J.E., Kanki, J.P., and Look, A.T. (2011). Zebrafish microRNA-126 determines hematopoietic cell fate through c-Myb. Leukemia *25*, 506-514.

Haar, J.L., and Ackerman, G.A. (1971). A phase and electron microscopic study of vasculogenesis and erythropoiesis in the yolk sac of the mouse. The Anatomical record *170*, 199-223.

Han, J.K., Chang, S.H., Cho, H.J., Choi, S.B., Ahn, H.S., Lee, J., Jeong, H., Youn, S.W., Lee, H.J., Kwon, Y.W.*, et al.* (2014). Direct conversion of adult skin fibroblasts to endothelial cells by defined factors. Circulation *130*, 1168-1178.

Hart, A., Melet, F., Grossfeld, P., Chien, K., Jones, C., Tunnacliffe, A., Favier, R., and Bernstein, A. (2000). Fli-1 is required for murine vascular and megakaryocytic development and is hemizygously deleted in patients with thrombocytopenia. Immunity *13*, 167-177.

Hartley, R.S., Lewellyn, A.L., and Maller, J.L. (1994). MAP kinase is activated during mesoderm induction in Xenopus laevis. Developmental biology *163*, 521-524.

Hassel, D., Cheng, P., White, M.P., Ivey, K.N., Kroll, J., Augustin, H.G., Katus, H.A., Stainier, D.Y., and Srivastava, D. (2012). MicroRNA-10 regulates the angiogenic behavior of zebrafish and human endothelial cells by promoting vascular endothelial growth factor signaling. Circulation research *111*, 1421-1433.

Hatakeyama, J., and Kageyama, R. (2004). Retinal cell fate determination and bHLH factors. Seminars in cell & developmental biology *15*, 83-89.

Hayashi, M., Pluchinotta, M., Momiyama, A., Tanaka, Y., Nishikawa, S., and Kataoka, H. (2012). Endothelialization and altered hematopoiesis by persistent Etv2 expression in mice. Experimental hematology *40*, 738-750 e711.

Hirata, H., Kawamata, S., Murakami, Y., Inoue, K., Nagahashi, A., Tosaka, M., Yoshimura, N., Miyamoto, Y., Iwasaki, H., Asahara, T.*, et al.* (2007). Coexpression of platelet-derived growth factor receptor alpha and fetal liver kinase 1 enhances cardiogenic potential in embryonic stem cell differentiation in vitro. Journal of bioscience and bioengineering *103*, 412-419.

Hirschi, K.K. (2012). Hemogenic endothelium during development and beyond. Blood *119*, 4823-4827.

Hollenhorst, P.C., Jones, D.A., and Graves, B.J. (2004). Expression profiles frame the promoter specificity dilemma of the ETS family of transcription factors. Nucleic acids research *32*, 5693-5702.

Hollenhorst, P.C., McIntosh, L.P., and Graves, B.J. (2011). Genomic and biochemical insights into the specificity of ETS transcription factors. Annual review of biochemistry *80*, 437-471.

Huang, X., Gschweng, E., Van Handel, B., Cheng, D., Mikkola, H.K., and Witte, O.N. (2011). Regulated expression of microRNAs-126/126* inhibits erythropoiesis from human embryonic stem cells. Blood *117*, 2157-2165.

Iacovino, M., Hernandez, C., Xu, Z., Bajwa, G., Prather, M., and Kyba, M. (2009). A conserved role for Hox paralog group 4 in regulation of hematopoietic progenitors. Stem Cells Dev *18*, 783-792.

Iwafuchi-Doi, M., and Zaret, K.S. (2014). Pioneer transcription factors in cell reprogramming. Genes Dev *28*, 2679-2692.

Jain, R.K. (2003). Molecular regulation of vessel maturation. Nat Med *9*, 685-693.

Kabir, A.U., Lee, T.J., Pan, H., Berry, J.C., Krchma, K., Wu, J., Liu, F., Kang, H.K., Hinman, K., Yang, L.*, et al.* (2018). Requisite endothelial reactivation and effective siRNA nanoparticle targeting of Etv2/Er71 in tumor angiogenesis. JCI Insight *3*.

Kappel, A., Ronicke, V., Damert, A., Flamme, I., Risau, W., and Breier, G. (1999). Identification of vascular endothelial growth factor (VEGF) receptor-2 (Flk-1) promoter/enhancer sequences sufficient for angioblast and endothelial cell-specific transcription in transgenic mice. Blood *93*, 4284-4292.

Kappel, A., Schlaeger, T.M., Flamme, I., Orkin, S.H., Risau, W., and Breier, G. (2000). Role of SCL/Tal-1, GATA, and ets transcription factor binding sites for the regulation of flk-1 expression during murine vascular development. Blood *96*, 3078-3085.

Kataoka, H., Hayashi, M., Nakagawa, R., Tanaka, Y., Izumi, N., Nishikawa, S., Jakt, M.L., Tarui, H., and Nishikawa, S. (2011a). Etv2/ER71 induces vascular mesoderm from Flk1+PDGFRalpha+ primitive mesoderm. Blood *118*, 6975-6986.

Kataoka, H., Hayashi, M., Nakagawa, R., Tanaka, Y., Izumi, N., Nishikawa, S., Jakt, M.L., Tarui, H., and Nishikawa, S.I. (2011b). Etv2/ER71 induces vascular mesoderm from Flk1+PDGFRα+ primitive mesoderm. Blood *118*, 6975-6986.

Kim, J.H., Lee, S.R., Li, L.H., Park, H.J., Park, J.H., Lee, K.Y., Kim, M.K., Shin, B.A., and Choi, S.Y. (2011). High cleavage efficiency of a 2A peptide derived from porcine teschovirus-1 in human cell lines, zebrafish and mice. PLoS One *6*, e18556.

Kim, J.Y., Lee, R.H., Kim, T.M., Kim, D.W., Jeon, Y.J., Huh, S.H., Oh, S.Y., Kyba, M., Kataoka, H., Choi, K.*, et al.* (2014). OVOL2 is a critical regulator of ER71/ETV2 in generating FLK1+, hematopoietic, and endothelial cells from embryonic stem cells. Blood *124*, 2948-2952.

Kissa, K., and Herbomel, P. (2010). Blood stem cells emerge from aortic endothelium by a novel type of cell transition. Nature *464*, 112-115.

Knebel, J., De Haro, L., and Janknecht, R. (2006). Repression of transcription by TSGA/Jmjd1a, a novel interaction partner of the ETS protein ER71. J Cell Biochem *99*, 319-329.

Kodandapani, R., Pio, F., Ni, C.Z., Piccialli, G., Klemsz, M., McKercher, S., Maki, R.A., and Ely, K.R. (1996). A new pattern for helix-turn-helix recognition revealed by the PU.1 ETS-domain-DNA complex. Nature *380*, 456-460.

Koyano-Nakagawa, N., Kweon, J., Iacovino, M., Shi, X., Rasmussen, T.L., Borges, L., Zirbes, K.M., Li, T., Perlingeiro, R.C., Kyba, M.*, et al.* (2012). Etv2 is expressed in the yolk sac hematopoietic and endothelial progenitors and regulates Lmo2 gene expression. Stem Cells *30*, 1611-1623.

Koyano-Nakagawa, N., Shi, X., Rasmussen, T.L., Das, S., Walter, C.A., and Garry, D.J. (2015). Feedback Mechanisms Regulate Ets Variant 2 (Etv2) Gene Expression and Hematoendothelial Lineages. The Journal of biological chemistry *290*, 28107-28119.

Kuhnert, F., Mancuso, M.R., Hampton, J., Stankunas, K., Asano, T., Chen, C.Z., and Kuo, C.J. (2008). Attribution of vascular phenotypes of the murine Egfl7 locus to the microRNA miR-126. Development *135*, 3989-3993.

Kume, T., Jiang, H., Topczewska, J.M., and Hogan, B.L. (2001). The murine winged helix transcription factors, Foxc1 and Foxc2, are both required for cardiovascular development and somitogenesis. Genes Dev *15*, 2470-2482.

Lee, D., Kim, T., and Lim, D.S. (2011). The Er71 is an important regulator of hematopoietic stem cells in adult mice. Stem cells *29*, 539-548.

Lee, D., Park, C., Lee, H., Lugus, J.J., Kim, S.H., Arentson, E., Chung, Y.S., Gomez, G., Kyba, M., Lin, S*., et al.* (2008a). ER71 acts downstream of BMP, Notch, and Wnt signaling in blood and vessel progenitor specification. Cell Stem Cell *2*, 497-507.

Lee, D., Park, C., Lee, H., Lugus, J.J., Kim, S.H., Arentson, E., Chung, Y.S., Gomez, G., Kyba, M., Lin, S*., et al.* (2008b). ER71 acts downstream of BMP, Notch, and Wnt signaling in blood and vessel progenitor specification. Cell stem cell *2*, 497-507.

Lee, S., Park, C., Han, J.W., Kim, J.Y., Cho, K., Kim, E.J., Kim, S., Lee, S.J., Oh, S.Y., Tanaka, Y*., et al.* (2017). Direct Reprogramming of Human Dermal Fibroblasts Into Endothelial Cells Using ER71/ETV2. Circulation research *120*, 848-861.

Lindsley, R.C., Gill, J.G., Murphy, T.L., Langer, E.M., Cai, M., Mashayekhi, M., Wang, W., Niwa, N., Nerbonne, J.M., Kyba, M*., et al.* (2008). Mesp1 coordinately regulates cardiovascular fate restriction and epithelial-mesenchymal transition in differentiating ESCs. Cell stem cell *3*, 55-68.

Liu, F., Bhang, S.H., Arentson, E., Sawada, A., Kim, C.K., Kang, I., Yu, J., Sakurai, N., Kim, S.H., Yoo, J.J*., et al.* (2013). Enhanced hemangioblast generation and improved vascular repair and regeneration from embryonic stem cells by defined transcription factors. Stem cell reports *1*, 166-182.

Liu, F., Kang, I., Park, C., Chang, L.-W., Wang, W., Lee, D., Lim, D.-S., Vittet, D., Nerbonne, J.M., and Choi, K. (2012a). ER71 specifies Flk-1+ hemangiogenic mesoderm by inhibiting cardiac mesoderm and Wnt signaling. Blood *119*, 3295-3305.

Liu, F., Kang, I., Park, C., Chang, L.W., Wang, W., Lee, D., Lim, D.S., Vittet, D., Nerbonne, J.M., and Choi, K. (2012b). ER71 specifies Flk-1+ hemangiogenic mesoderm by inhibiting cardiac mesoderm and Wnt signaling. Blood *119*, 3295-3305.

Liu, F., Kang, I., Park, C., Chang, W., Wang, W., Lee, D., Lim, D.S., Vittet, D., Nerbonne, J.M., and Choi, K. (2012c). ER71 specifies Flk-1(+) hemangiogenic mesoderm by inhibiting cardiac mesoderm and Wnt signaling. Blood *119*, 3295-3305.

Liu, F., Li, D., Yu, Y.Y., Kang, I., Cha, M.J., Kim, J.Y., Park, C., Watson, D.K., Wang, T., and Choi, K. (2015). Induction of hematopoietic and endothelial cell program orchestrated by ETS transcription factor ER71/ETV2. EMBO reports *16*, 654-669.

Liu, N., and Olson, E.N. (2010). MicroRNA regulatory networks in cardiovascular development. Developmental cell *18*, 510-525.

Liu, T., Qian, W.J., Strittmatter, E.F., Camp, D.G., 2nd, Anderson, G.A., Thrall, B.D., and Smith, R.D. (2004). High-throughput comparative proteome analysis using a quantitative cysteinyl-peptide enrichment technology. Anal Chem *76*, 5345-5353.

Love, M.I., Huber, W., and Anders, S. (2014). Moderated estimation of fold change and dispersion for RNA-seq data with DESeq2. Genome Biol *15*, 550.

Lugus, J.J., Chung, Y.S., Mills, J.C., Kim, S.I., Grass, J., Kyba, M., Doherty, J.M., Bresnick, E.H., and Choi, K. (2007). GATA2 functions at multiple steps in hemangioblast development and differentiation. Development *134*, 393-405.

Lyons, I., Parsons, L.M., Hartley, L., Li, R., Andrews, J.E., Robb, L., and Harvey, R.P. (1995). Myogenic and morphogenetic defects in the heart tubes of murine embryos lacking the homeo box gene Nkx2-5. Genes Dev *9*, 1654-1666.

Ma, Q., Jones, D., Borghesani, P.R., Segal, R.A., Nagasawa, T., Kishimoto, T., Bronson, R.T., and Springer, T.A. (1998). Impaired B-lymphopoiesis, myelopoiesis, and derailed cerebellar neuron migration in CXCR4- and SDF-1-deficient mice. Proceedings of the National Academy of Sciences of the United States of America *95*, 9448-9453.

Mackay, D.R., Hu, M., Li, B., Rheaume, C., and Dai, X. (2006). The mouse Ovol2 gene is required for cranial neural tube development. Dev Biol *291*, 38-52.

Mansour, S.J., Matten, W.T., Hermann, A.S., Candia, J.M., Rong, S., Fukasawa, K., Vande Woude, G.F., and Ahn, N.G. (1994). Transformation of mammalian cells by constitutively active MAP kinase kinase. Science *265*, 966-970.

Meadows, S.M., Myers, C.T., and Krieg, P.A. (2011). Regulation of endothelial cell development by ETS transcription factors. Seminars in cell & developmental biology *22*, 976-984.

Moore, J.C., Sheppard-Tindell, S., Shestopalov, I.A., Yamazoe, S., Chen, J.K., and Lawson, N.D. (2013). Post-transcriptional mechanisms contribute to Etv2 repression during vascular development. Developmental biology *384*, 128-140.

Morita, R., Suzuki, M., Kasahara, H., Shimizu, N., Shichita, T., Sekiya, T., Kimura, A., Sasaki, K., Yasukawa, H., and Yoshimura, A. (2015). ETS transcription factor ETV2 directly converts human fibroblasts into functional endothelial cells. Proceedings of the National Academy of Sciences of the United States of America *112*, 160-165.

Motoike, T., Markham, D.W., Rossant, J., and Sato, T.N. (2003). Evidence for novel fate of Flk1+ progenitor: contribution to muscle lineage. Genesis *35*, 153-159.

Muhl, B., Hagele, J., Tasdogan, A., Loula, P., Schuh, K., and Bundschu, K. (2015). SPREDs (Sprouty related proteins with EVH1 domain) promote self-renewal and inhibit mesodermal differentiation in murine embryonic stem cells. Developmental dynamics : an official publication of the American Association of Anatomists *244*, 591-606.

Nagasawa, T., Hirota, S., Tachibana, K., Takakura, N., Nishikawa, S., Kitamura, Y., Yoshida, N., Kikutani, H., and Kishimoto, T. (1996). Defects of B-cell lymphopoiesis and bone-marrow myelopoiesis in mice lacking the CXC chemokine PBSF/SDF-1. Nature *382*, 635-638.

Neuhaus, H., Muller, F., and Hollemann, T. (2010a). Xenopus er71 is involved in vascular development. Developmental dynamics : an official publication of the American Association of Anatomists *239*, 3436-3445.

Neuhaus, H., Müller, F., and Hollemann, T. (2010b). Xenopus er71 is involved in vascular development. Dev Dyn *239*, 3436-3445.

Nobuhisa, I., Kato, R., Inoue, H., Takizawa, M., Okita, K., Yoshimura, A., and Taga, T. (2004). Spred-2 suppresses aorta-gonad-mesonephros hematopoiesis by inhibiting MAP kinase activation. J Exp Med *199*, 737-742.

Oh, S.Y., Kim, J.Y., and Park, C. (2015). The ETS Factor, ETV2: a Master Regulator for Vascular Endothelial Cell Development. Mol Cells *38*, 1029-1036.

Palencia-Desai, S., Kohli, V., Kang, J., Chi, N.C., Black, B.L., and Sumanas, S. (2011). Vascular endothelial and endocardial progenitors differentiate as cardiomyocytes in the absence of Etsrp/Etv2 function. Development *138*, 4721-4732.

Palis, J., Robertson, S., Kennedy, M., Wall, C., and Keller, G. (1999). Development of erythroid and myeloid progenitors in the yolk sac and embryo proper of the mouse. Development *126*, 5073-5084.

Park, C., Afrikanova, I., Chung, Y.S., Zhang, W.J., Arentson, E., Fong Gh, G., Rosendahl, A., and Choi, K. (2004). A hierarchical order of factors in the generation of FLK1- and SCL-expressing hematopoietic and endothelial progenitors from embryonic stem cells. Development *131*, 2749-2762.

Park, C., Kim, T.M., and Malik, A.B. (2013). Transcriptional regulation of endothelial cell and vascular development. Circulation research *112*, 1380-1400.

Park, C., Lee, T.J., Bhang, S.H., Liu, F., Nakamura, R., Oladipupo, S.S., Pitha-Rowe, I., Capoccia, B., Choi, H.S., Kim, T.M.*, et al.* (2016). Injury-Mediated Vascular

Regeneration Requires Endothelial ER71/ETV2. Arteriosclerosis, thrombosis, and vascular biology *36*, 86-96.

Park, C., Ma, Y.D., and Choi, K. (2005). Evidence for the hemangioblast. Experimental hematology *33*, 965-970.

Patan, S. (2004). Vasculogenesis and angiogenesis. Cancer treatment and research *117*, 3-32.

Paterson, M.R., and Kriegel, A.J. (2017). MiR-146a/b: a family with shared seeds and different roots. Physiological genomics *49*, 243-252.

Pham, V.N., Lawson, N.D., Mugford, J.W., Dye, L., Castranova, D., Lo, B., and Weinstein, B.M. (2007). Combinatorial function of ETS transcription factors in the developing vasculature. Developmental biology *303*, 772-783.

Potu, H., Peterson, L.F., Kandarpa, M., Pal, A., Sun, H., Durham, A., Harms, P.W., Hollenhorst, P.C., Eskiocak, U., Talpaz, M.*, et al.* (2017). Usp9x regulates Ets-1 ubiquitination and stability to control NRAS expression and tumorigenicity in melanoma. Nature communications *8*, 14449.

Randi, A.M., Sperone, A., Dryden, N.H., and Birdsey, G.M. (2009). Regulation of angiogenesis by ETS transcription factors. Biochemical Society transactions *37*, 1248-1253.

Rasmussen, T.L., Kweon, J., Diekmann, M.A., Belema-Bedada, F., Song, Q., Bowlin, K., Shi, X., Ferdous, A., Li, T., Kyba, M.*, et al.* (2011). ER71 directs mesodermal fate decisions during embryogenesis. Development *138*, 4801-4812.

Rechsteiner, M., and Rogers, S.W. (1996). PEST sequences and regulation by proteolysis. Trends Biochem Sci *21*, 267-271.

Ritchie, M.E., Phipson, B., Wu, D., Hu, Y., Law, C.W., Shi, W., and Smyth, G.K. (2015). limma powers differential expression analyses for RNA-sequencing and microarray studies. Nucleic acids research *43*, e47.

Saba-El-Leil, M.K., Vella, F.D., Vernay, B., Voisin, L., Chen, L., Labrecque, N., Ang, S.L., and Meloche, S. (2003). An essential function of the mitogen-activated protein kinase Erk2 in mouse trophoblast development. EMBO reports *4*, 964-968.

Sakurai, H., Era, T., Jakt, L.M., Okada, M., Nakai, S., Nishikawa, S., and Nishikawa, S. (2006). In vitro modeling of paraxial and lateral mesoderm differentiation reveals early reversibility. Stem cells *24*, 575-586.

Schoenebeck, J.J., Keegan, B.R., and Yelon, D. (2007). Vessel and blood specification override cardiac potential in anterior mesoderm. Developmental cell *13*, 254-267.

Selvaraj, N., Kedage, V., and Hollenhorst, P.C. (2015). Comparison of MAPK specificity across the ETS transcription factor family identifies a high-affinity ERK interaction required for ERG function in prostate cells. Cell Commun Signal *13*, 12.

Seo, S., Fujita, H., Nakano, A., Kang, M., Duarte, A., and Kume, T. (2006). The forkhead transcription factors, Foxc1 and Foxc2, are required for arterial specification and lymphatic sprouting during vascular development. Developmental biology *294*, 458-470.

Shalaby, F., Rossant, J., Yamaguchi, T.P., Gertsenstein, M., Wu, X.-F., Breitman, M.L., and Schuh, A.C. (1995). Failure of blood-island formation and vasculogenesis in Flk-1-deficient mice. Nature *376*, 62-66.

Sharrocks, A.D. (2001a). The ETS-domain transcription factor family. Nat Rev Mol Cell Biol *2*, 827-837.

Sharrocks, A.D. (2001b). The ETS-domain transcription factor family. Nat Rev Mol Cell Biol *2*, 827-837.

Shi, X., Zirbes, K.M., Rasmussen, T.L., Ferdous, A., Garry, M.G., Koyano-Nakagawa, N., and Garry, D.J. (2015). The transcription factor Mesp1 interacts with cAMP-responsive element binding protein 1 (Creb1) and coactivates Ets variant 2 (Etv2) gene expression. The Journal of biological chemistry *290*, 9614-9625.

Simoes, F.C., Peterkin, T., and Patient, R. (2011). Fgf differentially controls cross-antagonism between cardiac and haemangioblast regulators. Development *138*, 3235-3245.

Sivak, J.M., Petersen, L.F., and Amaya, E. (2005). FGF signal interpretation is directed by Sprouty and Spred proteins during mesoderm formation. Developmental cell *8*, 689-701.

Spyropoulos, D.D., Pharr, P.N., Lavenburg, K.R., Jackers, P., Papas, T.S., Ogawa, M., and Watson, D.K. (2000). Hemorrhage, impaired hematopoiesis, and lethality in mouse embryos carrying a targeted disruption of the Fli1 transcription factor. Molecular and cellular biology *20*, 5643-5652.

Stainier, D.Y., Weinstein, B.M., Detrich, H.W., 3rd, Zon, L.I., and Fishman, M.C. (1995). Cloche, an early acting zebrafish gene, is required by both the endothelial and hematopoietic lineages. Development *121*, 3141-3150.

Stenman, J.M., Rajagopal, J., Carroll, T.J., Ishibashi, M., McMahon, J., and McMahon, A.P. (2008). Canonical Wnt signaling regulates organ-specific assembly and differentiation of CNS vasculature. Science *322*, 1247-1250.

Sturgeon, C.M., Chicha, L., Ditadi, A., Zhou, Q., McGrath, K.E., Palis, J., Hammond, S.M., Wang, S., Olson, E.N., and Keller, G. (2012). Primitive erythropoiesis is regulated by miR-126 via nonhematopoietic Vcam-1+ cells. Developmental cell *23*, 45-57.

Sumanas, S., and Choi, K. (2016). ETS Transcription Factor ETV2/ER71/Etsrp in Hematopoietic and Vascular Development. Curr Top Dev Biol *118*, 77-111.

Sumanas, S., Jorniak, T., and Lin, S. (2005). Identification of novel vascular endothelial-specific genes by the microarray analysis of the zebrafish cloche mutants. Blood *106*, 534-541.

Sumanas, S., and Lin, S. (2006). Ets1-related protein is a key regulator of vasculogenesis in zebrafish. PLoS biology *4*, e10.

Takeuchi, M., Fuse, Y., Watanabe, M., Andrea, C.S., Takeuchi, M., Nakajima, H., Ohashi, K., Kaneko, H., Kobayashi-Osaki, M., Yamamoto, M.*, et al.* (2015). LSD1/KDM1A promotes hematopoietic commitment of hemangioblasts through downregulation of Etv2. Proceedings of the National Academy of Sciences of the United States of America *112*, 13922-13927.

Tanaka, M., Chen, Z., Bartunkova, S., Yamasaki, N., and Izumo, S. (1999). The cardiac homeobox gene Csx/Nkx2.5 lies genetically upstream of multiple genes essential for heart development. Development *126*, 1269-1280.

Taniguchi, K., Kohno, R., Ayada, T., Kato, R., Ichiyama, K., Morisada, T., Oike, Y., Yonemitsu, Y., Maehara, Y., and Yoshimura, A. (2007). Spreds are essential for embryonic lymphangiogenesis by regulating vascular endothelial growth factor receptor 3 signaling. Molecular and cellular biology *27*, 4541-4550.

Tsai, F.Y., Keller, G., Kuo, F.C., Weiss, M., Chen, J., Rosenblatt, M., Alt, F.W., and Orkin, S.H. (1994). An early haematopoietic defect in mice lacking the transcription factor GATA-2. Nature *371*, 221-226.

Tsai, F.Y., and Orkin, S.H. (1997). Transcription factor GATA-2 is required for proliferation/survival of early hematopoietic cells and mast cell formation, but not for erythroid and myeloid terminal differentiation. Blood *89*, 3636-3643.

Umbhauer, M., Marshall, C.J., Mason, C.S., Old, R.W., and Smith, J.C. (1995). Mesoderm induction in Xenopus caused by activation of MAP kinase. Nature *376*, 58-62.

Unezaki, S., Horai, R., Sudo, K., Iwakura, Y., and Ito, S. (2007). Ovol2/Movo, a homologue of Drosophila ovo, is required for angiogenesis, heart formation and placental development in mice. Genes to cells : devoted to molecular & cellular mechanisms *12*, 773-785.

Veldman, M.B., and Lin, S. (2012). Etsrp/Etv2 is directly regulated by Foxc1a/b in the zebrafish angioblast. Circulation research *110*, 220-229.

Veldman, M.B., Zhao, C., Gomez, G.A., Lindgren, A.G., Huang, H., Yang, H., Yao, S., Martin, B.L., Kimelman, D., and Lin, S. (2013). Transdifferentiation of fast skeletal muscle into functional endothelium in vivo by transcription factor Etv2. PLoS biology *11*, e1001590.

Ventura, A., Young, A.G., Winslow, M.M., Lintault, L., Meissner, A., Erkeland, S.J., Newman, J., Bronson, R.T., Crowley, D., Stone, J.R.*, et al.* (2008). Targeted deletion reveals essential and overlapping functions of the miR-17 through 92 family of miRNA clusters. Cell *132*, 875-886.

Verger, A., and Duterque-Coquillaud, M. (2002). When Ets transcription factors meet their partners. Bioessays *24*, 362-370.

Vlachos, I.S., Zagganas, K., Paraskevopoulou, M.D., Georgakilas, G., Karagkouni, D., Vergoulis, T., Dalamagas, T., and Hatzigeorgiou, A.G. (2015). DIANA-miRPath v3.0: deciphering microRNA function with experimental support. Nucleic acids research *43*, W460-466.

Wakioka, T., Sasaki, A., Kato, R., Shouda, T., Matsumoto, A., Miyoshi, K., Tsuneoka, M., Komiya, S., Baron, R., and Yoshimura, A. (2001). Spred is a Sprouty-related suppressor of Ras signalling. Nature *412*, 647-651.

Wang, H., Qian, W.J., Mottaz, H.M., Clauss, T.R., Anderson, D.J., Moore, R.J., Camp, D.G., 2nd, Khan, A.H., Sforza, D.M., Pallavicini, M.*, et al.* (2005a). Development and evaluation of a micro- and nanoscale proteomic sample preparation method. J Proteome Res *4*, 2397-2403.

Wang, L.C., Kuo, F., Fujiwara, Y., Gilliland, D.G., Golub, T.R., and Orkin, S.H. (1997). Yolk sac angiogenic defect and intra-embryonic apoptosis in mice lacking the Ets-related factor TEL. The EMBO journal *16*, 4374-4383.

Wang, S., Aurora, A.B., Johnson, B.A., Qi, X., McAnally, J., Hill, J.A., Richardson, J.A., Bassel-Duby, R., and Olson, E.N. (2008). The endothelial-specific microRNA miR-126 governs vascular integrity and angiogenesis. Developmental cell *15*, 261-271.

Wang, Z.Y., Sato, H., Kusam, S., Sehra, S., Toney, L.M., and Dent, A.L. (2005b). Regulation of IL-10 gene expression in Th2 cells by Jun proteins. Journal of immunology *174*, 2098-2105.

Watanabe, K., Villarreal-Ponce, A., Sun, P., Salmans, M.L., Fallahi, M., Andersen, B., and Dai, X. (2014). Mammary morphogenesis and regeneration require the inhibition of EMT at terminal end buds by Ovol2 transcriptional repressor. Developmental cell *29*, 59-74.

Wei, G., Srinivasan, R., Cantemir-Stone, C.Z., Sharma, S.M., Santhanam, R., Weinstein, M., Muthusamy, N., Man, A.K., Oshima, R.G., Leone, G.*, et al.* (2009). Ets1 and Ets2 are required for endothelial cell survival during embryonic angiogenesis. Blood *114*, 1123-1130.

Weintraub, H., Davis, R., Tapscott, S., Thayer, M., Krause, M., Benezra, R., Blackwell, T.K., Turner, D., Rupp, R., Hollenberg, S.*, et al.* (1991). The myoD gene family: nodal point during specification of the muscle cell lineage. Science *251*, 761-766.

Wells, J., Lee, B., Cai, A.Q., Karapetyan, A., Lee, W.J., Rugg, E., Sinha, S., Nie, Q., and Dai, X. (2009). Ovol2 suppresses cell cycling and terminal differentiation of

keratinocytes by directly repressing c-Myc and Notch1. The Journal of biological chemistry *284*, 29125-29135.

Yamamizu, K., Matsunaga, T., Katayama, S., Kataoka, H., Takayama, N., Eto, K., Nishikawa, S., and Yamashita, J.K. (2012). PKA/CREB signaling triggers initiation of endothelial and hematopoietic cell differentiation via Etv2 induction. Stem cells *30*, 687-696.

Yamashita, J., Itoh, H., Hirashima, M., Ogawa, M., Nishikawa, S., Yurugi, T., Naito, M., Nakao, K., and Nishikawa, S. (2000). Flk1-positive cells derived from embryonic stem cells serve as vascular progenitors. Nature *408*, 92-96.

Yao, Y., Li, W., Wu, J., Germann, U.A., Su, M.S., Kuida, K., and Boucher, D.M. (2003). Extracellular signal-regulated kinase 2 is necessary for mesoderm differentiation. Proceedings of the National Academy of Sciences of the United States of America *100*, 12759-12764.

Zhang, T., Zhu, Q., Xie, Z., Chen, Y., Qiao, Y., Li, L., and Jing, N. (2013). The zinc finger transcription factor Ovol2 acts downstream of the bone morphogenetic protein pathway to regulate the cell fate decision between neuroectoderm and mesendoderm. J Biol Chem *288*, 6166-6177.

Zou, Y.R., Kottmann, A.H., Kuroda, M., Taniuchi, I., and Littman, D.R. (1998). Function of the chemokine receptor CXCR4 in haematopoiesis and in cerebellar development. Nature *393*, 595-599.

Zovein, A.C., Hofmann, J.J., Lynch, M., French, W.J., Turlo, K.A., Yang, Y., Becker, M.S., Zanetta, L., Dejana, E., Gasson, J.C.*, et al.* (2008). Fate tracing reveals the endothelial origin of hematopoietic stem cells. Cell stem cell *3*, 625-636.